Politecnico di Torino

Master's *Degree in Civil Engineering*

A.Y. 2026/2027

Defense session: March 2026

Experimental Investigation on Waste Plastic Incorporation in Sustainable Bituminous Mixtures

Supervisors:

Prof. Davide Dalmazzo

Prof. Tsantilis Lucia

Prof. Ezio Santagata

Davide Cimenti

Candidate:

Mohammadmahdi Esmaeili

Abstract

This thesis investigates the development of sustainable bituminous mixtures for base course applications, with a specific focus on evaluating the influence of recycled plastic on mixture performance. The study aims to assess how the incorporation of recycled plastic affects the volumetric and mechanical behavior of base course mixtures and how these effects can be exploited to support an optimized mix design approach.

The experimental campaign was designed to analyze bituminous mixtures characterized by different recycled plastic contents and varying bitumen dosages. Volumetric and mechanical analyses were carried out to identify performance trends and to evaluate the role of recycled plastic within the mixture, supporting the definition of suitable mix design parameters for base course applications. In parallel, all constituent materials were thoroughly characterized to ensure a consistent material framework and to clarify the influence of material properties on mixture behavior. The performance of the developed mixtures was subsequently compared with reference base course mixtures adopted in industrial practice, enabling a direct assessment of the proposed solutions against real-world standards.

The results show that recycled plastic significantly affects the volumetric and mechanical performance of base course mixtures, supporting the development of more sustainable and high-performing asphalt layers. In addition, the efficiency of traditional production methods was assessed with particular attention to temperature-related aspects. Overall, the findings confirm the potential of recycled plastic as an effective strategy for optimizing base course mix design while promoting resource efficiency and circular economy principles in road engineering.

Keywords: bituminous mixtures, recycled plastic, base course, mix design, volumetric properties, mechanical properties, sustainability.

Summary

ACKNOWLEDGEMENTS

This thesis is not only the result of academic work, but also the outcome of a long journey filled with challenges, sacrifices, and unwavering support from the people who mean the most to me.

First and foremost, I would like to express my deepest gratitude to my beloved parents. Every step I have taken and every hardship I have endured was driven by the hope of bringing even a small amount of happiness and pride to your hearts. You dedicated your entire lives to me, setting aside your own dreams so that I, along with my brother and sister, could pursue ours. During my journey abroad, although I was physically alone, you never allowed me to feel lonely. Your constant care, support, and encouragement gave me the strength to move forward, especially in moments when I felt exhausted or lost. If today I stand here with valuable experiences and achievements, it is because of your endless sacrifices. I only wish you could be here beside me, so I could proudly show you to the world and say: *these are my parents*. Please know that I hold my head high because of you. I may never be able to be as good a son as you have been parents to me, but I am deeply grateful for every single moment of my life, which I owe to you. Today is truly yours. From afar, I kiss your hands with all my love.

I would also like to sincerely thank my dear brother and sister, who have always been my motivation to keep going. I love you deeply, and you have been in my thoughts every single moment. Please know that your brother loves you more than words can express. I only wish you could have been here beside me. My greatest wish is to always see you happy and smiling.

I would like to express my sincere appreciation to my supervisors, Prof. Davide Dalmazzo, Prof. Lucia Tsantilis, and Prof. Ezio Santagata, for their invaluable guidance, continuous support, and for treating me with kindness that felt like family. Thank you for sharing your knowledge so generously and for giving me the opportunity to learn and grow under your supervision. I feel truly honored to have been your student. Although I may not have been a perfect student, I can confidently say that I always did my best, and I am genuinely grateful for the time I had the privilege to spend working with you.

My heartfelt thanks also go to Davide Cimenti, who supported me like an older brother throughout this journey. There were many moments when I lacked knowledge or experience, but with great patience and kindness, he stood by me and guided me until the very end. I sincerely wish him the very best in his academic and professional future, along with happiness and success in his personal life.

Finally, I would like to thank my dear friends who stood by me during this journey, as well as the city of Turin and Politecnico di Torino, which provided me with meaningful experiences, beautiful memories, and a sense of belonging.

Thank you all for being part of my journey

خدایا شکرت

Introduction

Background and motivation

Over the past decades, global plastic production and consumption have increased steadily, driven by population growth, urbanization, and the expansion of industrial and consumer markets. Recent global assessments report that annual plastic production remains above 400 million tons, while less than 10% of generated plastic waste is effectively recycled, despite ongoing improvements in waste management technologies and regulatory frameworks [1].

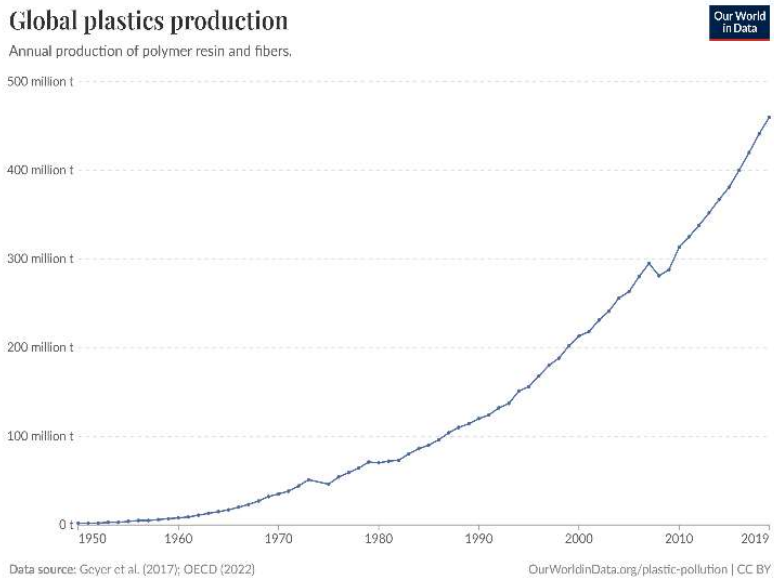

Figure 1 Global plastic production over the past decades [1]

Beyond the sheer growth in plastic production, there is increasing concern regarding the accumulation of mismanaged waste and the limitations of current recycling capabilities. Focusing solely on total plastic generation fails to accurately reflect the magnitude of the pollution crisis. This disparity is clearly reported in the scatterplot of Figure 2; while the horizontal axis shows the amount of plastic waste generated per capita, the vertical axis measures the per capita emission of the plastic pollution, more specifically plastic burned or lost as debris to rivers, ecosystems, and oceans. High – income nations, such as Australia, Qatar and Hong Kong, generate high amount of waste but maintain negligible pollution levels due to environmental awareness and effective recycling systems. Conversely, low-income countries like Rwanda, Burundi and Malawi produce far less waste but face significant pollution challenges due to infrastructure gap. The emphasis of such geographical disparities linked to infrastructure efficiency and consumption intensity is widely documented in scientific literature [1, 2], and requires reflection on plastic economy.

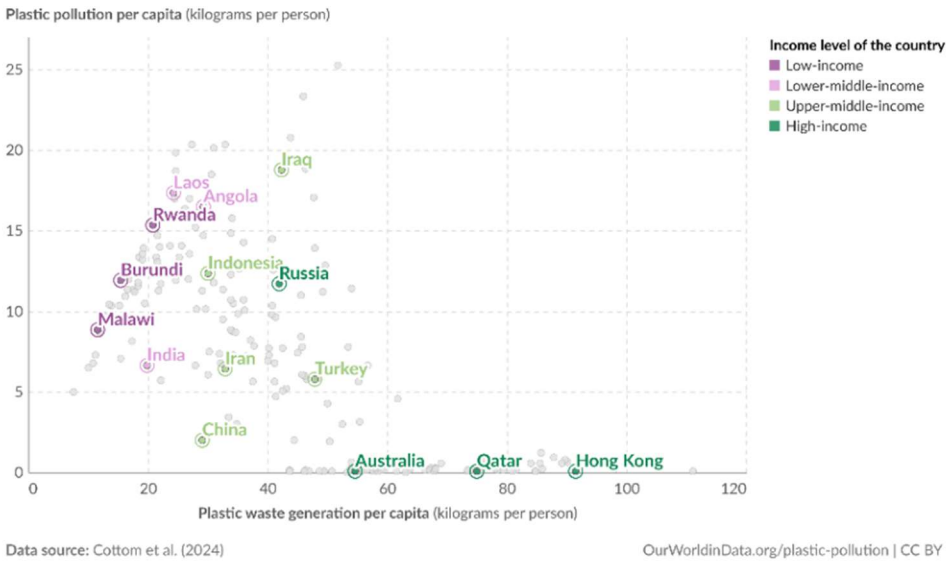

Figure 2 Plastic pollution vs plastic waste generation per capita values [3]

The global challenge of plastic waste management is increasingly addressed through a paradigm shift from a traditional linear model to a more sustainable circular economy framework. The conventional linear approach, characterized by a "*produce, use, and dispose*" trajectory (Figure 3A), relies heavily on landfilling and incineration. While pervasive and scalable, these methods are associated with significant environmental degradation, including the long-term release of microplastics into terrestrial and aquatic ecosystems, the emission of toxic combustion by products and the generation of greenhouse gases. Furthermore, the linear model remains critically dependent on finite petroleum resources, which is fundamentally incompatible with growing global energy demands and environmental preservation goals.

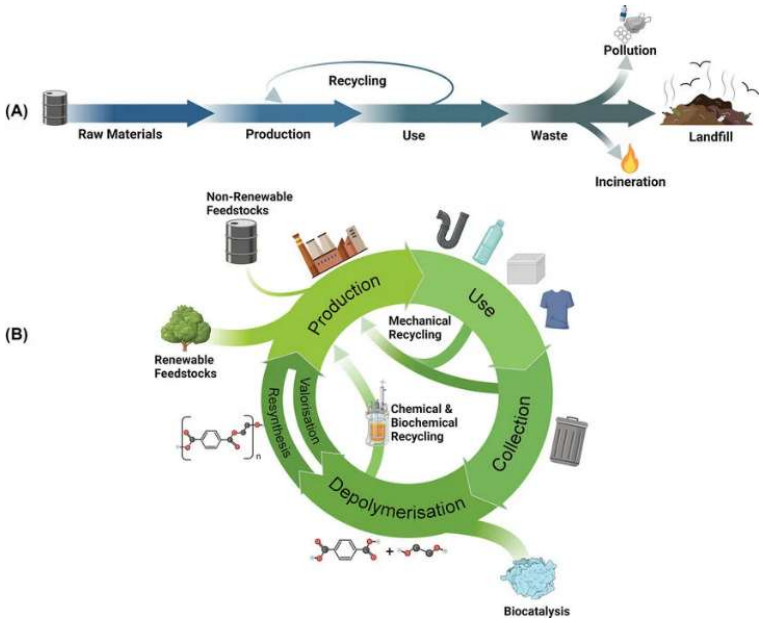

Figure 3 Linear and circular models of plastics economy [4]

In contrast, the circular economy approach seeks to integrate resource efficiency and waste reduction by closing the plastic value chain loop (Figure 3 B). This paradigm is based on using renewable feedstocks, improved waste collection, plastic waste recycling to monomers using physical and chemical technologies, monomer valorization or polymer resynthesis, and production of new plastic material [4].

Addressing plastic pollution therefore requires not only upstream reduction and improved recycling systems but also the development of technically feasible downstream valorization pathways capable of absorbing significant volumes of waste materials. In this context, the pavement sector represents a promising domain for the sustainable utilization of recycled plastics within existing industrial production systems. From a material engineering perspective, incorporating recycled plastics into asphalt mixtures modifies the internal structure and mechanical behavior of the composite system. Depending on their physical form, thermal characteristics, and interaction mechanisms, plastics may influence stiffness, strength, resistance to permanent deformation and moisture susceptibility [5, 6]. However, the magnitude and direction of these effects depend strongly on mixture composition, processing conditions, and the structural role assigned to the plastic material within the mixture. Within the pavement structure, the base course plays a fundamental role in distributing traffic-induced stresses and ensuring overall structural integrity. Unlike surface layers, which are primarily exposed to environmental actions and functional performance requirements, the base course must sustain repeated mechanical loading while maintaining volumetric stability and structural coherence. Consequently, evaluating the feasibility of recycled plastics in base course mixtures requires careful assessment of both volumetric and mechanical properties under controlled experimental conditions.

Objective of the Study

The primary objective of this research is to investigate the feasibility of incorporating wastes from plastic recycling operations into asphalt mixtures, specifically for the base course. The study aims to systematically evaluate the influence of plastic modifiers on both volumetric characteristics and mechanical performances ensuring compliance both with ANAS technical specifications and the Minimum Environmental Criteria (CAM, December 2024). The core of this investigation lies in the valorization of plastic waste streams that would otherwise be relegated to landfills or incinerators aiming to determine whether the integration of these secondary raw materials can serve not only enhancing mechanical performance but also facilitating partial binder replacement and therefore with economic and environmental implications.

Document outline

This thesis is structured in the following way:

- ***Background and literature review*:** here the Green Road project is introduced, followed by a general overview of waste plastic management and its incorporation into asphalt concrete (AC) mixtures according to different technological processes.
- ***Materials and Experimental methodology*:** This chapter describes the materials used in the experimental investigation and the methodology adopted to evaluate the feasibility of incorporating recycled plastic waste into AC for base course applications. The chapter first presents the objectives and overall structure of the experimental program, followed by a detailed description of the materials employed, including mineral aggregates, recycled plastic wastes, bituminous binder and chemical additives. Subsequently, the procedures adopted for mix design and specimen preparation are described. Finally, the laboratory testing program used to evaluate both volumetric and mechanical properties of the produced mixtures is presented.
- ***Experimental results and discussion**:* This chapter deals with the mechanical and volumetric outcomes of the overall asphalt mixtures produced at the laboratory scale, providing the basis for determining the optimum binder content (OBC). In addition, the dataset is supplemented with results from analogous tests performed on the optimized formulations manufactured at industrial plants and placed in full-scale field sections. This approach enabled to compare results produced with different mixing processes.
- ***Conclusions*:** This final section evaluates whether the research objectives have been successfully addressed and offers recommendations for future study.

1 Background and Literature Review

1.1 “Green Roads” project

From the environmental point of view, sustainable strategies in the road sector focus on reducing greenhouse gas emissions, conserving natural resources, and limiting waste generation through the adoption of recycled and low-carbon materials. Several studies have demonstrated that impacts can be significantly mitigated through the entire life duration when recycled constituents are incorporated into pavement structures due to the enhancement of mechanical properties and consequently the reduction in the frequency of rehabilitation interventions [7, 8].

Within this framework, the “Green roads” project – a collaboration between the asphalt manufacturer company Brillada. located in Borgaro Torinese and the Politecnico di Torino – aims to integrate recycled plastic waste into asphalt mixtures with the objective to commercialize such innovative products in base, binder and wearing courses in compliance with CAM. Commencing in September 2024, this two-year project follows a structured methodology. The process began with the selection of recycled plastic wastes based on their chemical and physical properties, followed by a comprehensive characterization of the constituents used in both traditional and innovative mixtures. Subsequently, a laboratory mix design process is carried out to determine the optimum binder content and evaluate the influence of plastic additives on volumetric and mechanical performance. The optimized mixtures are then replicated in plant, followed by advanced mechanical assessment with respect to flexible pavements most relevant distresses. The project concludes with field tests and environmental impact assessment to validate the development of this new line of products.

1.2 Asphalt mix design approaches

The optimal composition of an asphalt mixture cannot be defined in a univocal manner; rather, it must be determined case-by-case based on the available constituent materials and through adequate laboratory characterization. Starting from the same components, it is possible to identify multiple design recipes, each satisfying specific performance requirements and tailoring the choice to its intended destination of use [9]. Traditional methodologies aim to achieve an optimal balance between aggregate gradation, binder content, and air void content to ensure adequate resistance against common flexible pavement distresses, such as fatigue cracking and rutting.

In general, the asphalt mix design procedure consists of selecting suitable materials, defining the aggregate gradation, and preparing trial mixtures with different binder contents. The mixtures are then compacted and evaluated through laboratory tests in order to determine the optimum binder content and verify the expected volumetric and mechanical performance. This systematic approach allows the mixture composition to be adjusted to meet the required performance criteria [10].

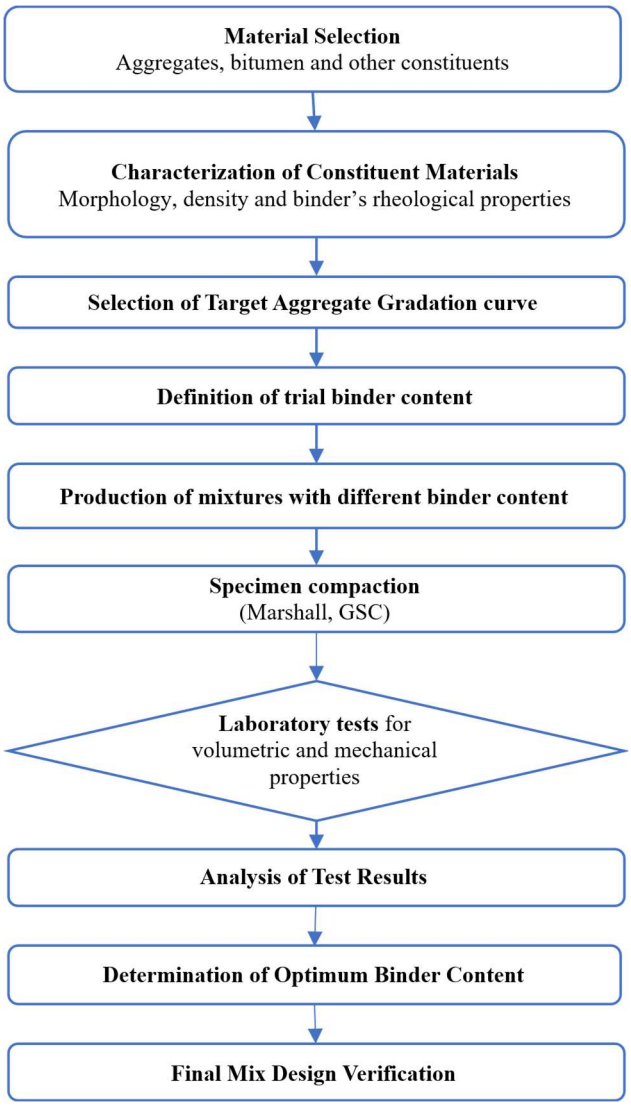

Figure 4 General procedure of asphalt mixture design [10]

Over the past several decades, mix design philosophies have progressive evolved from prescriptive methods towards performance – oriented concepts, in which volumetric requirements are complemented by mechanical testing to capture the in-service behavior more accurately. The Marshall method, for instance, determines the optimum binder content (OBC) through the assessment of volumetric properties and empirical characteristics, namely Marshal stability and flow. These are evaluated on specimens compacted via the Marshal impact technique and tested at 60°C under a constant loading rate of 50.8 mm/min until failure. However, this approach is limited by the static nature of the applied load, the potential discrepancy between the 60°C test temperature and actual operating conditions, and the fact that the measured parameters are not fundamental properties. Despite these inherent empirical limitations, this method remains widely used due to its simplicity, minimal equipment requirements, and cost-effectiveness.

Jitsangiam et al. (2023) [13] proposed a modified Marshall mix design to incorporate recycled plastic into asphalt mixtures, comparing conventional asphalt concrete (AC) with plastic-modified asphalt

concrete (ACP). They introduced a new parameter, the plastic-to-binder ratio (PBR), to better determine the appropriate plastic dosage within the mix design framework. The results showed that the optimum mixture was obtained at about 5.7% binder content corresponding to 4% air voids, satisfying the Marshall volumetric requirements. In the same way, ACP mixture demonstrated improved performance compared with the conventional AC, including approximately 16% higher Marshall stability and a 49% increase in resilient modulus, indicating the potential of plastic incorporation to enhance mixture mechanical performance. The design procedure involves an initial estimation of the PBR through a series of trial mixtures at fixed binder content, followed by the preparation of specimens with varying binder–plastic combinations based on the replacement concept. For each mixture, Marshall stability, flow, and volumetric parameters (air voids, VMA, and VFB) are determined, and the optimum binder content is identified through graphical analysis at the target air void level (4%). Subsequently, the corresponding PBR is refined to ensure consistency with the optimum binder content, leading to the final selection of mixture proportions that satisfy both volumetric criteria and mechanical performance requirements.

To address the above-mentioned limitations, the Strategic Highway Research Program introduced the Superpave (Superior Performing Asphalt Pavements) mix design approach. Superpave integrates mechanistic–empirical principles, incorporating binder performance grade (PG), aggregate angularity, and volumetric properties, while simulating field compaction more accurately through the gyratory compactor. In this method, specimens are compacted using the Superpave Gyratory Compactor (SGC), which better simulates field compaction conditions. The compaction is performed under a vertical pressure of approximately 600 kPa with a gyration angle of 1.25°**,** applied at a rotation rate of 30 gyrations per minute. The number of gyrations **(**Ni, N_d, and N_m**)** is selected according to traffic level and climatic conditions. During mix design, the binder content is adjusted so that the mixture achieves 4% air voids at the design number of gyrations (N_d)**.** Prior to compaction, loose mixtures are short-term aged in an oven at 135 °C for about 2 hours to simulate plant production conditions. The resulting specimens (typically 150 mm diameter and about 115 mm height**)** are then evaluated based on volumetric properties such as air voids (V_a), VMA, and VFA to determine the optimum binder content [11].

Performance-based mix design frameworks seek to directly relate material properties to distress mechanisms such as rutting, cracking, and moisture damage, thereby improving the reliability of laboratory-based mixture evaluation [12]. This evolution has become particularly relevant in the context of non-conventional and recycled materials, whose behavior cannot always be fully described through volumetric parameters alone.

Balanced Mix Design (BMD) represents another advanced approach in asphalt mixture design, which focuses on integrating volumetric properties with performance-based criteria. This method has been developed to overcome the limitations of traditional mix design procedures, particularly when dealing with recycled or non-conventional materials. For instance, Li et al. (2023) [33], investigated the implementation of BMD in asphalt mixtures and demonstrated that the optimum binder content is not a single fixed value, but rather a range defined by performance requirements, typically between 5.1% and 5.7%, depending on the balance between rutting resistance and cracking performance. Furthermore, their results showed that different cracking tests can lead to different minimum acceptable binder contents,

ranging from 5.3% to 5.9%, highlighting the sensitivity of mixture design to the selected performance criteria.

This approach is particularly relevant for asphalt mixtures incorporating recycled plastics, where the presence of plastic can significantly influence stiffness, deformation resistance, and cracking behavior. Therefore, adopting a BMD framework enables the identification of an optimal balance between rutting resistance and cracking susceptibility, ensuring that plastic-modified mixtures satisfy both volumetric and mechanical performance requirements.

The incorporation of recycled plastics adds complexity to the asphalt mix design process, as these materials can modify the interaction between aggregates and binder, affecting coating efficiency, mixture workability, and compaction behavior. Due to their diverse physical and thermal properties, plastics may also lead to heterogeneous mixture responses during production. Therefore, careful control of mix design parameters is required to ensure adequate volumetric stability and performance compliance [5]. Plastics with low melting temperatures may soften during production and interact with the binder, modifying its rheology, while high-melting plastics remain as solid inclusions within the aggregate skeleton, affecting load transfer and stress distribution. As a result, different mechanical responses may occur, including variations in stiffness, strength, deformation resistance, and moisture susceptibility.

Literature indicates that the impact of plastics strongly depends on the adopted mix design strategy and the role assigned to the plastic within the mixture. When plastics act as binder modifiers, adequate dispersion and compatibility with bitumen are required; when used as aggregate substitutes or reinforcement elements, particle size and distribution become critical. Therefore, mix design plays a key role in determining the feasibility and performance of plastic-modified asphalt mixtures [6].

Establishing a clear mix design methodology improves the comparability of experimental studies and facilitates the transfer of laboratory findings to practical pavement applications. This is particularly important for plastic-modified asphalt mixtures, where the lack of standardized design procedures has often limited large-scale implementation. Therefore, a rigorous mix design approach is essential for evaluating the potential of recycled plastics as sustainable components in asphalt base course mixtures and for supporting their adoption in industrial practice.

1.3 Recycled plastics and their incorporation methods in asphalt mixtures

The physical characteristics of a polymer depend not only on its morphology and molecular weight, but also on differences of structural configuration of molecular chains. Linear polymers (Figure 5.a) are composed of monomeric units connected end-to-end along a singles continuous chain. These macromolecules exhibit a high degree of flexibility. In this arrangement, numerous van der Waals and hydrogen bonds can form between adjacent chain. Owing to their mobility and ability to align, linear polymers can pack efficiently, resulting in a high degree of crystallinity. Typical examples include HDPE,

PVC, PS, PMMA and nylon. During polymer synthesis, side-branching may occur, giving rise to branched polymers (Figure 5b) in which lateral chains are attached to the main backbone. The presence of these branches reduces chain mobility and limits the ability of macromolecules to pack in ordered fashion, thereby decreasing both density and crystallinity. A representative example is LDPE, characterized by the presence of numerous short-chain branches. In cross-linked polymers (Figure 5c), adjacent linear chain are interconnected through localized covalent bonds introduced either during synthesis or through subsequent irreversible chemical reactions. These bonds are commonly formed by adding atoms or molecular groups capable of establishing covalent linkages with the main chain. Many elastomers acquire their cross-linked structure through vulcanization reactions. Finally, network or reticulated polymers (Figure 5d) are formed from multifunctional monomers capable of generating three or more active covalent bonds. This results in a fully interconnected three-dimensional network, which imparts distinctive mechanical and thermal properties that are markedly different from those of linear or lightly cross-linked systems.

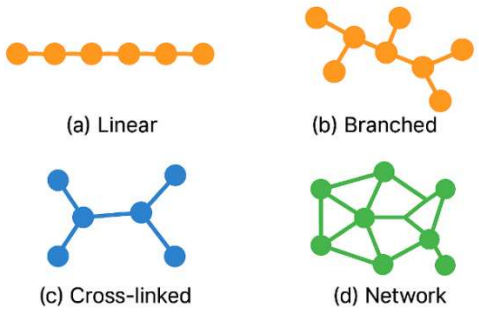

Figure 5 Schematic representation of polymer molecular structures

The molecular structure strongly influences their physical and mechanical behavior, including melting temperature and softening response, aspects that are particularly relevant in asphalt modification. These thermal and interaction mechanisms have led to two main approaches for incorporating recycled plastics into asphalt mixtures: the wet and dry processes. In the wet process, plastics are blended with hot bitumen to produce a modified binder, whereas in the dry process plastics are added directly to the mixture and integrate into the aggregate skeleton. These methods involve different interaction mechanisms and can produce distinct performance outcomes.

García-Morales et al. (2006) [14] investigated the effect of different waste polymers (EVA, EVA/LDPE blends, crumb rubber and ABS) on bitumen behavior. Their study showed that the thermal and molecular structure of polymers influences how they interact with bitumen during mixing. Rheological tests indicated that polymer addition increases the stiffness and viscoelastic response of the binder at high temperatures. As shown in below Figure**,** polymer-modified binders present higher complex modulus compared with neat bitumen due to the formation of polymer networks within the binder. These results highlight that polymer melting behavior and compatibility with bitumen are key factors governing how recycled plastics can be incorporated into asphalt mixtures.

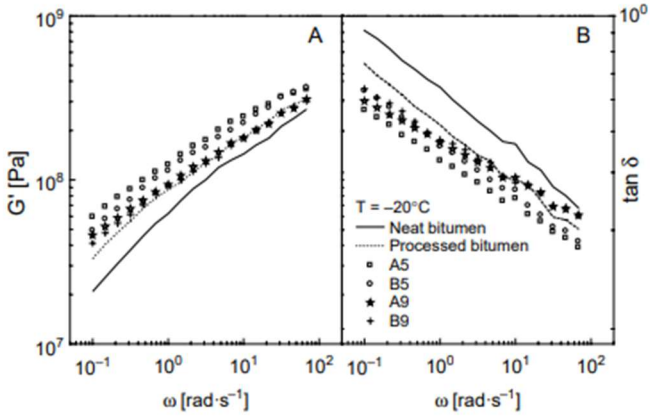

Figure 6 Frequency dependence of the viscoelastic functions of neat and polymer-modified bitumen at −20 °C [14]

As shown in Figure 6, polymer-modified binders exhibit higher storage modulus G′ than neat bitumen, indicating increased stiffness due to the interaction between polymer chains and the bitumen matrix [14]. This behavior highlights the importance of polymer thermal properties in the incorporation of recycled plastics into asphalt mixtures.

The thermal and rheological characteristics of polymers therefore play a key role in determining how recycled plastics interact with bitumen during asphalt production. Depending on their melting behavior and compatibility with the binder phase, plastics may either blend with the bitumen or remain as discrete particles within the mixture. Consequently, different technological approaches have been developed to incorporate recycled plastics into asphalt mixtures. In practice, these approaches are mainly classified into two methods: the wet process and the dry process. Based on these thermal and interaction mechanisms, different technological approaches have been developed to incorporate recycled plastics into asphalt mixtures. In the wet process, plastics are blended with hot bitumen to produce a modified binder before mixing with aggregates. In contrast, in the dry process plastics are directly added during the mixing stage and become part of the aggregate structure. These two approaches lead to different interaction mechanisms and may result in distinct mixture performance.

In the wet process, recycled plastics are mixed with hot bitumen, where low-melting polymers can soften and interact with the binder, altering its rheology and typically increasing stiffness and resistance to permanent deformation. Plastics are commonly introduced as powders or pellets at contents of about 2–8% by binder weight [15]. Although this method enables direct modification of binder properties, it may require additional facilities to control phase separation, increasing operational complexity and cost. [14]. investigated the effect of different waste polymers (EVA, EVA/LDPE blends, crumb rubber and ABS) on bitumen behavior. Rheological tests indicated that polymer addition increases the stiffness and viscoelastic response of the binder at high temperatures. As shown in Figure 6 Frequency dependence of the viscoelastic functions of neat and polymer-modified bitumen at −20 °C [14] **,** polymer-modified binders present higher storage modulus compared with neat bitumen due to the formation of polymer chains and the bitumen matrix.

In the dry process, recycled plastics are introduced directly into the asphalt mixture during the

mixing stage together with the aggregates, becoming part of the mixture structure rather than modifying the binder beforehand. This method can generally be implemented in conventional asphalt plants without requiring specific binder modification facilities. However, the performance of dry-processed mixtures largely depends on parameters such as plastic dosage, particle size, and mixing conditions, which affect mixture homogeneity and compaction behavior [5, 16].

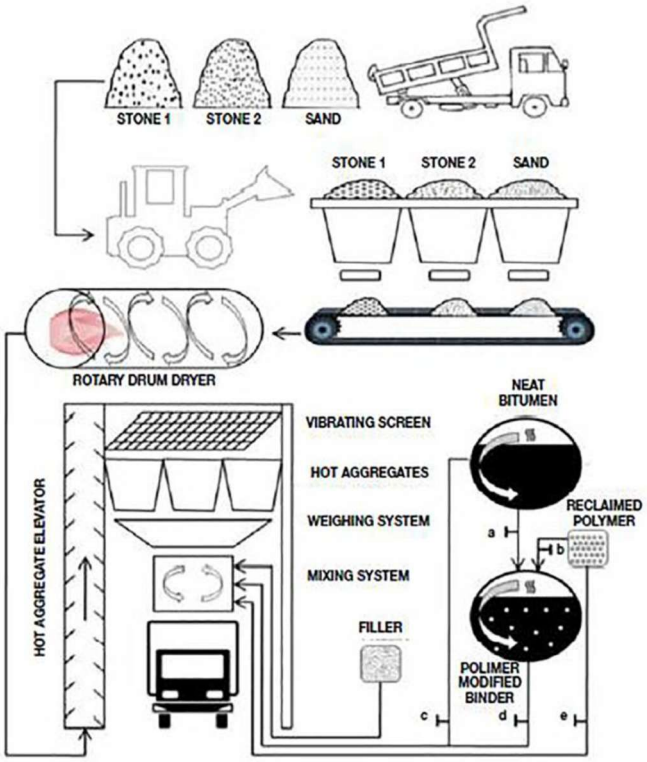

Figure 7 Wet and dry incorporation processes of recycled plastics in asphalt plants [5].

this Figure 7 illustrates the main stages of incorporating recycled plastics into asphalt production through wet and dry processes. In the wet process plastics are blended with the binder to produce a polymer-modified binder, whereas in the dry process plastic particles are added directly during the aggregate mixing stage.

Comparative studies indicate that both wet and dry incorporation processes present specific advantages and limitations. The wet process allows a more controlled modification of the binder and may enhance binder rheological properties; however, it requires specialized mixing and storage facilities, which increases production complexity and cost. In contrast, the dry process can be implemented using conventional asphalt plants and offers a simpler and more economical production procedure. Nevertheless, it may present challenges related to mixture homogeneity and moisture stability. Therefore, the selection between these two approaches should consider not only the desired performance of the mixture but also practical aspects related to production infrastructure and industrial feasibility [16].

Method	Production Cost	Technological Problem		Performance of Mixture	
		Advantage	Drawback	Advantage	Drawback
Wet process	Expensive (AC-16)	Normative guidance and engineering experience	Complex production process (specialized mixing and storage facilities)	Higher viscosity	Poor storage stability
Dry process	Cheap (AC-16)	Lack of normative guidance	Simple production process (no need of professional facility)	-	Poor water stability

Figure 8 The advantages and drawbacks of different processes [16].

To further investigate the dry incorporation method, [17] examined the behavior of plastic particles added directly to hot aggregates during mixing. Their results showed that incorporating polyethylene-based plastics improved mixture performance, particularly Marshall stability and rutting resistance, with stability increases of approximately two to three times compared with the conventional mixture at optimal plastic contents. In the dry process, plastics such as PET or HDPE typically maintain their particle form during mixing and become part of the aggregate skeleton. The mixing sequence used in this approach is illustrated in Figure 9**,** where plastic particles are blended with heated aggregates before the addition of bitumen.

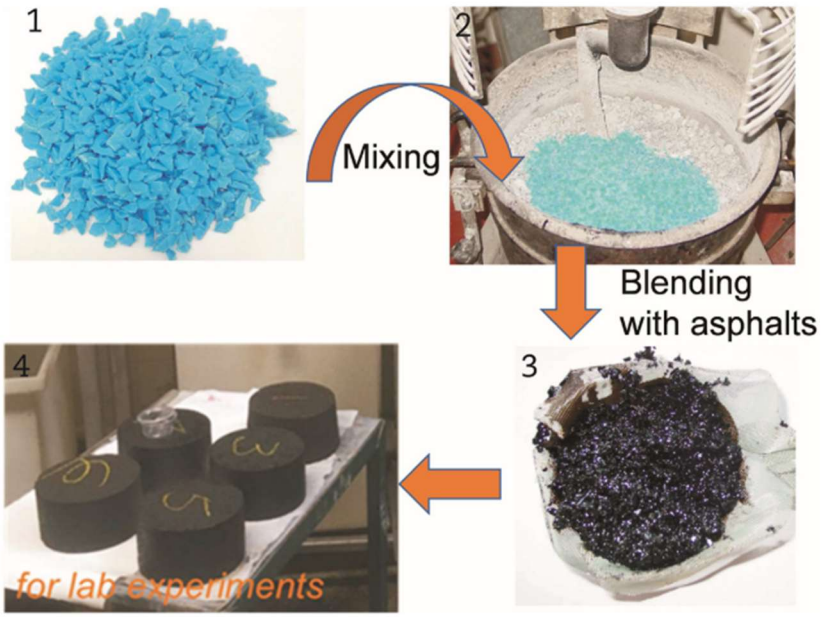

Figure 9 Dry processed asphalt mixtures with plastics waste [17].

The performance of plastic-modified asphalt mixtures is strongly affected by the mix design methodology. Different design approaches influence binder content, aggregate structure, and compaction, which consequently affect volumetric and mechanical properties. While the Marshall method mainly evaluates stability and flow, Superpave uses gyratory compaction and performance-based binder grading. More recently, Balanced Mix Design (BMD) has been developed to simultaneously control rutting and cracking. Therefore, the same plastic additive may lead to different performance outcomes depending on the selected mix design procedure.

The effect of recycled plastics in asphalt mixtures also depends on the mix design method

adopted. In Marshall design, plastic incorporation is often reflected by an increase in Marshall stability while maintaining air voids close to the typical design value of about 4%. In Superpave mixtures, the improved aggregate structure and gyratory compaction generally lead to higher rutting resistance, often associated with increases in VMA. More recently, Balanced Mix Design (BMD) approaches evaluate both rutting and cracking performance, and several studies report improvements in fatigue resistance while maintaining a balanced response between rutting and cracking. These results highlight the importance of considering the mix design framework when evaluating plastic-modified asphalt mixtures.

To further illustrate the influence of mix design procedures on the performance of plastic-modified mixtures, several examples reported in the literature are presented. The following charts summarize typical volumetric and mechanical responses observed in different studies, highlighting how recycled plastics may affect parameters such as air voids, VMA, stability, rutting resistance, and fatigue performance depending on the adopted design framework.

As an example, Almeida et al. (2020) [18] investigated asphalt mixtures containing LDPE plastic flakes using the Marshall mix design method. The plastic content varied from 0% to 8% by weight of bitumen. The results showed that the addition of LDPE slightly increased the Marshall stability, which reached values around 20–21 kN, compared with approximately 16–18 kN for the reference mixture. The volumetric analysis indicated that the air void content remained close to the typical design value of about 4%, showing that the incorporation of plastic did not significantly disturb the volumetric balance of the mixture. In addition, mechanical tests revealed improvements in stiffness and rutting resistance, while the reduction in rut depth reached approximately 30–60% compared with the reference mixture. The variation of volumetric parameters and stability with plastic content is illustrated in Figure 10**.**

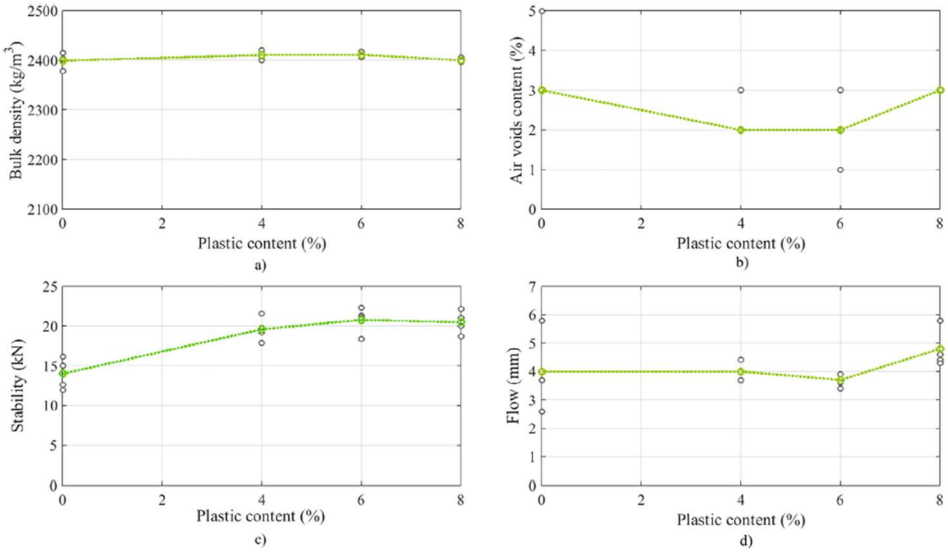

Figure 10 Variation of bulk density, air voids, Marshall stability and flow with plastic content [18].

Overall, recycled plastics can be incorporated into asphalt mixtures through different technological approaches, each leading to different interaction mechanisms within the mixture. Their effectiveness depends on factors such as plastic type, particle size, and processing condition. in this study, the

following section investigates how the incorporation of recycled plastics affects the volumetric and mechanical properties of asphalt mixtures.

2 Materials and Experimental Methodology

The experimental methodology was developed to simulate realistic asphalt production conditions while ensuring controlled laboratory evaluation of the effects of recycled plastics on mixture behavior. Particular attention was given to parameters influencing mixture volumetrics, compaction characteristics, and mechanical performance, which are critical for base course layers subjected to repeated traffic loading. The program was structured to allow a systematic comparison between mixtures produced with recycled plastics and reference mixtures prepared using conventional materials. Through this approach, the influence of plastic inclusion on mixture composition, volumetric characteristics, and mechanical performance could be evaluated under consistent testing conditions.

Figure 11 Experimental program flowchart

2.1 Objectives and experimental program

The experimental program was designed to evaluate the feasibility of incorporating recycled plastic waste into asphalt mixtures intended for base course applications and to analyze its influence on mixture performance under controlled laboratory conditions. To achieve this objective, several asphalt mixtures were produced varying binder contents and two distinct mixing protocols – manual and automatic mixing - to simulate diverse production environments and assess their impact on mixture homogeneity and compaction behavior.

The experimental matrix employed a comparative framework: for each selected composition, a reference mixture without polymer was compared against a modified mixture containing a fixed amount of plastic content of 0.8%. This approach allowed for a direct assessment of plastic's influence on the bituminous matrix across varying binder dosages. The resulting specimens were subsequently tested to evaluate both volumetric characteristics and mechanical properties of the mixtures. Volumetric analysis included parameters such as bulk density and air void content, which are essential for assessing mixture compaction and internal structure. Mechanical performance was evaluated through laboratory testing aimed at determining the resistance of the mixtures to tensile stresses and deformation.

In addition to laboratory-produced mixtures, the results were also compared with mixtures produced in the asphalt plant, allowing an assessment of the effect of the mixing procedure on overall properties, and therefore have feedback about the practical applicability of recycled plastics in asphalt mixtures.

Through this structured experimental program, the study aims to identify an appropriate mix design configuration and to evaluate the extent to which recycled plastics can act as a partial replacement of the bituminous binder, while maintaining acceptable volumetric stability and mechanical performance in asphalt mixtures for base course applications.

2.2 Materials

The materials employed in the present experimental investigation were selected to represent the conventional components typically used in asphalt base course mixtures while allowing the incorporation of recycled plastic waste as an alternative material. The study involved three primary material categories: mineral aggregates, recycled plastic waste, and bituminous binder. Each material plays a distinct role in determining the volumetric composition, workability, and mechanical properties of the asphalt mixture. Aggregates form the load-bearing skeleton of the mixture, the bituminous binder provides cohesion and viscoelastic behavior, and the recycled plastic material acts as a modifying constituent capable of altering the interaction mechanisms within the mixture acting as aggregate or as binder phase. Consequently, careful material characterization is necessary to ensure compatibility among the components and to guarantee reliable interpretation of the experimental results. The following subsections describe the origin, characteristics, and functional role of each material used in the experimental program.

2.2.1 Mineral aggregate and RAP

Mineral aggregates constitute the largest fraction of asphalt mixtures and play a critical role in determining the structural performance of pavement layers. As part of sustainable pavement engineering strategy, it is common practice the integration into the aggregate skeleton of a certain percentage of reclaimed asphalt which is material obtained from the milling or removal of existing asphalt pavement and therefore contribute on the final composition both with bitumen and mineral aggregate. In compliance with CAM for the base layer 35% is set as the minimum percentage to adopt.

2.2.1.1 Particle size distribution

Prior to mixture preparation, the aggregates were characterized through particle size distribution analysis using sieve analysis in accordance with EN 933-1 [22]. To ensure reliable grading measurements, representative aggregate samples were prepared according to the recommendations of Table 1.

Table 1 Minimum test portion size for sieve analysis [22]

Table 1 — Minimum size of test portions

Aggregate size D (maximum) mm	mass of aggregates kg	volume of lightweight aggregates (litres)
90	80	-
32	10	2,1
16	2,6	1,7
8	0,6	0,8
≤ 4	0,2	0,3

NOTE 1 For aggregates of other sizes below 90 mm, the minimum test portion mass may be interpolated from the masses given in Table 1 using the following formulae: $M = (D/10)^2$

where M = minimum mass of test portion in kg

D = aggregate size in mm

NOTE 2 The precision of the test method may be reduced if the test portion size is less than the value in Table 1. In such a case, the test portion size should be stated in the test report (9.2).

NOTE 3 For aggregates of particle density higher than 3,00 Mg/m^3 (see EN 1097-6), an appropriate correction should be applied to the test portion masses given in Table 1 based on the density ratio, in order to produce a test portion of approximately the same volume as those for aggregates of normal density.

NOTE 4 For lightweight aggregates complying with EN 13055, use the volume column to choose the appropriate minimum size of test portions. The volumes for other aggregate sizes may be interpolated.

Figure 12 Aggregate 15/25

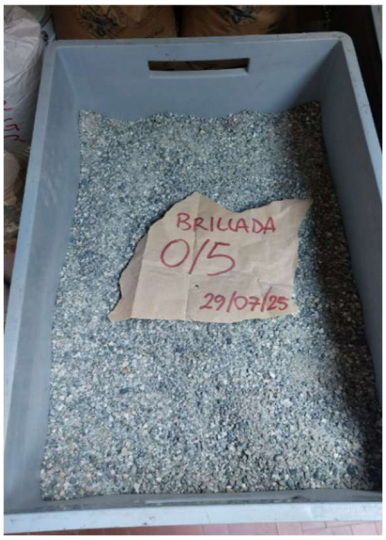

Figure 13 Aggregate 0/5

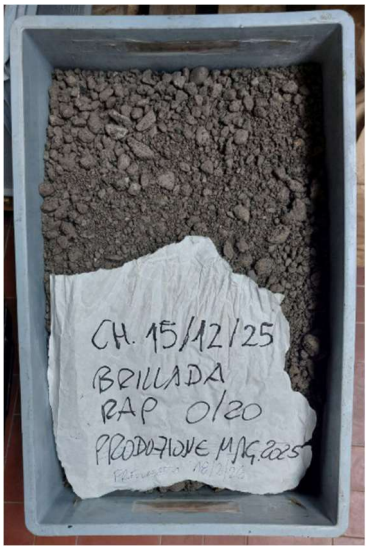

Figure 14 RAP 0/20 black

Figure 15 Filler

The obtained gradation curves for the fractions 0/5, 15/25, extracted RAP 0/20 and filler are reported in Table 2 and Figure 16. For the aggregate skeleton the granular sizes 0/5, 15/25 and extracted RAP 0/20 were combined to obtain the target gradation required for the base course mixture design. This resulting distribution was carefully selected in order to ensure proper particle interlocking, adequate compaction behavior, and satisfactory volumetric properties.

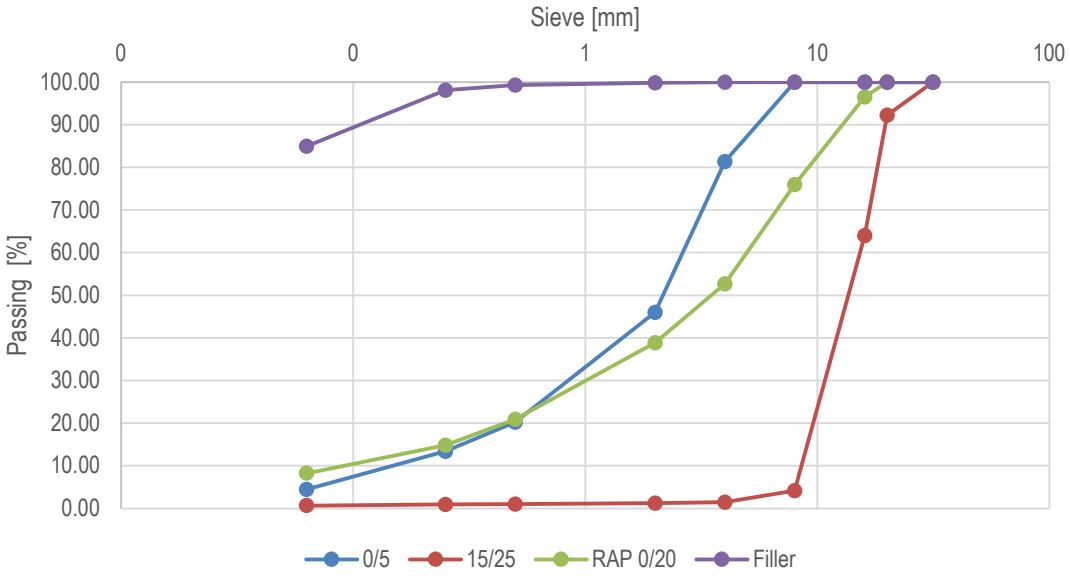

Figure 16 Particle size distribution curves of the aggregate fractions.

Table 2 Sieve analysis results showing the particle size distribution of the individual aggregate components.

Sieve size [mm]	Passing [%]			
	Filler	0/5	15/25	Extracted RAP 0/20
31.5	100.00	100.00	100.00	100.00
20	100.00	100.00	92.22	100.00
16	100.00	100.00	63.99	96.54
8	100.00	100.00	4.18	75.95
4	100.00	81.36	1.42	52.66
2	99.86	45.96	1.18	38.86
0.50	99.30	20.21	1.01	20.87
0.25	98.08	13.36	0.92	14.84
0.063	85.00	4.44	0.68	8.27

2.2.1.2 Aggregate particle density

The particle density of the aggregates was determined using the pycnometer method according to EN 1097-6: 2002 Annex A. Table 3 shows the results of the test.

Table 3 Summary of aggregate density values used for mix design

Fraction	Average density (Mg/m³)	Standard deviation (Mg/m³)
15/25	2.813	0.025
0/5	2.726	0.004
RAP 0/20	2.524	0.006

2.2.2 Plastic wastes

Wastes from plastic recycling operations were used in this study as an alternative material in the asphalt mixtures in order to evaluate its potential application in sustainable pavement construction as well as its binder substitution attitudes. The material employed in the experimental program, identified as MEGPO, is a polyolefin blend provided by a supplier operating in the recycling of post-consumer plastics located in the North of Italy.

Previous morphological and thermal characterizations conducted by the research group focused on grading curve, density and high-temperature interaction between the polymer and the aggregate skeleton, specifically assessing the efficiency of the polymer coating on the mineral surfaces. The physical properties of the MEGPO additive are detailed below.

Figure 17 Waste plastics MEGPO used in the experimental mixtures

2.2.2.1 Particle size distribution

The gradation analysis of MEGO flakes indicates a material predominantly sized between 4.0 mm and 10.0 mm, with a negligible percentage of passing through 2.0 mm sieve (<2%). The results from sieving are reported in Table 4 Sieving analysis results for MEGPO and Figure 18.

Table 4 Sieving analysis results for MEGPO

Sieve (mm)	Cumulative passing (%)
16.0	100.0
12.5	100.0
10.0	97.7
8.0	87.9
6.3	66.2
4.0	19.9
2.0	1.8
1.0	0.2
0.5	0.1
F	0.0

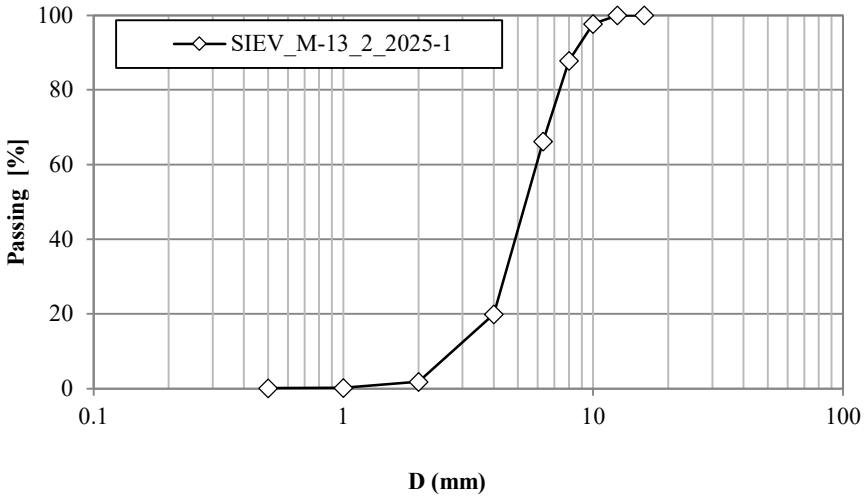

Figure 18 Particle size distribution of the waste plastic used in the study, obtained from sieve analysis

2.2.2.2 Density analysis

The density of MEGPO was determined according to EN 1097:6 Annex A, as in the case for the mineral aggregates. The average value assumed in the calculations is 1.166 Mg/m^3.

2.2.2.3 Ignition residue

Ignition tests performed on the polymer revealed that it does not fully combust. An average mass residue of 21% remains after the cycle. This recalcitrant fraction is incorporated into subsequent volumetric and dosage calculations to prevent the overestimation of the binder content.

2.2.3 Neat bitumen

The bituminous binder acts as the primary cohesive matrix within asphalt mixtures. Its fundamental role is to encapsulate mineral aggregates in a thin, continuous film, providing a lubricating effect that facilitates the internal rearrangement of the lithic skeleton. This mechanism ensures optimal particle interlocking and maintains the structural integrity of the composite material. In the present study, a 70/100 penetration grade bitumen was used, sourced directly from the production plant. Previous tests performed in the laboratory reported a penetration value of 96 dmm and a softening point of 45.2°C.

Figure 19 Bitumen used in the experimental program

2.2.4 Rejuvenator additive

Rejuvenators are commonly used in asphalt technology to restore or improve the rheological properties of aged or modified binders in RAP by reintroducing lighter molecular fractions that may be lost during ageing processes. The use of rejuvenating agents can enhance binder flexibility, improve workability during mixture production, and contribute to maintaining desirable mechanical properties of the asphalt mixture. Within this study, the quantity the rejuvenator introduced is 0.2% by the weight of RAP, sprayed directly on this latter conditioned on large trays such to maximize the exposition to the restoring agent.

2.3 Laboratory mix design procedure

The mix design procedure represents a fundamental stage in asphalt mixture development, as it defines the composition and preparation process used to obtain mixtures with suitable volumetric and mechanical properties for pavement applications. In this study, the mix design procedure was developed to evaluate the incorporation of recycled plastic materials within asphalt mixtures intended for base course layers.

The design methodology was structured to ensure that the produced mixtures were compatible with conventional asphalt production practices while allowing the controlled introduction of recycled plastic materials. Particular attention was given to parameters influencing mixture volumetrics, aggregate interlocking, binder distribution, and compaction behavior.

The overall procedure involved several sequential steps, including the definition of the target aggregate gradation, the selection of mixture components, specimen preparation, and laboratory compaction. These stages were designed to ensure repeatability of the experimental process and consistency among the produced mixtures.

The mix design process was therefore organized to allow the preparation of different asphalt mixtures while maintaining controlled laboratory conditions. This approach enabled a systematic evaluation of mixture behavior during subsequent volumetric and mechanical testing.

2.3.1 Design grading curve

The optimization of the combined grading curve was performed through spreadsheet calculations in which the percentage of each aggregate fraction presented in 2.2.1 was determined through an optimization process aiming to minimize the root mean square error (RMSE) between the designed grading curve and the target grading curve defined by the ANAS specifications [20].

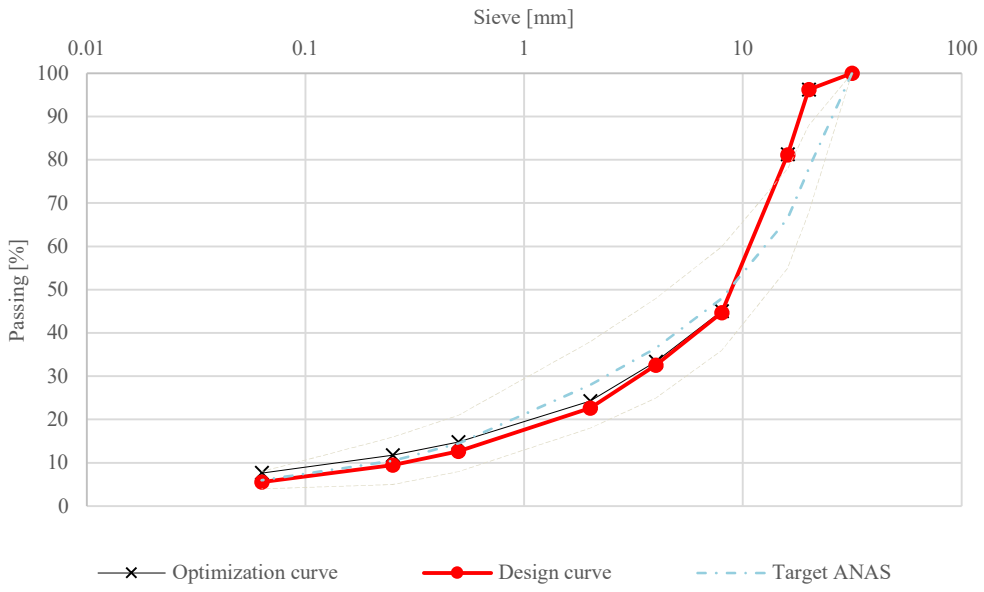

Figure 20 Combined aggregate grading curve obtained through optimization compared with the design curve

Following the optimization procedure, an initial aggregate gradation curve was obtained showing an amount of filler exceeding the 7%. Aggregate proportions were subsequently adjusted, moving from the initial optimized curve toward the final design gradation curve (

Table 6, Figure 20). While the adjustment ensured compliance with ANAS specifications limits for most fractions, a slight variation was observed for sieve sizes exceeding 16 mm. Despite this discrepancy, the final grading was validated and accepted by the asphalt producer, as the curve closely aligns with the standard production benchmarks used at the plant.

Table 5 Adopted aggregate fractions in the mix design

Aggregate fraction	Percentage (%)
Filler	2
0/5	14
15/25	49
RAP 0/20	35

Table 6 Target gradation curve used for the mix design (SL1)

Sieve (mm)	Design curve
32	100.00
20	96.19
16	81.15
8	44.63
4	32.52
2	22.61
0.50	12.62
0.25	9.48
0.063	5.55

2.3.2 Laboratory specimen preparation

The preparation of laboratory specimens represents a critical stage in the experimental investigation of asphalt mixtures, as it ensures the reproducibility of mixture properties and the reliability of the subsequent volumetric and mechanical tests. In this study, asphalt concrete mixtures were prepared under controlled laboratory conditions in order to simulate the manufacturer's procedure on real scale.

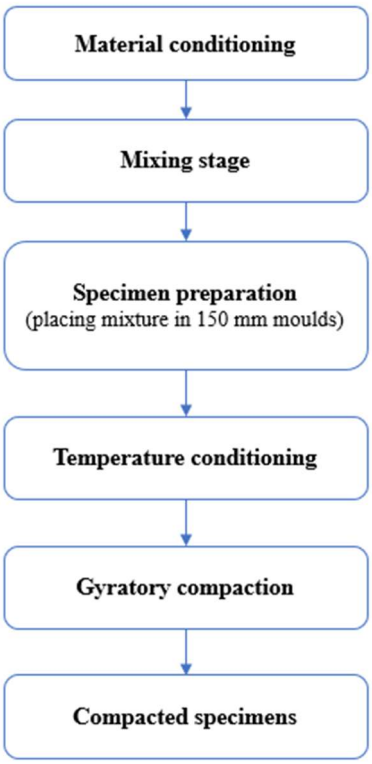

Figure 21 Flowchart of the overall procedure

Prior to mixing, all materials were conditioned to the required temperatures in order to ensure proper workability and homogeneity of the mixtures. The aggregate fractions 0/5 and 15/25 were pre-dried at 110°C for at least 9 hours and then heated at 250 °C for about 2 hours; waste plastics and RAP 0/20 were heated at 75 °C for maximum two hours in order to avoid excessive ageing of the aged binder in the latter one. Filler and neat bitumen were conditioned at the mixing temperature of 165°C. Through this procedure, all materials were brought to suitable thermal conditions before the mixing stage, ensuring consistent mixture preparation and proper interaction between aggregates, binder, and recycled plastic.

Figure 22 Heating of aggregates prior to mixing

After reaching the required temperatures, the heated aggregates were introduced into the laboratory mixing equipment. The binder was then added to the aggregate mixture in accordance with the predetermined mixture composition defined in the mix design procedure. The materials were mixed until a uniform coating of aggregates by the bituminous binder was obtained. In mixtures containing recycled plastic material, the plastic particles were incorporated during the mixing stage according to the selected incorporation procedure. The mixing process was carefully controlled to ensure homogeneous distribution of the recycled plastic within the asphalt mixture. After reaching the required conditioning temperatures, the laboratory mixer was first preheated to the mixing temperature in order to minimize heat losses during the mixing stage. Once the equipment and materials were properly prepared, the mixing process was initiated.

The heated aggregate fractions (0/5 and 15/25) were first introduced into the mixer and blended for two minutes with the waste plastics in accordance with the dry incorporation procedure and allowing partial aggregate coating. The RAP 0/20, which had previously been treated with the required amount of rejuvenator to restore part of the aged binder properties, was incorporated and determined a temperature drop due to the temperature difference and the significant amount of this material. The hand mixing proceeds until the target temperature of 165°C was reached observing an improvement in workability of the mixture because of lubricant action of RAP bitumen. At this temperature, neat bitumen was incorporated in three additions, each followed by a proportional amount of mineral filler and 30 seconds of mixing to ensure uniform texture. Once all components were added, the mixture was blended for an

additional 60 seconds, followed by a minute pause to simulate the thermal effects of transport prior to compaction.

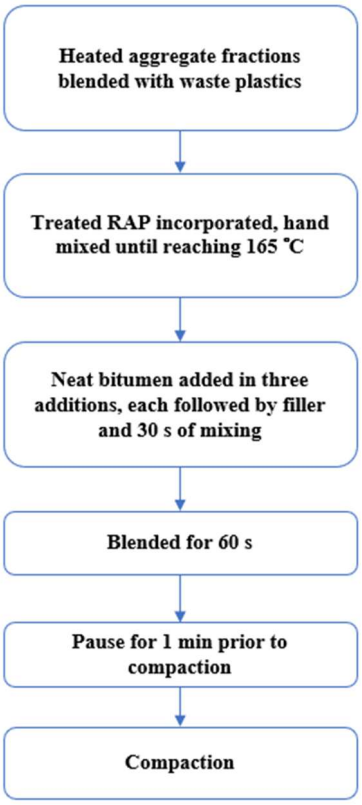

Figure 23 Laboratory mixing sequence for asphalt mixtures with waste plastic (dry process)

During the entire mixing procedure, the temperature inside the mixer was maintained between 165 °C and 170 °C to ensure proper workability and uniform mixture preparation.

Figure 24 Mixing procedure of the asphalt mixture in the laboratory

The asphalt mixture was transferred into cylindrical moulds for specimen preparation. The material was carefully sampled from mixing bowl in order to avoid segregation and to maintain the representative distribution of aggregates within the specimen. In this study, 150 mm diameter moulds were used according to the standard [23] since the maximum nominal diameters of aggregate is 20 mm. The mass of the mixture to be introduced into the mould was determined on the basis of the following equation:

$$M = 10^{-3}\pi \frac{D^2}{4} h_{MIN}\, \rho_M$$

Where:

- M, mass of a dry mixture to be introduced in the mould (g);
- D, internal diameter of the mould, equals to 150 mm.
- h_{MIN}, minimum height of compacted specimen corresponding to zero percent of voids, equals to 100 mm.
- ρ_M, maximum density of the mixture (Mg/m^3).

Moulds with material were placed in an oven at the compaction temperature and kept there until the mixture reached thermal equilibrium. This conditioning step ensured that the mixture temperature was appropriate for the gyratory compaction process. Once the required compaction temperature was reached, the specimens were compacted using the Superpave Gyratory Compactor (SGC) at 145°C according to [24].

Figure 25 Placement of asphalt mixture into the mould

After the compaction process was completed, the specimens were extracted from the moulds. The compacted samples were subsequently allowed to cool at room temperature before being subjected to the volumetric and mechanical tests described in the following sections. Prior to testing, the specimens were stored under controlled laboratory conditions to ensure consistent handling and testing procedures.

2.3.3 Determination for the maximum theoretical density

The maximum theoretical density (TMD) of the asphalt mixtures was determined to estimate the density of the mixture under conditions where air voids are assumed to be absent. This parameter is fundamental for the evaluation of volumetric characteristics of asphalt mixtures, including air void content and voids in mineral aggregate (VMA). The test procedure followed the requirements specified in [25].

Prior to testing, the loose asphalt mixture was carefully spread on a clean working surface and manually separated in order to break down any agglomerations and ensure a uniform distribution of aggregate particles. After a short cooling period, the material was gently re-mixed and divided into representative portions according to the relevant standard procedure.

Figure 26 Quartering of the loose asphalt [25].

The prepared portions were then placed in calibrated pycnometers with known internal volume. The mass of the pycnometer containing the mixture was first recorded. Subsequently, the vessel was filled with de-aired distilled water and connected to a vacuum system to facilitate the removal of air trapped within the mixture. During this stage, the pycnometer was periodically agitated to enhance the release of entrapped air bubbles. When the air removal process was completed, the pycnometer was filled to the reference level with de-aired water and closed with its cap. The final mass of the pycnometer assembly was then measured, and the temperature of the water inside the vessel was recorded before completing the test.

Figure 27 Pycnometer apparatus used for the determination of the maximum theoretical density

The preparation of the test portion followed the recommendations of [25], which specifies the minimum mass of the test specimen depending on the maximum aggregate size in the mixture. Ensuring a sufficient sample mass improves the reliability of the density measurement and reduces potential experimental errors.

Table 7 Minimum mass of test specimens according to EN 12697-5 [25]

Table H.1 — Minimum mass of test specimens

Upper aggregate size (*D*) mm	Minimum mass of test specimens kg
31,5	1,5
16	1,0
8	0,5
4 (or less)	0,25
For other *D* values, the minimum mass of the test specimen may be interpolated from the masses specified.	

Prior to testing, the pycnometer volume was calibrated using distilled and de-aired water at controlled temperature conditions. The density of water used in the calculations was determined as a function of temperature according to the relationship provided in the standard.

$$\rho_w = 1.00025205 + \left(\frac{7.59 \times t - 5.32 \times t^2}{10^6}\right)$$

Where:

- ρ_W, density of water at temperature t. expressed in g/cm^3;
- t, temperature of the water, expressed in degrees Celsius (°C).

The maximum theoretical density of the mixture was calculated using the volumetric method according to [25] as follows:

$$\rho_{mv} = \frac{(m_2 - m_1)}{10^6 \times V_p - \frac{(m_3 - m_2)}{\rho_w}}$$

Where:

- ρ_{mv}, the maximum density of the bituminous mixture, as determined by the volumetric procedure, in megagrams per cubic meter (Mg/m³) to the nearest 0.001 Mg/m³;
- m_1, the mass of the pycnometer plus head piece and spring, if any, in grams (g);
- m_2, the mass of the pyknometer plus head piece, spring and test sample, in grams (g);
- m_3, the mass of the pyknometer plus head piece, spring, test sample and water or solvent, in grams (g);
- V_p, the volume of the pyknometer, when filled up to the reference mark, in cubic meters (m³);
- ρ_w, the density of water in accordance with the previous equation at the test temperature, in megagrams per cubic meter (Mg/m³) to the nearest 0.0001 Mg/m³.

To verify the consistency of the experimental results, the test was repeated for multiple specimens of the same mixture. The obtained values were then used to calculate the mean maximum theoretical density, the standard deviation, and the coefficient of variation, ensuring that the results satisfied the reproducibility requirements specified by the standard.

The mathematical maximum theoretical density, considering the heterogeneity of the different aggregate fractions, is determined on the basis of the following equation:

$$\rho_{mc} = \frac{100}{\frac{p_{a_1}}{\rho_{a_1}} + \frac{p_{a_2}}{\rho_{a_2}} + \cdots + \frac{p_B}{\rho_B} + \frac{p_r}{\rho_r} + \frac{p_{WP}}{\rho_{WP}}}$$

Where:

- ρ_{mc}, maximum density of the material by calculation, in megagrams per cubic meter (Mg/m³) to the nearest 0.001 Mg/m³;
- p_{a_i}, the percentage of the i-th aggregate approximated to the nearest 0.1 % (by mass);
- ρ_{a_i}, the apparent density of the i-th aggregate, in megagrams per cubic meter (Mg/m³) to the nearest 0.001 Mg/m³;
- p_B, the proportion of binder in the material in percent (%) to the nearest 0.1 % (by mass);
- ρ_B, the density of the binder at 25 °C, in megagrams per cubic meter (Mg/m³) to the nearest 0.001 Mg/m³;
- p_r , the percentage of rejuvenating agent in the mixture, approximated to the nearest 0.1 % (by mass);
- ρ_r, the density of rejuvenating agent in the mixture, in megagrams per cubic meter (Mg/m³) to the nearest 0.001 Mg/m³;

- p_{WP} , the percentage of waste plastics in the mixture, approximated to the nearest 0.1 % (by mass);
- ρ_{WP}, the density of waste plastics, in megagrams per cubic meter (Mg/m³) to the nearest 0.001 Mg/m³.

2.3.4 Determination for the binder content

The binder content of the asphalt mixtures was determined using the ignition furnace method, which is commonly employed to quantify the bitumen content of asphalt mixtures through controlled combustion. This method allows the separation of bitumen from the aggregate skeleton by burning the organic binder at high temperature while leaving the mineral aggregates intact. The test procedure was carried out in accordance with [26].

Figure 28 Ignition furnace used for the determination of binder content

Inside the furnace, the asphalt mixture was exposed to a high temperature of 540 °C, which is sufficient to burn off the bituminous binder. During the combustion process, the organic binder is removed while the mineral aggregates remain inside the metallic basket. The furnace continuously monitors the mass of the sample and determines the mass loss associated with binder combustion.

Prior to placing the sample in the furnace, the empty metallic basket was first weighed. Afterwards, the loose asphalt mixture with a representative portion was prepared in accordance with the recommendations of the standard was evenly distributed inside the basket, and both the net mass of the mixture and the combined mass of the basket and mixture were recorded using a precision balance. The basket containing the mixture was then placed inside the ignition furnace to start the combustion process.

Figure 29 Metallic basket containing the loose asphalt mixture before the ignition test

After completion of the test, the basket containing the remaining aggregates was removed from the furnace and allowed to cool down to room temperature. The final mass of the basket together with the remaining aggregates was then measured again using the precision balance.

Figure 30 Aggregates remaining after binder combustion during the ignition test

The binder content of the mixture was determined based on the difference between the initial mass of the asphalt mixture and the mass of the aggregates remaining after ignition. The calculation was performed using the relationships shown in the below formula, which account for the mass of the mixture before ignition and the mass of the aggregates after the combustion process.

$$B_{\text{mix}} = \frac{m_{mix} - m_{\text{agg}}}{m_{mix}} \times 100$$

$$B_{\text{agg}} = \frac{m_{mix} - m_{\text{agg}}}{m_{agg}} \times 100$$

where:

- B_{mix} , binder content with respect to the total asphalt mixture (%);
- B_{agg}, binder content with respect to the aggregates (%);

- m_{mix}, mass of the asphalt concrete mixture before the ignition test (g);
- m_{agg}, mass of the aggregate fraction remaining after the ignition test (g).

The ignition method represents a reliable and widely used technique for determining the binder content of asphalt mixtures and is commonly applied in laboratory testing and quality control procedures in pavement engineering.

2.3.5 Compaction with SGC

The compaction of asphalt mixtures plays a fundamental role in determining the internal structure of the material and its volumetric characteristics. Proper compaction ensures the development of a stable aggregate skeleton and allows laboratory specimens to reproduce, as closely as possible, the density conditions achieved during field compaction. In this study, the asphalt specimens were compacted using a Superpave Gyratory Compactor (SGC), which is widely adopted in asphalt mixture design and laboratory specimen preparation. The gyratory compactor simulates field compaction by applying a combination of vertical pressure and gyratory motion, producing cylindrical specimens with controlled density and aggregate orientation. The compaction procedure was carried out in accordance with [27], which specifies the equipment requirements and operational parameters for laboratory compaction of asphalt mixtures.

Figure 31 Superpave Gyratory Compactor used for specimen preparation

Compaction in the gyratory compactor is achieved through the combined effect of a constant vertical pressure of approximately 600 kPa and a rotational shearing action applied to the specimen. This shearing mechanism is generated by a slight inclination of the mould (1.25°) with respect to the vertical axis, producing a conical gyratory motion during compaction. The interaction between the vertical load and the inclined rotation promotes a gradual rearrangement of the aggregate particles, allowing the mixture to reach a compacted structure that closely simulates field compaction conditions.

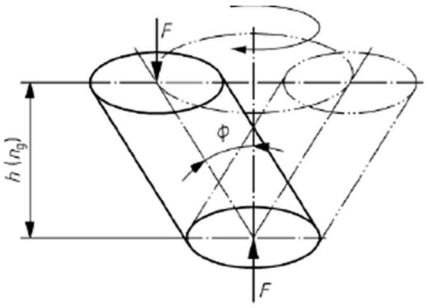

Key

F	axial resultant force
$h\ (n_g)$	height of specimen after a number of gyrations
ϕ	angle

Figure 32 Schematic representation of the gyratory compaction mechanism [27].

In the present experimental program, cylindrical specimens with a diameter of 150 mm were produced. The compaction level was set to 180 gyrations, corresponding to the level typically adopted for base course mixtures according to ANAS specifications [20], in order to obtain specimens representative of field-compacted asphalt layers and to achieve stable and reproducible specimen densities for subsequent volumetric and mechanical testing.

The selection of the number of gyrations is associated with the expected traffic level and structural function of the asphalt layer. Higher gyration numbers simulate higher compaction energy and are typically adopted for mixtures designed for heavier traffic conditions.

Table 8 Reference values for base and binder AC according to ANAS specifications

Variable	Performance class	Number of gyrations	Minimum air voids (%)	Maximum air voids (%)
N1	Low traffic	10	11	15
N2	Medium traffic	100	3	6
N3	High traffic	180	2	6

The compaction process continues until the specified number of gyrations is reached. During this procedure, the gyratory compactor records the evolution of specimen height and compaction effort, allowing the monitoring of mixture densification behavior. After reaching the target number of gyrations, the compacted specimen is removed from the mould and allowed to cool at room temperature before further volumetric and mechanical testing.

2.4 In plant production process

The production of bituminous mixtures for road pavements is carried out in asphalt plants specifically designed to ensure homogeneous mixing of the overall constituents under controlled conditions. Modern

asphalt plants are capable of producing between 100 and 400 ton/h of asphalt mixture depending on the plant configuration and production capacity. Two main plant typologies are commonly adopted in asphalt production: batch plants deal with the indirect production process while drum plants with the direct one. These two configurations differ mainly in the heating system and the sequence in which materials are introduced into the mixing unit.

2.4.1 Indirect process

In a batch plant weighted aggregate fractions, according with the mix design grading curve, are heated and dried in a rotary drying drum, where they reach temperatures typically between 160 °C and 180 °C. The heating is indirect because the aggregates are not mixed with the binder during the heating stage. After drying, the aggregates are transported through a hot elevator to a vibrating screen system where they are separated into different size fractions and weighted for a second time. These fractions are temporarily stored in hot bins. The mixing process then takes place in a pugmill mixer, where the different aggregate fractions are weighed and combined with bitumen, filler and possible additives. Bitumen is usually heated to approximately 150–170 °C before injection into the mixer. The mixing phase generally lasts 30–45 seconds, ensuring complete coating of aggregates by the binder. Once the mixing process is completed, the produced asphalt mixture is transferred to a storage silo before being loaded into trucks for transportation to the construction site.

Batch plants are particularly suitable for laboratory research and specialized asphalt mixtures because they allow precise control of the composition of each production batch.

2.4.2 Direct Process

In drum plants the heating and mixing phases occur within the same rotating drum. Aggregates are introduced through a cold feeder system, which controls the feed rate of each aggregate fraction. Inside the rotating drum, aggregates are dried and heated by direct contact with hot gases generated by the burner. The internal temperature of the drum typically reaches 150–180 °C, allowing efficient moisture removal and heating of aggregates.

Once the aggregates reach the desired temperature, bitumen is injected directly into the drum together with mineral filler and possible additives. The rotation of the drum ensures continuous mixing and coating of aggregates. The residence time inside the drum is generally between 45 and 60 seconds, after which the produced asphalt mixture is discharged and transported to storage silos.

Drum plants are commonly used for high-volume asphalt production, as they allow continuous operation and higher productivity compared with batch plants. The comparison highlights the main operational differences between the indirect and direct processes. In the batch plant, aggregates are first screened and stored in hot bins, and the mixing process is carried out in a separate mixer under controlled conditions. This allows precise control over aggregate gradation and material proportions. In contrast, in the drum plant, bitumen, filler, and additives are injected directly into the rotating drum, where drying and mixing occur simultaneously. As a result, the process is continuous and more efficient, but with less control over mixture composition. These differences mainly affect the mixing mechanism, production

continuity, and level of control, which may influence the final volumetric and mechanical properties of asphalt mixtures.

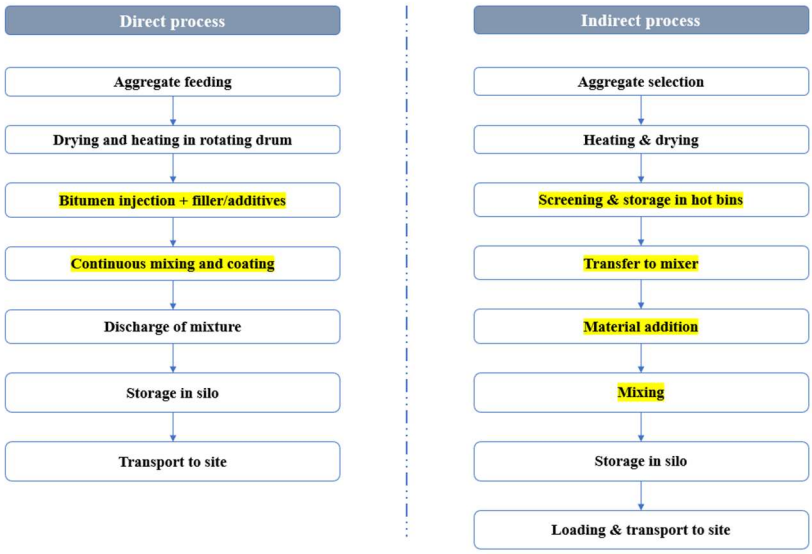

Figure 33 Comparison between direct and indirect processes

2.4.3 Transportation and Laying Operations

After production, the asphalt mixture is transported to the construction site by insulated trucks in order to minimize heat loss during transport. The temperature of the mixture during transportation is typically maintained between 140 °C and 160 °C.

At the construction site, the mixture is placed using an asphalt paver, which distributes the material uniformly across the pavement surface. The paving thickness depends on the layer being constructed, but base layers generally range between 6 and 12 cm.

Following placement, the mixture is compacted using steel or pneumatic rollers to achieve the required density and mechanical performance. Compaction usually begins when the mixture temperature is around 140 °C and continues until it drops to approximately 90 °C.

In December 2025, a site visit to the asphalt production and paving site was conducted in order to observe the laying operations and collect material samples. The observations obtained during this visit helped to better understand the industrial production process and were taken into account when defining the laboratory mixing procedure adopted in this study.

Figure 34 Field observation of asphalt laying operation

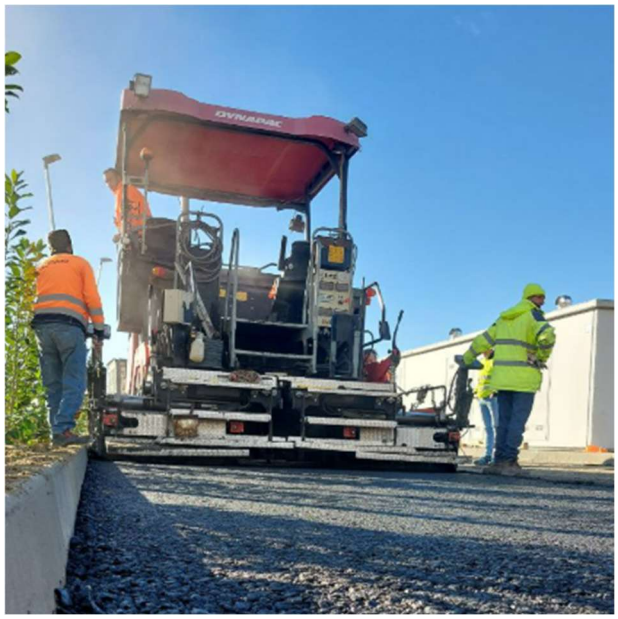

Figure 35 Field observation of asphalt laying operation

2.5 Laboratory testing program

The performance of the asphalt mixtures produced in this study was evaluated through a laboratory testing program aimed at assessing both volumetric and mechanical properties. These tests were selected in order to provide a comprehensive characterization of the mixtures and to verify their suitability for base course applications.

The laboratory testing program was structured to investigate the internal volumetric condition of the compacted specimens as well as their response under mechanical loading. Volumetric testing was performed to determine properties related to specimen density and air void distribution, while mechanical

testing was carried out to evaluate the structural behavior of the mixtures in terms of stiffness and tensile resistance.

All tests were conducted on compacted laboratory specimens prepared according to the procedures described in the previous sections. Depending on the purpose of the test, both sawn and unsawn specimens were considered. The selected laboratory methods were performed in accordance with the relevant European standards for asphalt mixtures, ensuring consistency, reproducibility, and comparability of the experimental results. The testing program included the assessment of volumetric and mechanical properties.

2.5.1 Assessment of volumetric properties on SGC specimens

The volumetric properties of the asphalt mixtures were evaluated in order to characterize the internal structure of the compacted specimens and to determine parameters related to density and air void distribution. These properties are fundamental for understanding the behavior of asphalt mixtures, as they influence mechanical performance, durability, and resistance to deformation.

In the present experimental program, volumetric properties were assessed on both unsawn and sawn specimens. Immediately after the gyratory compaction process, the bulk density of the cylindrical specimens was determined in accordance with [28]. This initial measurement allowed the evaluation of the density of the specimens in their original compacted condition.

Following the determination of bulk density, the compacted cylindrical specimens were cut using a laboratory saw in order to obtain specimens with the appropriate geometry required for subsequent mechanical testing. The cutting process ensured that the samples used for mechanical testing had uniform dimensions and parallel surfaces, which are necessary to obtain reliable test results.

After the cutting procedure, additional measurements were performed on the sawn specimens, including a second determination of bulk density as well as mechanical testing. This approach allowed the comparison of density conditions before and after cutting and ensured that the volumetric characteristics of the specimens were properly considered in the interpretation of mechanical test results.

The combination of volumetric measurements on both unsawn and sawn specimens provided a more accurate assessment of specimen conditions prior to mechanical testing, allowing a consistent evaluation of mixture performance.

Figure 36 Cutting of gyratory-compacted specimens and cut specimens

2.5.2 Bulk density

The bulk density of the asphalt specimens was determined in order to evaluate the compacted density of the mixtures and to provide the basis for the calculation of volumetric parameters such as air voids, VMA, and VFB. The determination of bulk density represents a fundamental step in the volumetric characterization of asphalt mixtures, as it reflects the internal structure of the compacted material.

Measurements were performed in accordance with [28]: Determination of bulk density of bituminous specimens using the saturated surface-dry (SSD) method. This method is widely adopted in asphalt mixture testing as it allows an accurate determination of specimen density through measurements performed in air and in water.In this procedure, each specimen was first dried and weighed in air to determine its dry mass. The specimen was then immersed in water to measure its apparent mass while submerged. Subsequently, the specimen was removed from the water, carefully dried to achieve a saturated surface-dry condition and weighed again.

Figure 37 Asphalt specimen suspended in water for determination of submerged mass [28].

The density of water used in the calculations was determined as a function of the water temperature according to the relationship provided in the standard.

$$\rho_w = 1.00025205 + \left(\frac{7.59t - 5.32t^2}{10^6}\right)$$

Where

- ρ_w is the density of water at temperature t, expressed in g/cm³;
- t is the temperature of the water, expressed in degrees Celsius (°C).

The bulk density of the specimen was then calculated according to the following expression:

$$\rho_{bssd} = \left(\frac{m_1}{\mathrm{m_3 - m_2}}\right) \times \rho_w$$

Where

- ρ_{bssd} is the bulk density (SSD), in megagram per cubic meter (Mg/m³);
- m_1 is the mass of the dry specimen, in gram (g);
- m_2 is the mass of the specimen in water, in gram (g);
- m_3 is the mass of the saturated surface-dried specimen, in gram (g);
- ρ_w is the density of the water at test temperature, in megagram per cubic meter (Mg/m³).

In the present study, the bulk density was determined for both unsawn specimens, immediately after the compaction process, and for sawn specimens obtained after the cutting procedure. The second measurement allowed the verification of the volumetric condition of the specimens prior to the execution of the mechanical tests.

2.5.3 Volumetric parameters

The volumetric properties of asphalt mixtures were evaluated in order to assess the internal structure of the compacted specimens and to verify their compliance with the design requirements. More specifically air voids (Va), voids in mineral aggregate (VMA) and voids filled with bitumen (VFB) were evaluated according to EN 12697-8 [29].

2.5.3.1 Air Void content

Air voids represent one of the most important volumetric parameters for asphalt mixtures, as they describe the amount of air spaces within the compacted mixture, In this study, the air voids content was determined using the SGC at three different compaction levels: 10, 100 and 180 gyrations. These compaction levels correspond to different stages of mixture densification and allow assessment of workability of the various blends. In the present analysis, the following acceptance criteria were considered [20]:

- air voids at 10 gyrations (N_{10}) between 11% and 15%,
- air voids at 100 gyrations (N_{100}) between 3% and 6%,
- air voids at 180 gyrations (N max) greater than 2%.

For 10 and 100 gyrations the evaluations has been carried out through compaction height array recorded by the device and then corrected with bulk density information. Air voids at the maximum number of gyrations were determined using the relationship between the bulk density of the compacted specimen and the maximum theoretical density of the mixture**.**

$$V_a = 100 \times \frac{\rho_{mv} - \rho_b}{\rho_{mv}}$$

Where:

- V_a, is the percentage of voids at N max gyrations;
- ρ_{mv}, is the maximum theoretical density of the mixture (Mg/m^3);
- ρ_b, is the bulk density of compacted specimen (Mg/m^3).

2.5.3.2 Voids in Mineral Aggregate

The Voids in Mineral Aggregate (VMA) represent the intergranular void space between aggregate particles in a compacted asphalt mixture. This void space includes both the air voids and the volume occupied by the binder. VMA is a key parameter in asphalt mix design because it determines the space available for binder within the mixture structure. Adequate VMA ensures sufficient binder content to provide durability while maintaining structural stability.

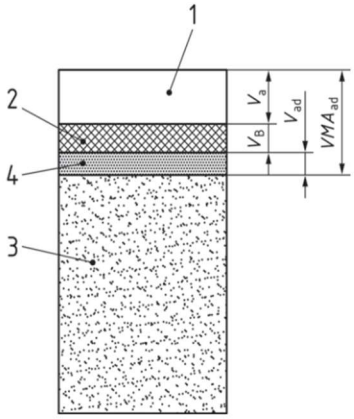

Figure 38 Schematic representation of volumetric components in asphalt mixtures [29]

According to the schematic representation of Figure 38, VMA can be defined as

$$VMA_{ad} = \frac{V_1 + V_2 + V_4}{\sum_{i=1}^{4} V_i} \cdot 100$$

Where 1,2,3 and 4 represents respectively the volumes occupied by air, bitumen, additive and mineral aggregate phases. In the experimental investigation this parameter is calculated according with the following relationship [29]:

$$VMA_{ad} = V_a + \frac{B \times \rho_b}{\rho_B} + \frac{\Sigma_i (P_{ad}, i \times \rho_b)}{\rho_{ad}, i}$$

Where:

- VFB_{ad}, is the percentage of the voids in the mineral aggregate filled with binder and additive in 0.1 % (by volume);
- B, is the percentage of binder in the specimen (in 100 % mixture) in 0.1 % (by mass) and it is obtained from ignition test value subtracting the contributions of plastic and rejuvenator;
- ρ_b is the bulk density of the specimen, in megagram per cubic meter (Mg/m³);
- ρ_B is the density of the binder, in megagram per cubic meter (Mg/m³);
- $P_{ad,i}$ is the percentage of additive *i-th* in the specimen (in 100 % mixture) in 0.1 % (by mass);
- ρ_{ad}, i is the density of the additive *i*, in megagram per cubic meter (Mg/m³);
- VMA_{ad} is the voids content in the mineral aggregate in 0.1 % (by volume) for mixtures containing additives;
- V_a is the air voids content of the specimen in 0.1 % (by volume).

The volumetric parameters calculated through these procedures provide essential information regarding the internal structure of asphalt mixtures and are widely used to verify compliance with mix design specifications and performance requirements. For the interpretation of the results, the limits commonly adopted in the Superpave volumetric mix design specification [32] were used as reference criteria. According to Superpave specifications, mixtures with a nominal maximum aggregate size of 19 mm

should satisfy a minimum VMA value of 13%.

Table 9 Superpave HMA volumetric design requirements [32]

Design ESALs,[a] million	Required Relative Density, Percent of Theoretical Maximum Specific Gravity			Voids in the Mineral Aggregate (VMA), % Minimum						Voids Filled with Asphalt (VFA) Range,[b] %	Dust-to-Binder Ratio Range[c]
				Nominal Maximum Aggregate Size, mm							
	$N_{initial}$	N_{design}	N_{max}	37.5	25.0	19.0	12.5	9.5	4.75		
<0.3	≤91.5	96.0	≤98.0	11.0	12.0	13.0	14.0	15.0	16.0	70–80[d,e]	0.6–1.2
0.3 to <3	≤90.5	96.0	≤98.0	11.0	12.0	13.0	14.0	15.0	16.0	65–78[f]	0.6–1.2
3 to <10	≤89.0	96.0	≤98.0	11.0	12.0	13.0	14.0	15.0	16.0	65–75[e,f,g]	0.6–1.2
10 to <30	≤89.0	96.0	≤98.0	11.0	12.0	13.0	14.0	15.0	16.0	65–75[e,f,g]	0.6–1.2
≥30	≤89.0	96.0	≤98.0	11.0	12.0	13.0	14.0	15.0	16.0	65–75[g]	0.6–1.2

2.5.3.3 Voids Filled with Bitumen

The Voids Filled with Bitumen (VFB) represent the percentage of the VMA that is occupied by bitumen. This parameter indicates how effectively the binder fills the void structure of the aggregate skeleton. High VFB values indicate a greater proportion of binder within the void system, which generally improves durability but may reduce resistance to deformation if excessive. VFB value was calculated, according to [29], using the following relationship:

$$VFB_{ad} = \left(\frac{B \times \rho_b}{\rho_B} + \frac{\Sigma_i\left(P_{ad,i} \times \rho_b\right)}{\rho_{ad,i}}\right) \times \left(\frac{100}{VMA_{ad}}\right)$$

Superpave prescriptions set limitations on VFB values depending on the traffic level (Table 10). For this dissertation 65-75 is considered as the recommended range.

Table 10 Recommended design ranges for VFB [32].

Traffic Level (ESALs)	Design Voids Filled With Asphalt (%)
$<3 \times 10^5$	70 - 80
$<3 \times 10^6$	65 - 78
$<1 \times 10^8$	65 - 75
$> 1 \times 10^8$	65 - 75

2.5.4 Mechanical properties

In order to evaluate the mechanical behavior of the asphalt mixtures, a laboratory testing program was conducted using a Universal Testing Machine (UTM). The mechanical characterization focused on two primary parameters: Indirect Tensile Stiffness Modulus (ITSM), to assess the material's elastic response and Indirect Tensile Strength (ITS), to determine resistance to tensile failure and cracking.

Prior to mechanical testing, the compacted specimens were cut into smaller samples using a laboratory saw in order to obtain specimens with the appropriate geometry for the indirect tensile configuration. Following the cutting procedure, the specimens were subjected to further bulk density measurements before performing the mechanical tests.

Figure 39Universal Testing Machine (UTM) used for the mechanical testing of asphalt specimens.

2.5.4.1 Indirect Tensile Modulus

The mechanical response of the asphalt mixtures was evaluated through the Indirect Tensile Stiffness Modulus (ITSM) test, in accordance with EN 12697-26 (Annex C) [30]. This test quantifies the material's ability to distribute traffic loads and resist elastic deformation under cyclic loading.

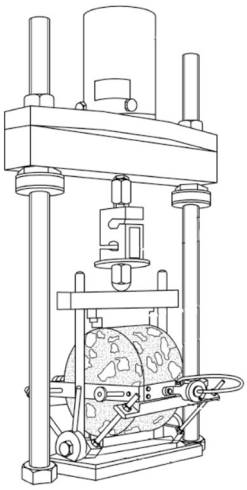

Figure 40 Schematic configuration of the ITSM [30]

In the ITSM test, a cylindrical specimen is subjected to repeated vertical loading along its diametral axis. This loading configuration generates horizontal tensile stresses and strains at the center of the specimen, allowing the stiffness modulus of the mixture to be determined from the relationship between the applied load and the resulting horizontal deformation. Prior to testing, the specimens were conditioned in a temperature-controlled climatic chamber at 25 °C for at least 4 hours to ensure thermal equilibrium.

During the test, cyclic loads were applied through curved loading strips positioned on the upper and lower surfaces of the specimen. The load was applied in the form of haversine loading pulses, as specified in the reference [30]. The horizontal deformation induced by the applied load was measured using displacement transducers mounted on the specimen.

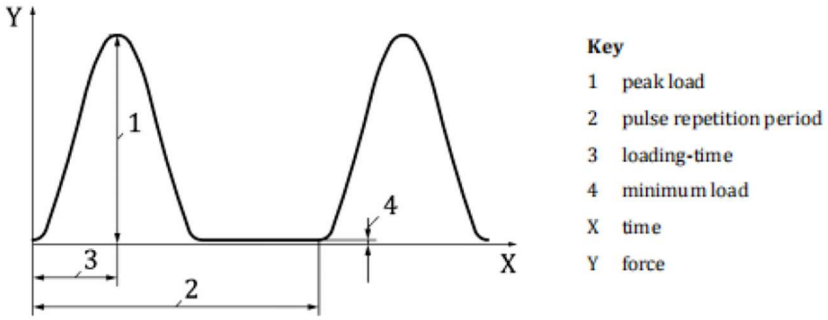

Figure 41 haversine load pulse used during the ITSM test [30]

To ensure elastic behavior and specimen integrity, the horizontal deformation was strictly controlled below a threshold of 9 µm, based on the testing temperature of 25°C. Following initial conditioning pulses to stabilize the material response, measurements were recorded, and the specimen was rotated 90° to verify consistency and isotropy, as required by the standard.

The stiffness modulus was calculated from the relationship between the applied load and the measured horizontal deformation according to the expression proposed by [30].

$$E = \frac{F \times (\nu + 0.27)}{z \times h}$$

Where:

- E, is the stiffness modulus (MPa);
- F, is the applied vertical load (N);
- z, is the horizontal deformation (mm);
- h, is the average specimen thickness (mm);
- ν, is the Poisson's ratio, usually assumed equal to 0.35.

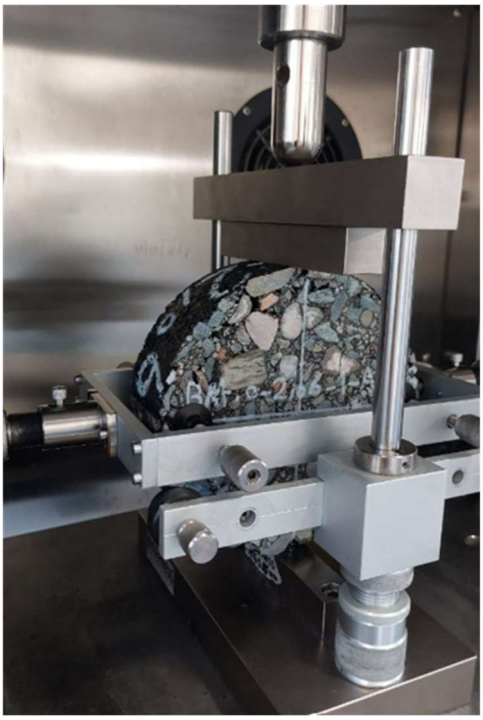

Figure 42 Experimental setup for the ITSM test [30]

2.5.4.2 Indirect Tensile Strength

The tensile strength of asphalt mixtures was evaluated using the Indirect Tensile Strength (ITS) test, which provides an indication of the resistance of asphalt materials to cracking under tensile stresses. Tensile stresses play a critical role in asphalt pavements, particularly in the lower layers of the asphalt structure where fatigue cracking may initiate due to repeated traffic loading.

The test was carried out in accordance with [31], which specifies the procedure for determining the indirect tensile strength of cylindrical bituminous specimens. In this test configuration, a cylindrical asphalt specimen is placed between two curved steel loading strips and subjected to a vertical compressive load applied along the vertical diametral plane.

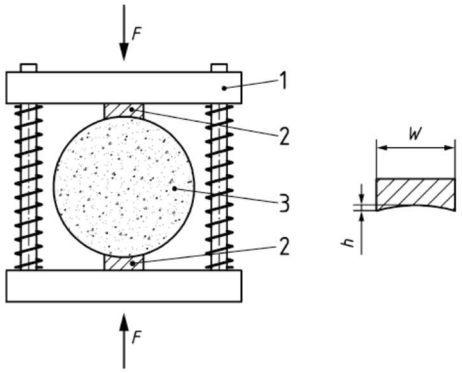

Figure 43 Schematic representation of the ITS test configuration [31]

Although the applied load is compressive, the stress distribution generated within the specimen produces tensile stresses perpendicular to the loading direction. The maximum tensile stress develops at the center

of the specimen, and failure occurs when this tensile stress exceeds the tensile strength of the asphalt mixture. Prior to testing, the specimens were conditioned at the target test temperature to ensure a uniform temperature distribution within the material. In this study, the tests were performed at a temperature of 25°C, which is commonly used as a reference temperature for the mechanical characterization of asphalt mixtures.

The specimens were positioned inside the UTM device, where the load was applied through curved loading strips to ensure a uniform stress distribution along the loading line. The vertical load was applied continuously at a constant displacement rate of 50 mm/min until failure occurred. During the test, the applied load and the corresponding vertical displacement were continuously recorded by the data acquisition system. The maximum load reached at failure (peak load) was used for the calculation of the indirect tensile strength.

The indirect tensile strength was calculated using the following expression:

$$ITS = \frac{2P}{\pi DH}$$

Where

- ITS, indirect tensile strength (MPa);
- P is the maximum applied load at failure (N);
- D is the average specimen diameter (mm);
- H is the average specimen high (mm).

After testing, the specimens typically exhibited a diametral failure pattern, which is characteristic of the ITS test. This failure mode confirms that tensile stresses were correctly generated within the specimen during loading.

Figure 44 Failure pattern after the ITS test: (L) diametral crack; (R) fracture surfaces along the loading diameter.

The ITS test provides an important indicator of the cracking resistance of asphalt mixtures and is widely

used for evaluating mixture quality, aggregate–binder adhesion, and the susceptibility of asphalt mixtures to cracking. The results of this test complement the stiffness modulus measurements presented in the previous section.

3 Experimental results and discussion

3.1 Mixture coding

The experimental campaign included the production and characterization of several bituminous mixtures designed for the base layer of flexible pavements. In order to track the different mixtures produced during the laboratory activities and to keep the experimental results organized, a specific identification code was adopted. This coding system summarizes the main characteristics of each mixture identifying the main specification variables., including the mixing procedure, the percentage of waste plastic incorporated in the mix, the amount of neat bitumen referred to aggregates and RAP weight, and the main production parameters like the aggregate skeleton and the thermal protocol followed.

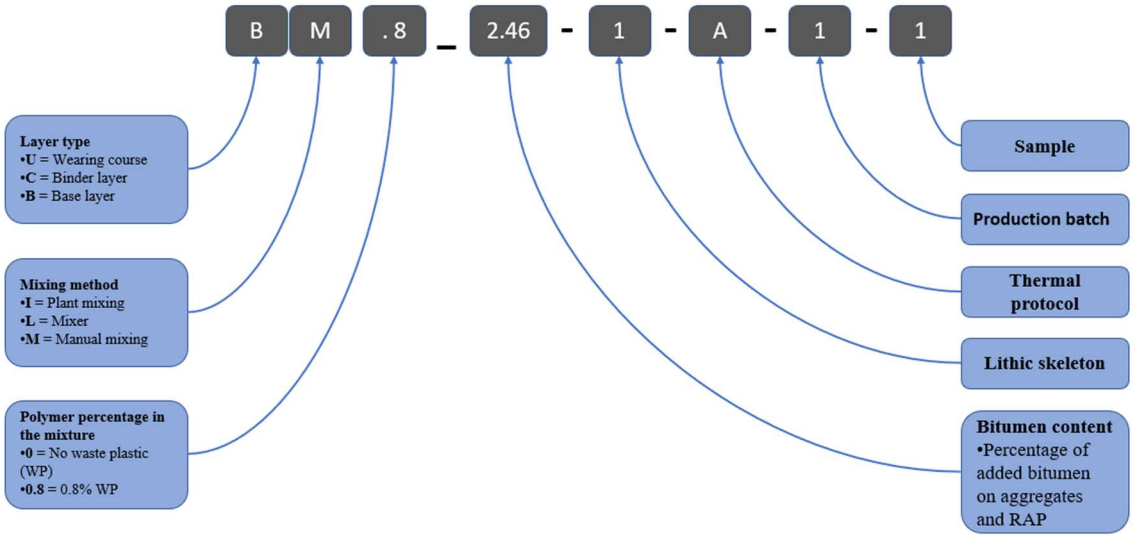

Figure 45 Identification system adopted for the produced mixtures

The value reported in the fourth field corresponds to the percentage of neat bitumen added to the aggregate–RAP blend, indicated as BA.A. This parameter represents the additional binder introduced during the production process. Another parameter used in the analysis is B.M, which represents the total binder content in the mixture, including both the binder coming from RAP and the added neat bitumen. The following fields of the code describe the aggregate skeleton configuration, the thermal protocol adopted during mixing, the production batch, and the sample replicate. This identification system allows each specimen to be uniquely traced throughout the experimental program.

3.2 Outcomes of laboratory mixtures

The experimental matrix comprises various asphalt mixtures categorized by mixing methodology, recycled plastic content, and binder dosage. Table 11 details the laboratory – produced specimens based on the following key parameters:

- WP.M, is the waste plastic content in the mixture;
- BA. A, is the dosage of neat bitumen added to the mineral aggregates;
- BM.M, is the total binder content, incorporating both added bitumen and residual one from the RAP.
- BWPR.M, is the equivalent binder phase, calculated under the assumption that 50% of the recycled plastic acts as a partial bitumen replacement.

Table 11 Summary of the mixtures produced in laboratory

Mix ID	WP.M	BA.A	B.M	REJ.M	BWPR.M
BM.0_2.06-1-A-1	0.00	2.06	3.76	0.07	3.83
BM.0_2.06-1-A-2	0.00	2.06	3.76	0.07	3.83
BM.0_2.46-1-A-1	0.00	2.46	4.13	0.07	4.20
BM.0_2.46-1-A-2	0.00	2.46	4.13	0.07	4.20
BM.0_2.71-1-A-1	0.00	2.71	4.37	0.07	4.43
BM.0_3.10-1-A-1	0.00	3.10	4.73	0.07	4.80
BM.8_2.06-1-A-1	0.80	2.06	3.73	0.07	4.20
BL.8_2.06-1-A-1	0.80	2.06	3.73	0.07	4.20
BM.8_2.46-1-A-1	0.80	2.46	4.10	0.07	4.57
BM.8_2.71-1-A-1	0.80	2.71	4.33	0.07	4.80

The previous table provides an aggregated overview of the experimental activity and can be expanded to include all individual specimens produced. Table 12 reports the complete list of specimens, categorized by their respective mix designs. As indicated in the "Analysis Status", certain specimens were included in the primary analysis, whereas others were excluded after being identified as outliers during the data processing stage because of their inconsistency between theoretical and experimental outcomes.

Table 12 Main characteristics of the lab-produced mixtures

Test ID	WP.M (%)	BA.A (%)	B.M (%)	REJ.M (%)	BWPR.M (%)	TBP (%)	EBP (%)	TMD (Mat)	TMD (Exp)	Analysis Status
BL.8_2.06-1-A-1-1	0.80	2.06	3.73	0.07	4.20	4.43	4.49	2.585	2.588	Excluded
BL.8_2.06-1-A-1-2	0.80	2.06	3.73	0.07	4.20	4.43	4.49	2.585	2.588	Excluded
BL.8_2.06-1-A-1-3	0.80	2.06	3.73	0.07	4.20	4.43	4.49	2.585	2.588	Excluded
BL.8_2.06-1-A-1-4	0.80	2.06	3.73	0.07	4.20	4.43	4.49	2.585	2.588	Excluded
BM.0_2.06-1-A-1-1	0.00	2.06	3.76	0.07	3.83	3.83	3.88	2.609	2.609	Excluded
BM.0_2.06-1-A-2-1	0.00	2.06	3.76	0.07	3.83	3.83	3.49	2.609	2.565	Included
BM.0_2.06-1-A-2-2	0.00	2.06	3.76	0.07	3.83	3.83	3.49	2.609	2.565	Included
BM.0_2.06-1-A-2-3	0.00	2.06	3.76	0.07	3.83	3.83	3.49	2.609	2.565	Included
BM.0_2.46-1-A-1-1	0.00	2.46	4.13	0.07	4.20	4.20	3.45	2.592	2.606	Excluded
BM.0_2.46-1-A-1-2	0.00	2.46	4.13	0.07	4.20	4.20	3.45	2.592	2.606	Included
BM.0_2.46-1-A-1-3	0.00	2.46	4.13	0.07	4.20	4.20	3.45	2.592	2.606	Excluded
BM.0_2.46-1-A-2-1	0.00	2.46	4.13	0.07	4.20	4.20	3.45	2.592	2.610	Excluded

BM.0_2.46-1-A-2-2	0.00	2.46	4.13	0.07	4.20	4.20	3.45	2.592	2.610	Excluded
BM.0_2.71-1-A-1-1	0.00	2.71	4.37	0.07	4.43	4.43	3.94	2.587	2.604	Included
BM.0_2.71-1-A-1-2	0.00	2.71	4.37	0.07	4.43	4.43	3.94	2.587	2.604	Included
BM.0_2.71-1-A-1-3	0.00	2.71	4.37	0.07	4.43	4.43	3.94	2.587	2.604	Excluded
BM.0_2.71-1-A-1-4	0.00	2.71	4.37	0.07	4.43	4.43	3.94	2.587	2.604	Included
BM.0_3.10-1-A-1-1	0.00	3.10	4.73	0.07	4.80	4.80	4.80	2.571	2.569	Included
BM.0_3.10-1-A-1-2	0.00	3.10	4.73	0.07	4.80	4.80	4.80	2.571	2.569	Included
BM.0_3.10-1-A-1-3	0.00	3.10	4.73	0.07	4.80	4.80	4.80	2.571	2.569	Excluded
BM.8_2.06-1-A-1-1	0.80	2.06	3.73	0.07	4.20	4.43	4.38	2.585	2.579	Included
BM.8_2.06-1-A-1-2	0.80	2.06	3.73	0.07	4.20	4.43	4.38	2.585	2.579	Excluded
BM.8_2.46-1-A-1-1	0.80	2.46	4.10	0.07	4.57	4.80	4.61	2.569	2.569	Included
BM.8_2.46-1-A-1-2	0.80	2.46	4.10	0.07	4.57	4.80	4.61	2.569	2.569	Excluded
BM.8_2.46-1-A-1-3	0.80	2.46	4.10	0.07	4.57	4.80	4.61	2.569	2.569	Included
BM.8_2.71-1-A-1-1	0.80	2.71	4.33	0.07	4.80	5.03	4.97	2.561	2.568	Included
BM.8_2.71-1-A-1-2	0.80	2.71	4.33	0.07	4.80	5.03	4.97	2.561	2.568	Excluded
BM.8_2.71-1-A-1-3	0.80	2.71	4.33	0.07	4.80	5.03	4.97	2.561	2.568	Included

3.2.1 Composition and morphology of laboratory mixtures

3.2.1.1 Maximum theoretical density

For each mixture the maximum theoretical density was determined experimentally and compared with the theoretical value obtained during the mix design phase. This comparison is important in order to verify the consistency of the experimental measurements and to ensure the reliability of the volumetric calculations.

Table 13 Comparison between theoretical and experimental MMVT values

Mix ID	Theoretical TMD [g/cm³]	Experimental TMD [g/cm³]	Experimental - theoretical difference
BL.8_2.06-1-A-1	2.585	2.588	-0.003
BM.0_2.06-1-A-2	2.609	2.565	0.044
BM.0_2.46-1-A-1	2.592	2.606	-0.014
BM.0_2.46-1-A-2	2.592	2.610	-0.018
BM.0_2.71-1-A-1	2.587	2.604	-0.017
BM.0_3.10-1-A-1	2.571	2.569	0.002
BM.8_2.06-1-A-1	2.585	2.579	0.006
BM.8_2.71-1-A-1	2.561	2.568	-0.007

Table 13 and Figure 46 demonstrate strong alignment between experimental and theoretical values. The data points cluster closely along the equality line, validating the reliability of the maximum theoretical density determination and the consistency of the subsequent volumetric analysis. Minimal dispersion across the investigated mixtures indicates high repeatability. However, mixture BM.0_2.06-1-A-2, depicted as black dot, was excluded as an outlier due to sampling inconsistencies. Furthermore, standard deviations are omitted for two mixtures where experimental TMD testing was not performed.

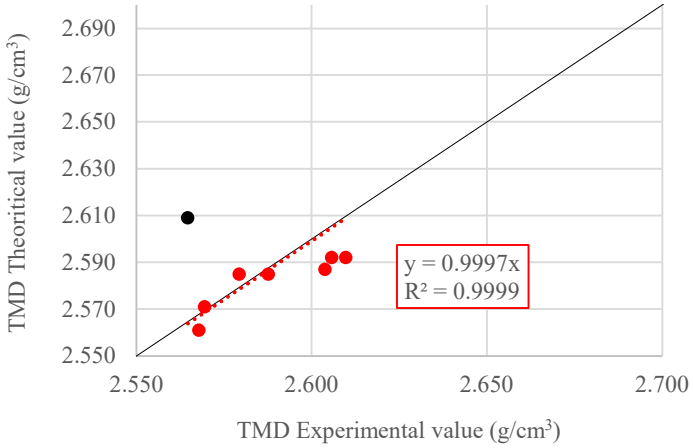

Figure 46 Comparison between theoretical and experimental values.

3.2.1.2 Gradation curves and statistical analysis

The gradation curves of the aggregate blends used in the experimental mixtures were then compared with the design grading curve in order to verify the consistency of the aggregate skeleton adopted during mixture preparation.

Table 14 Gradation values of the investigated mixtures

Sieve size (mm)	BM.8_2.46-1-A-1	BM.8_2.06-1-A-1	BM.0_2.71-1-A-1	BM.0_2.06-1-A-1	BM.0_2.46-1-A-2	BM.8_2.71-1-A-1	BL.8_2.06-1-A-1	BM.0_2.06-1-A-2	BM.0_2.46-1-A-1	BM.0_3.10-1-A-1
32	100.0	100.0	100.00	100.0	100.00	100.0	100.0	100.0	100.00	100.00
20	97.1	97.9	100.00	96.6	98.88	99.0	96.8	100.0	93.67	100.00
16	85.0	83.0	82.70	84.7	78.12	91.1	81.3	84.0	79.41	89.24
8	44.3	43.5	39.17	47.8	40.53	49.9	48.7	41.8	34.78	49.65
4	31.5	31.9	28.67	35.2	27.54	36.4	36.4	29.1	23.94	35.71
2	23.0	22.9	19.64	25.9	17.89	25.3	25.7	18.7	16.63	22.90
0.5	13.8	13.3	10.72	15.2	10.26	14.6	15.8	10.5	9.99	12.60
0.25	10.7	10.2	8.39	11.5	8.08	11.2	13.1	8.3	7.92	9.57
0.063	6.3	6.0	5.25	6.6	5.07	7.0	8.7	5.4	4.99	5.98

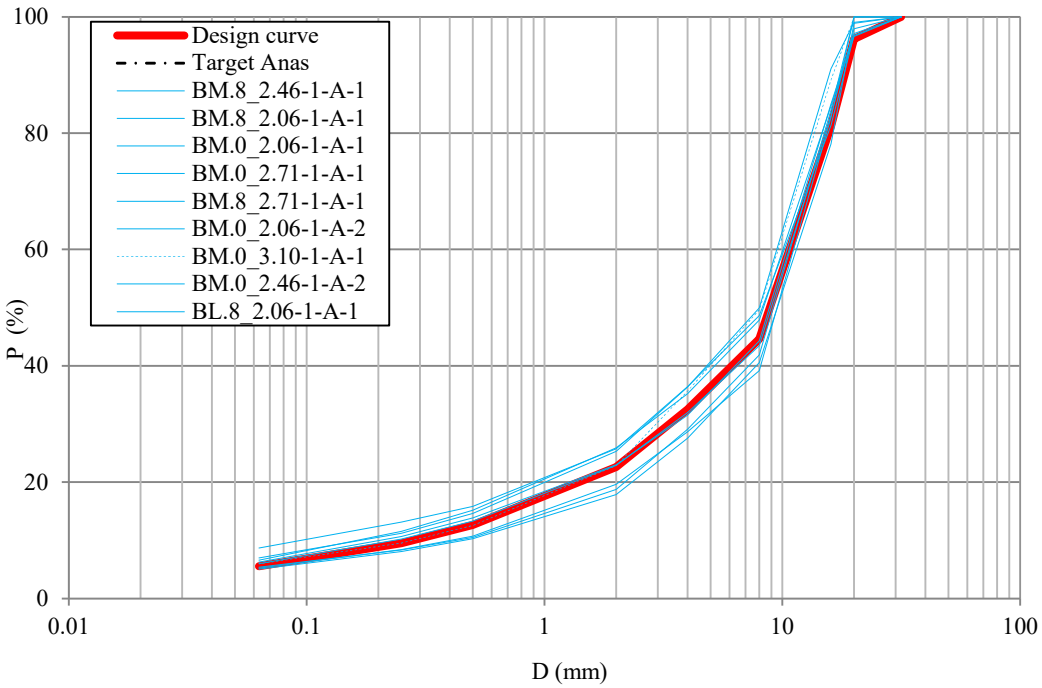

Figure 47 Gradation curves of the investigated mixtures compared with the design curve

As shown in Figure 47, the grading curves of the produced mixtures remain generally close to the design curve and fall within the specification limits for D<16.0 mm. Small deviations can be observed at some sieve sizes, mainly in the intermediate fractions, which is expected due to the variability associated with the preparation of the aggregate blends. However, these differences remain limited and do not significantly alter the overall grading structure of the mixtures. Therefore, the aggregate skeleton can be considered consistent across the investigated mixtures. To evaluate the consistency of the aggregate blends with respect to the target grading curve, a statistical analysis of the sieve passing values was performed. For each sieve size, the average passing value, standard deviation σ and the 2σ interval were calculated based on the available gradation data of the investigated mixtures.

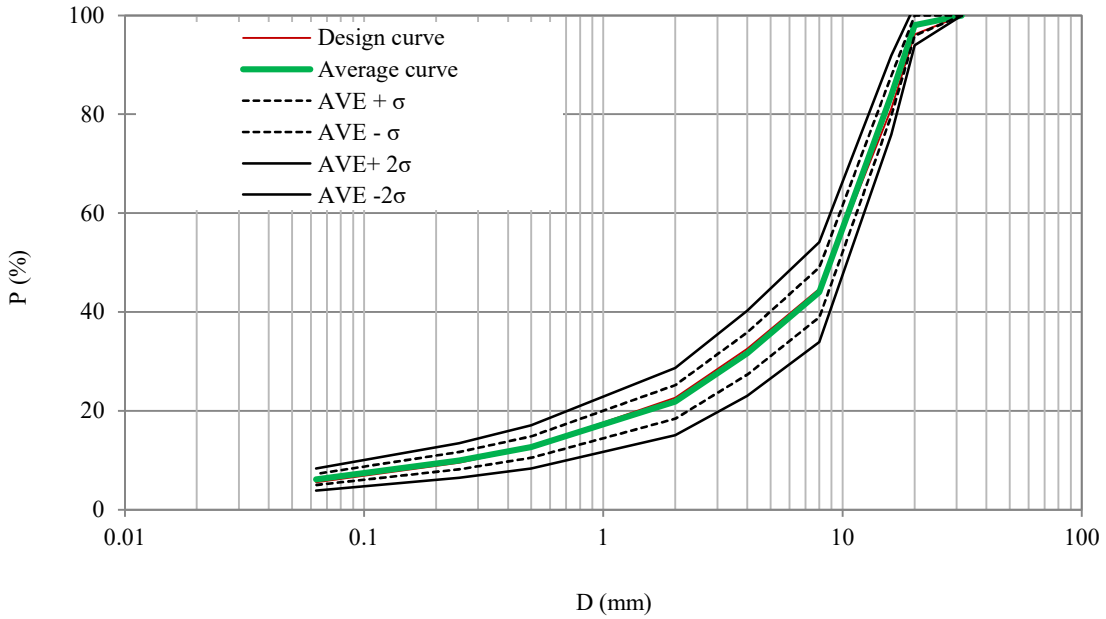

Figure 48 Design and average gradation curves with variability bands (±σ and ±2σ)

As indicated in Table 15 Difference between the passing values of the produced mixtures and the design curve for each sieve size., the variance between the average percentage passing and the target specifications remains negligible across the entire sieve spectrum. In every instance, the observed deviations are situated within the primary standard deviation interval, with all data points further contained within the 2σ threshold. This statistical alignment confirms that the grading variability is strictly controlled and falls within acceptable tolerance limits.

In order to further evaluate the agreement between the experimental gradations and the target gradation curve, the difference between the passing values of each mixture and the corresponding values of the target gradation curve was calculated for each sieve size. This comparison allows a clearer assessment of how closely the produced mixtures follow the design gradation.

Table 15 Difference between the passing values of the produced mixtures and the design curve for each sieve size.

Sieve size (mm)	BM.8_2.46-1-A-1	BM.8_2.06-1-A-1	BM.0_2.71-1-A-1	BM.0_2.06-1-A-1	BM.8_2.06-1-A-1	BM.8_2.71-1-A-1	BL.8_2.06-1-A-1	BM.0_2.06-1-A-2	BM.0_2.46-1-A-1	BM.0_3.10-1-A-1
32	0.0	0.0	0.00	0.0	0.0	0.0	0.0	0.0	0.00	0.00
20	0.9	1.8	3.81	0.4	1.8	2.8	0.6	3.8	-2.52	3.81
16	3.9	1.9	1.56	3.5	1.9	9.9	0.2	2.8	-1.74	8.10
8	-0.3	-1.2	-5.46	3.2	-1.2	5.3	4.0	-2.8	-9.85	5.02
4	-1.0	-0.6	-3.85	2.7	-0.6	3.9	3.9	-3.4	-8.58	3.18
2	0.4	0.3	-2.98	3.3	0.3	2.7	3.1	-3.9	-5.98	0.28
0.5	1.2	0.7	-1.89	2.6	0.7	2.0	3.2	-2.1	-2.63	-0.02
0.25	1.2	0.7	-1.09	2.1	0.7	1.7	3.6	-1.1	-1.55	0.10
0.063	0.7	0.4	-0.30	1.1	0.4	1.5	3.1	-0.1	-0.56	0.43

In Table 15 black values indicate differences between −5 and +5 with respect to the target gradation curve, while red ones represent differences outside this range. Most mixtures exhibit differences within the −5 to +5 range for the majority of sieve sizes, indicating a generally good agreement between the experimental gradations and the design gradation curve. This suggests that the aggregate skeleton of the mixtures was reproduced with satisfactory accuracy during the production process. Larger differences are mainly observed in a limited number of mixtures and sieve sizes, particularly in some intermediate and finer fractions, where small variations in material proportions may produce more noticeable differences in the passing values.

3.2.1.3 Comparison between Total Binder Phase and Effective Binder Phase

In asphalt mixture design, the specified Total Binder Phase (TBP) often differs from the Effective Binder Phase (EBP) due to aggregate absorption, binder content variability in RAP, and the presence of modifiers. Table 16 presents a comparison between these two variables, utilizing the ignition test to measure the experimental EBP. The results indicate a high degree of consistency, with most mixtures exhibiting negligible deviations. To facilitate analysis, differences were categorized by magnitude: values below 0.5% (shown in black) represent excellent agreement, while those reaching or exceeding 0.5% (in red) indicate minor discrepancies. Despite these localized variations, the differences remain limited across all specimens. This correlation is further substantiated by the control chart in Figure 49 Control chart comparing total binder phase and effective binder phase, which displays a clear linear relationship between TBP and EBP. The high coefficient of determination confirms a robust statistical agreement with the linear model, validating that the produced mixtures accurately reflect the intended design binder content.

Table 16 Comparison between total binder phase (TBP) and effective binder phase (EBP)

Mix ID	TBP (%)	EBP (%)	Difference between TPB and EBP (%)
BL.8_2.06-1-A-1	4.43	4.490	-0.1
BM.0_2.06-1-A-1	3.83	3.88	0.0
BM.0_2.06-1-A-2	3.83	3.490	0.3
BM.0_2.46-1-A-1	4.20	3.450	0.8
BM.0_2.46-1-A-2	4.20	3.450	0.8
BM.0_2.71-1-A-1	4.43	3.940	0.5
BM.0_3.10-1-A-1	4.80	4.800	0.0
BM.8_2.06-1-A-1	4.43	4.380	0.0
BM.8_2.46-1-A-1	4.8	4.61	0.2
BM.8_2.71-1-A-1	5.03	4.970	0.1

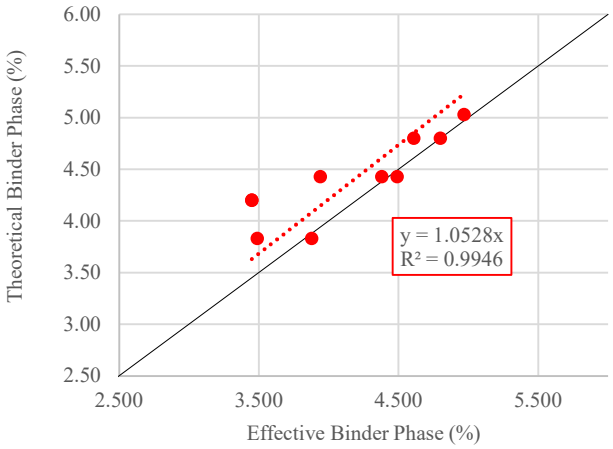

Figure 49 Control chart comparing total binder phase and effective binder phase

3.2.2 Volumetric properties of laboratory mixtures

3.2.2.1 Air void contents

In Table 17 are summarized voids at different gyrations for the mixtures included in the analysis. The values in red do not comply with the design requirements.

Table 17 Air voids values measured at different gyration levels for the mixtures included in the analysis

Mixture ID	10 GYR	100 GYR	180 GYR
BM.0_2.06-1-A-2-1	15.35	6.31	4.49
BM.0_2.06-1-A-2-2	15.32	6.24	4.32
BM.0_2.06-1-A-2-3	14.57	5.47	3.58
BM.0_2.46-1-A-1-2	15.24	5.90	4.96
BM.0_2.71-1-A-1-1	15.01	6.05	4.23
BM.0_2.71-1-A-1-2	14.76	6.21	4.31
BM.0_2.71-1-A-1-4	14.81	6.13	4.34
BM.0_3.10-1-A-1-1	13.45	3.90	1.92
BM.0_3.10-1-A-1-2	13.21	4.00	2.10
BM.8_2.06-1-A-1-1	14.41	5.48	3.57
BM.8_2.46-1-A-1-1	13.36	4.70	3.03
BM.8_2.46-1-A-1-3	13.86	5.31	3.52
BM.8_2.71-1-A-1-1	12.52	4.01	2.48
BM.8_2.71-1-A-1-3	12.25	4.20	2.48

To better understand the relationship between air voids and binder-related parameters, percentage of air voids at 10, 100 and 180 gyrations are plotted as a function of neat bitumen content (BA. A), total binder content in the mixture (B.M) and binder phase with 50% waste plastics acting as bitumen (BWPR.M).

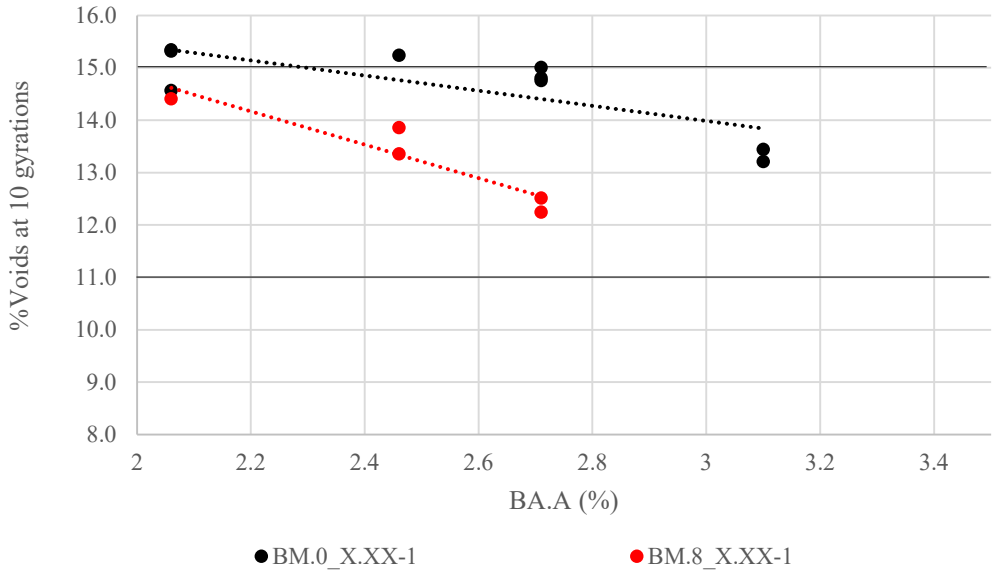

Figure 50 Air voids versus added bitumen content BA. A at 10 gyration levels

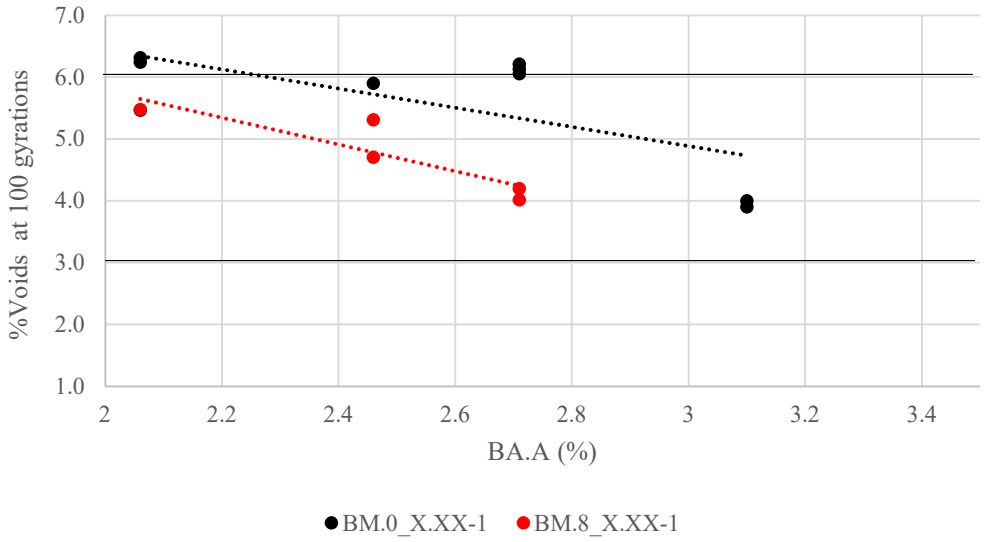

Figure 51 Air voids versus added bitumen content BA. A at 100 gyration levels

As expected, the air voids generally decrease with increasing binder content, since a higher amount of binder promotes a more effective filling of the void spaces between aggregates. This behavior is observed at all compaction levels, although it becomes more evident at higher gyration numbers, where the mixtures reach a more compact structure. A consistent regression trend is observed for both the control and the 0.8% waste plastic mixtures. Notably, the plastic-modified blends yield lower air void contents, suggesting that the polymer acts as an additional binding component that enhances void filling (Figure 50 and Figure 51).

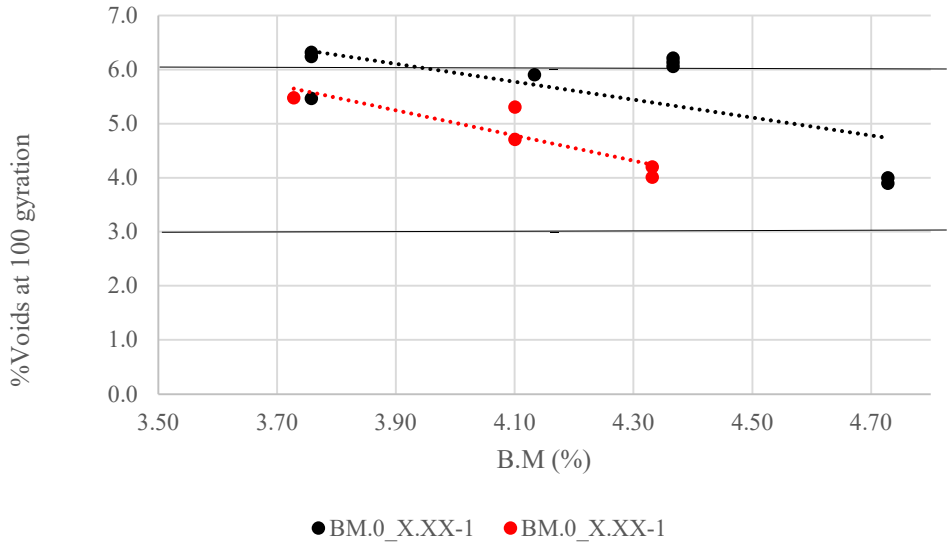

Figure 52 Air voids versus total binder content in the mixture (B.M) at 100 gyration

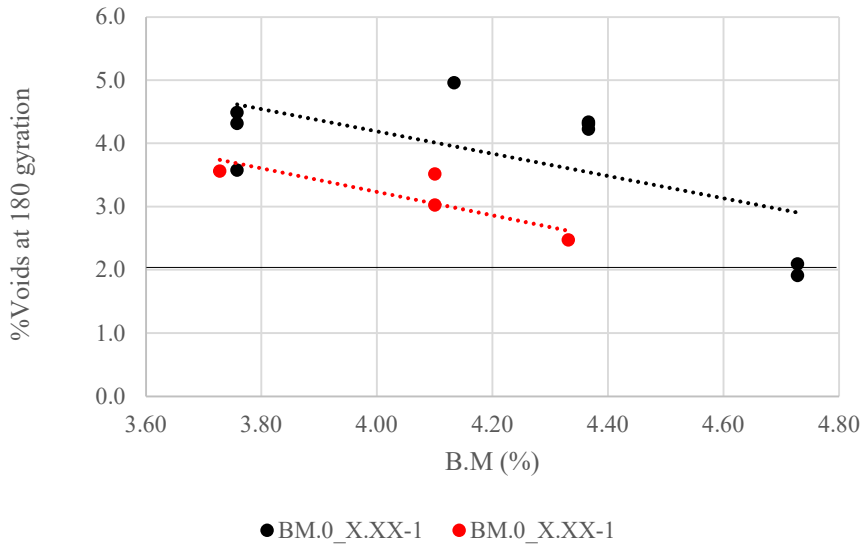

Figure 53 Air voids versus total binder content in the mixture (B.M) at 180 gyration

The volumetric analysis in the B.M domain reveals a characteristic horizontal shift among experimental data sharing the same BA. A, primarily driven by the repartition of total binder and its distribution within the mixture. The results show that, as the total binder content increases, the air voids tend to decrease, confirming what it has been observed with the previous plots: the air void values generally remain within the upper and lower reference limits for the considered gyration levels, indicating an overall satisfactory volumetric behavior of the investigated mixtures (Figure 52 and Figure 53).

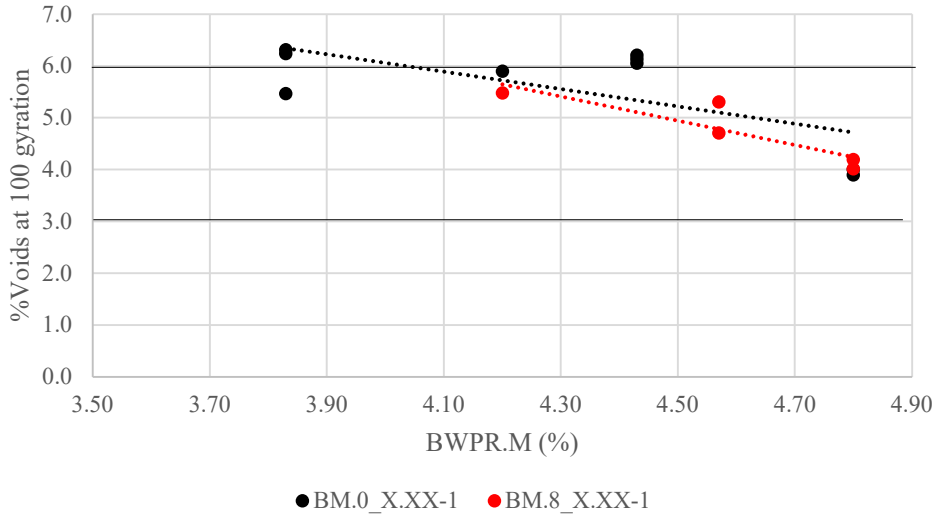

Figure 54 Air voids versus effective binder content considering waste plastic (BWPR.M) at 100 gyration level

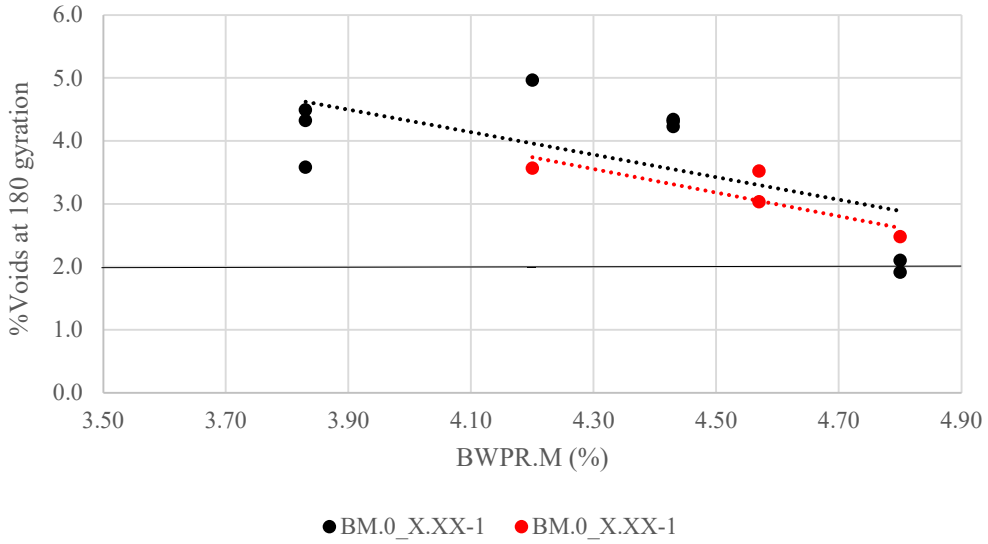

Figure 55 Air voids versus effective binder content considering waste plastic (BWPR.M) at 180 gyration level

Analyzing air voids relative to the effective binder content reveals a persistent decreasing trend as the total binder phase increases, with regression lines for the modified and control mixtures showing significant alignment. Notably, the plastic-modified mixtures exhibit slightly lower air void contents (Figure 54 and Figure 55). This divergence is attributed to the higher density of the polymer compared to bitumen; the partial mass substitution results in a lower volume of binder phase, yet the mineral aggregate skeleton accommodates the polymer more effectively. This suggests that the inclusion of waste plastic enhances compaction efficiency, allowing for a more densely packed aggregate matrix without compromising the overall volumetric structure of the mixture.

3.2.2.2 Voids in Mineral Aggregate (VMA)

The volumetric parameters obtained for the investigated mixtures are reported in the below Table 18. In accordance with Superpave specifications, the mixtures maintains a minimum VMA of 13.0% for 19 mm NMAS. The values satisfying this MSL are highlighted in black, while the values outside the acceptable ranges are indicated in red.

Table 18 Summary of VMA and VFB obtained for all the tested specimens

Test ID	WP.M	BA. A	B.M	BWPR.M	VMA
BM.0_2.06-1-A-2-1	0.0	2.06	3.76	3.83	12.9
BM.0_2.06-1-A-2-2	0.0	2.06	3.76	3.83	12.7
BM.0_2.06-1-A-2-3	0.0	2.06	3.76	3.83	12.1
BM.0_2.46-1-A-1-2	0.0	2.46	4.13	4.2	13.5
BM.0_2.71-1-A-1-1	0.0	2.71	4.37	4.43	14
BM.0_2.71-1-A-1-2	0.0	2.71	4.37	4.43	14.1
BM.0_2.71-1-A-1-4	0.0	2.71	4.37	4.43	14.2
BM.0_3.10-1-A-1-1	0.0	3.1	4.73	4.8	13.8
BM.0_3.10-1-A-1-2	0.0	3.1	4.73	4.8	14
BM.8_2.06-1-A-1-1	0.8	2.06	3.73	4.2	14.6
BM.8_2.46-1-A-1-1	0.8	2.46	4.10	4.57	14.5
BM.8_2.46-1-A-1-3	0.8	2.46	4.10	4.57	14.9
BM.8_2.71-1-A-1-1	0.8	2.71	4.33	4.8	15
BM.8_2.71-1-A-1-2	0.8	2.71	4.33	4.8	15.6

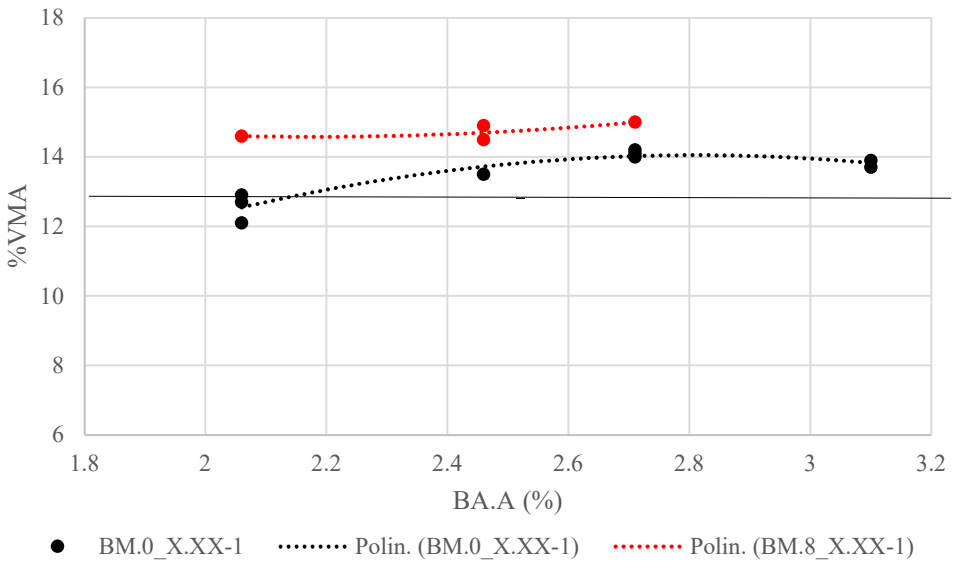

Figure 56 VMA in the BA.A domain

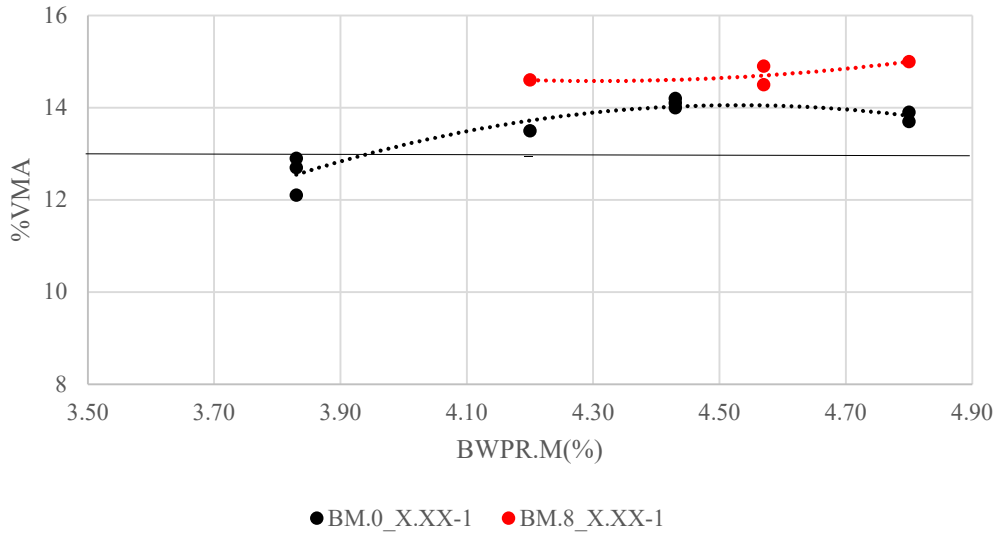

Figure 57 VMA as a function of effective binder content considering waste plastic (BWPR.M)

As illustrated in the figures, most of the mixtures exhibit VMA values exceeding the minimum specification limit, indicating that the aggregate skeleton provides sufficient void space to accommodate the binder phase, except for 2.06% neat bitumen blends. While the control mixtures show an atypical VMA trend in both considered domains, the modified ones follow the theoretical U-shaped behavior. This suggests that increasing the bitumen content toward 2.46% initially reduces VMA by lubricating the aggregates and promoting a more efficient packing; beyond this threshold (2.46% to 2.71%), the binder begins acting as spacer, increasing VMA.

In the BA.A domain, the 0.8% waste plastic content clearly increase VMA. This suggests that the plastic, by increasing the specific surface area of granular fraction, reduces the effective coating and lubrication of the aggregates. Notably, this does not result in higher air voids, as documented in previous part, because the aggregate skeleton remains adequate to accommodate plastic particles. When viewed in the effective binder domain (Figure 57), the discrepancy between the two curves diminishes, leading to the conclusion that the plastic undergoes partially melting during the process.

3.2.2.3 Voids Filled with Bitumen (VFB)

The VFB values of the analysed mixtures are reported in Table 19 in which red values do not comply with specifications. The relationship between VFB and binder-related parameters demonstrates that this parameter increases proportionally with the binder concentration as the bituminous phase progressively saturates the VMA. Both the control and the 0.8% waste plastic mixtures exhibit consistent regression trends, suggesting that the polymer inclusion does not fundamentally alter the void-filling mechanism. The mixtures containing 0.8% waste plastic tend to show slightly higher VFB values, which is consistent with the additional effective binding contribution introduced in the mixture.

Table 19 VFB values of the mixtures

Specimen ID	VFB (%)
BM.0_2.06-1-A-2-1	65.1
BM.0_2.06-1-A-2-2	66.3
BM.0_2.06-1-A-2-3	70.1
BM.0_2.46-1-A-1-2	62.9
BM.0_2.71-1-A-1-1	69.8
BM.0_2.71-1-A-1-2	69.3
BM.0_2.71-1-A-1-4	68.7
BM.0_3.10-1-A-1-1	85.8
BM.0_3.10-1-A-1-2	84.4
BM.8_2.06-1-A-1-1	75.1
BM.8_2.46-1-A-1-1	79.1
BM.8_2.46-1-A-1-3	76.6
BM.8_2.71-1-A-1-1	83.4
BM.8_2.71-1-A-1-2	79.6

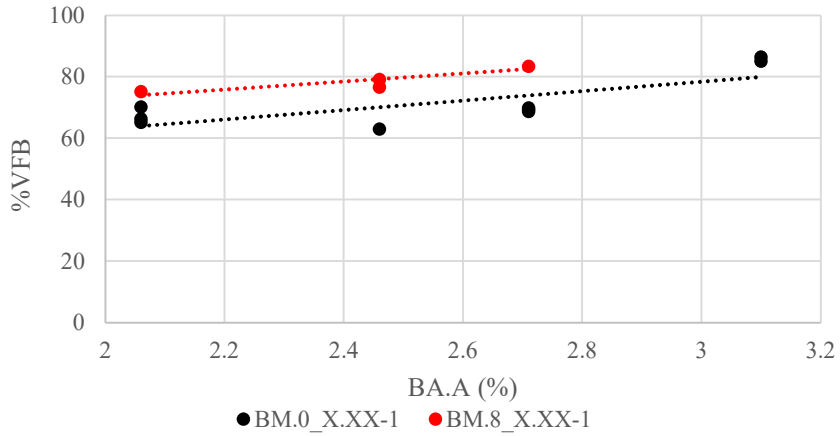

Figure 58 VFB as a function of added bitumen content (BA. A)

When evaluated against the effective binder content, the data further validates the study's hypothesis: approximately 50% of the waste plastic functions as an active binding component. The modified mixtures exhibit slightly higher VFB values, likely due to partial melting of the plastic during mixing.

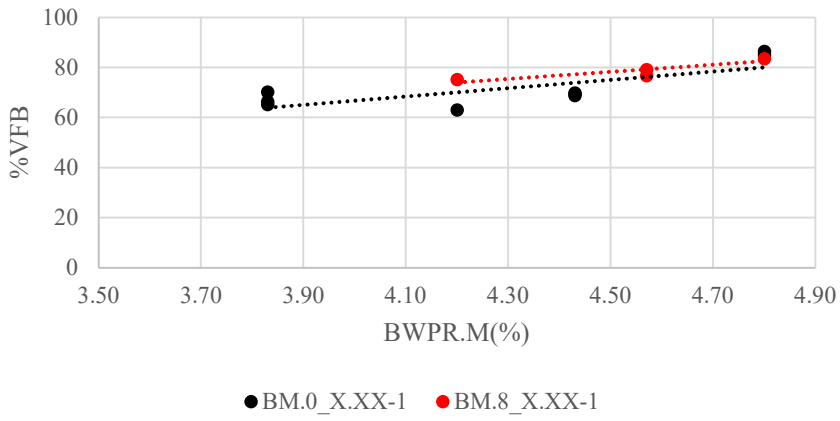

Figure 59 VFB as a function of effective binder content considering waste plastic (BWPR.M)

3.2.3 Mechanical properties of laboratory mixtures

The obtained results are analyzed as a function of the binder-related parameters previously considered in the volumetric analysis. This approach allows the influence of binder content and waste plastic addition on the mechanical response of the mixtures to be evaluated. The following sections present the analysis of the mechanical test results based on the experimental data obtained for the investigated mixtures.

Table 20 summarizes the main mechanical parameters obtained from the experimental program, including stiffness modulus, indirect tensile strength (ITS), and cracking tolerance index (CTI) for all the investigated mixtures. To streamline the evaluation of compliance, a color-coded classification system was implemented based on established performance thresholds. For the ITS, values are benchmarked against an optimal range of 0.72–1.4 MPa; results within this interval are presented in black, while non-compliant values are highlighted in red. Similarly, the CTI is evaluated against a minimum threshold of 65. All mixtures have value exceeding this limit to signify acceptable ductility.

Table 20 Summary of test results of laboratory mixtures

Test ID	STIFFNESS (MPa)	ITS (MPa)	CTI
BM.0_2.06-1-A-2-1	8129	1.472	146
BM.0_2.06-1-A-2-2	6872	1.333	138
BM.0_2.06-1-A-2-3	10324	1.696	149
BM.0_2.46-1-A-1-2	7850	1.696	133
BM.0_2.71-1-A-1-1	8325	1.669	208
BM.0_2.71-1-A-1-2	8328	1.535	171
BM.0_2.71-1-A-1-4	7632	1.600	196
BM.0_3.10-1-A-1-1	7398	1.742	184
BM.0_3.10-1-A-1-2	7125	1.326	98
BM.8_2.06-1-A-1-1	14349	2.040	225
BM.8_2.46-1-A-1-1	11732	1.954	237
BM.8_2.46-1-A-1-3	10190	1.801	160
BM.8_2.71-1-A-1-1	9686	2.069	281
BM.8_2.71-1-A-1-3	10552	1.950	222

3.2.3.1 Indirect Tensile Stiffness Modulus (ITSM)

From the master plots (Figure 60 and Figure 61), it can be observed that the stiffness modulus generally decreases as the binder content increases. This is consistent with the expected response of asphalt mixtures, since higher binder contents typically lead to a more flexible material with reduced stiffness.

A different sensitivity to binder content can be observed between the two mixture groups. The mixtures containing 0.8% waste plastic show a more pronounced decrease in stiffness as the binder content increases, whereas the mixtures without plastic exhibit a more gradual reduction. For similar binder contents, mixtures containing 0.8% waste plastic show higher stiffness values compared with control ones, indicating that the plastic slightly increases the rigidity of the mixture. While this higher stiffness may improve resistance to rutting, excessively high stiffness could also increase the susceptibility to

cracking, emphasizing the need for a balanced mixture design.

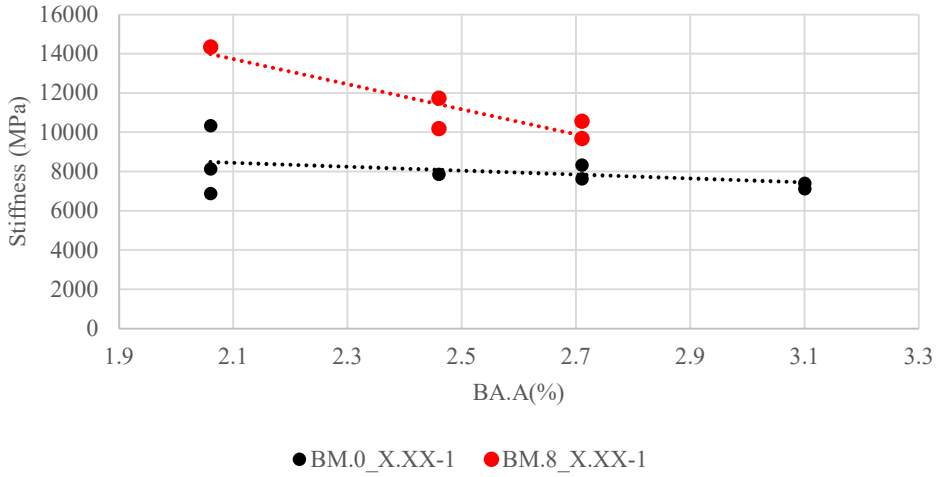

Figure 60 Stiffness modulus as a function of neat bitumen content (BA. A)

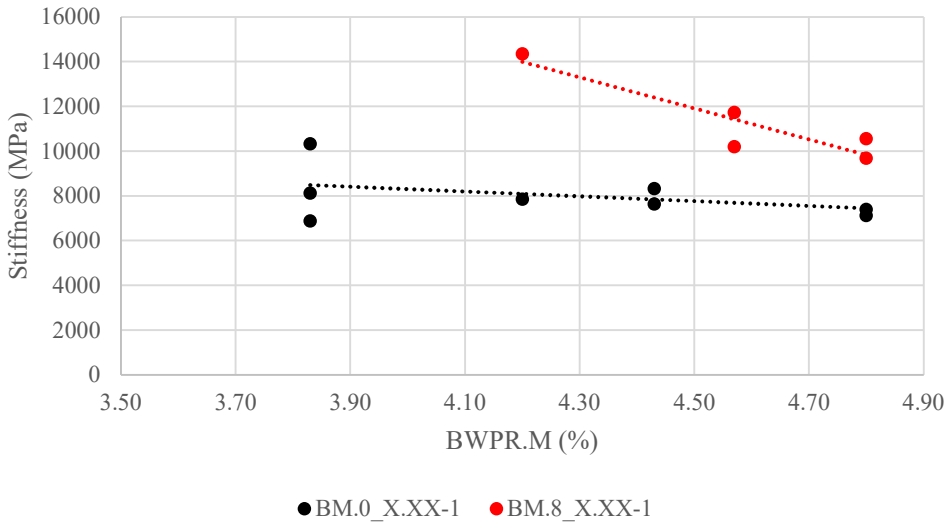

Figure 61 Stiffness modulus as a function of effective binder content considering waste plastic (BWPR.M)

3.2.3.2 Indirect Tensile Strength (ITS)

The experimental data confirms that mixtures modified with 0.8% waste plastic generally exhibit superior ITS compared to the control group, mirroring the trends observed in the stiffness modulus analysis. this enhancement indicates that the polymer fraction effectively reinforces the bituminous mastic, increasing internal cohesion and elevating the material's overall tensile resistance. Consequently, the waste plastic acts as a structural modifier, bolstering the mixture's capacity to withstand fracture-inducing stresses without compromising the fundamental aggregate interlock.

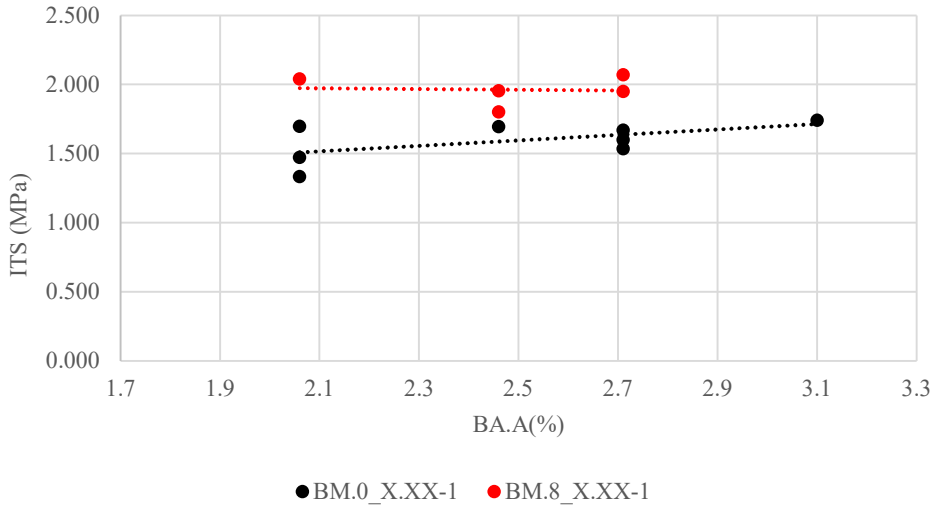

Figure 62 Indirect tensile strength (ITS) as a function of added bitumen content (B.A.A)

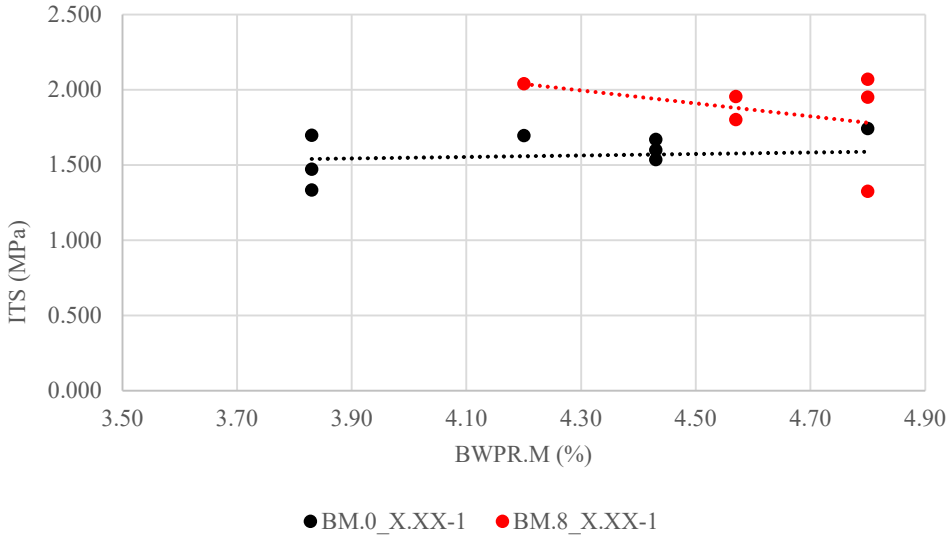

Figure 63 Indirect tensile strength (ITS) as a function of total binder content (BWPR.M)

3.3 Identification of the laboratory design mixtures

Based on volumetric requirements in Table 6 as well as Superpave prescriptions, the following findings were established. Adopting the target of 4% air voids at 100 gyrations (N design), the modified mixture achieves the design threshold at a neat bitumen content of 2.71%. This dosage represents the optimal candidate, as it remains consistent with both the air void content at 180 gyrations and the mechanical outcomes.

Conversely, the control mixture exhibited higher experimental dispersion of the data points than anticipated. This issue is probably related to sampling variations and material uncertainty. While regression line in Figure 64 identifies a 4% target at approximately 3.40%, the 3.10% neat bitumen mixture is selected as the optimal compromise to prevent VFB values from exceeding the recommended limits. the On the other way round for the control mixture it is observed more dispersion of experimental

data contrary as expected and due fundamentally to sampling operations and material uncertainly. In such case, whether the regression line reaches the 4% target around 3.40%, the mixture having 3.10% of neat bitumen is a good compromise because otherwise VFB would exceed the recommend values. This selection is further validated at N max where the candidate design mixture aligns effectively with the experimental point to the target void content of 2% and the regression model leads to 3% (Figure 65).

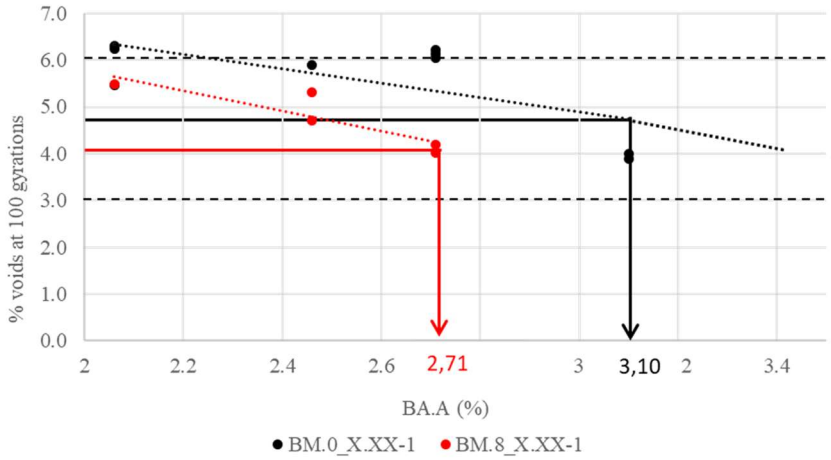

Figure 64 Identification of optimum bitumen content (B.A.A) based on air voids at 100 gyrations

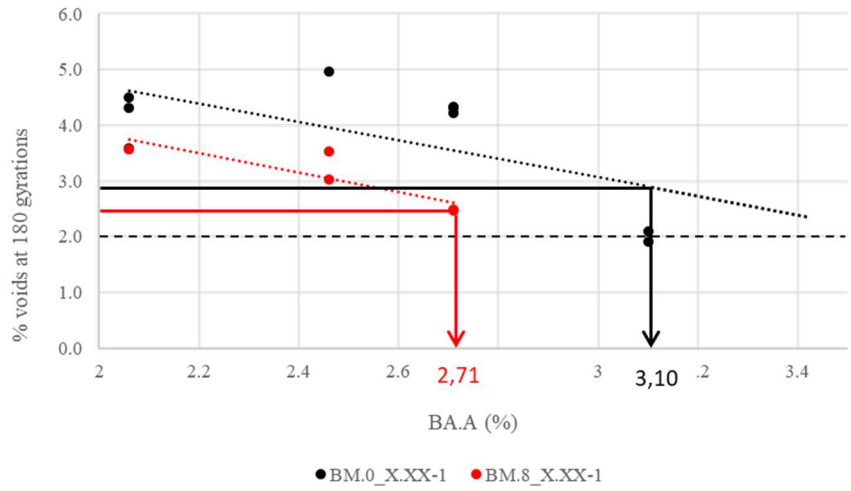

Figure 65Identification of optimum bitumen content (B.A.A) based on air voids at 180 gyrations

Therefore, comparing the design mixtures BM.8_2.71-1-A and BM.0_3.10-1-A, the incorporation of 0.8% of waste plastic leads to a neat bitumen reduction from 3.10% to 2.71%. The substitution rate, defined as the ratio between WP.M and BA. A gain, is close to 50%, confirming previous findings from the wearing course mix design. While thermal protocol A (165°C mixing, 145°C compaction) satisfies volumetric requirements, it is insufficient to confirm complete polymer melting; further investigations at higher temperatures are necessary to verify melting effectiveness. Nevertheless, a significant integration of polymers within the aggregate skeleton was observed, resulting in a measurable volumetric reduction in the asphalt concrete mixtures.

3.4 Outcomes of plant mixtures

In parallel with the laboratory production, additional asphalt mixtures produced at asphalt plant have been studied. This section evaluates the consistency between laboratory and industrial mixtures regarding composition, volumetric properties, and mechanical performance. This comparison serves to validate the scalability of the design approach and quantify the impact of production scale on material behavior.

Table 21 Main characteristics of the plant-produced mixtures,

Mixture ID	Mixing method	WP (%)	BA.A(%)	B.M(%)	REJ.M	BWPR.M
BI.0_2.46-00-A-1	I	0	2.46	4.136	0.07	4.14
BI.0_2.20-0-A-1	I	0	2.20	3.939	0.07	4.01
BI.8_2.20-0-A-1	I	0.8	2.20	3.908	0.07	4.38

Table 21 summarizes the main characteristics of the plant-produced mixtures, including the mixing method and the same variables discussed in 3.2. Table 22 provides disaggregate data of the various specimens analysed. For each mixture, multiple samples were collected in order to capture the variability associated with industrial production.

Table 22 Detailed summary of plant-produced specimens

Specimen ID	WP.M (%)	BA.A (%)	B.M (%)	REJ.M (%)	BWPR.M (%)	TBP (%)	EBP (%)	TMD (Mat)	TMD (Exp)	Analysis Status
BI.0_2.20-0-A-1-1	0.00	2.20	3.94	0.07	4.01	4.01	4.03	2.590	2.592	Included
BI.0_2.20-0-A-1-2	0.00	2.20	3.94	0.07	4.01	4.01	4.03	2.590	2.592	Included
BI.0_2.20-0-A-1-3	0.00	2.20	3.94	0.07	4.01	4.01	4.03	2.590	2.592	Included
BI.0_2.46-00-1-1	0.00	2.46	4.14	0.00	4.14	4.14	3.97	2.586	2.586	Included
BI.0_2.46-00-1-2	0.00	2.46	4.14	0.00	4.14	4.14	3.97	2.586	2.586	Included
BI.0_2.46-00-1-3	0.00	2.46	4.14	0.00	4.14	4.14	3.97	2.586	2.586	Included
BI.0_2.46-00-1-4	0.00	2.46	4.14	0.00	4.14	4.14	3.97	2.586	2.586	Included
BI.0_2.46-00-1-5	0.00	2.46	4.14	0.00	4.14	4.14	3.97	2.586	2.586	Included
BI.8_2.20-0-A-1-1	0.80	2.20	3.91	0.07	4.38	4.61	4.92	2.573	2.596	Excluded
BI.8_2.20-0-A-1-2	0.80	2.20	3.91	0.07	4.38	4.61	4.92	2.573	2.596	Included
BI.8_2.20-0-A-1-3	0.80	2.20	3.91	0.07	4.38	4.61	4.92	2.573	2.596	Included
BI.8_2.20-0-A-1-4	0.80	2.20	3.91	0.07	4.38	4.61	4.92	2.573	2.596	Included
BI.8_2.20-0-A-1-5	0.80	2.20	3.91	0.07	4.38	4.61	4.92	2.573	2.596	Included
BI.8_2.20-0-A-1-6	0.80	2.20	3.91	0.07	4.38	4.61	4.92	2.573	2.596	Included
BI.8_2.20-0-A-1-7	0.80	2.20	3.91	0.07	4.38	4.61	4.92	2.573	2.596	Included
BI.8_2.20-0-A-1-8	0.80	2.20	3.91	0.07	4.38	4.61	4.92	2.573	2.596	Included

During the data processing stage, a selection of specimens was performed based on consistency criteria, leading to the exclusion of a limited number of samples identified as outliers, while the remaining specimens were retained for the subsequent analysis.

3.4.1 Composition and morphology of plant mixtures

3.4.1.1 Maximum theoretical density

For the plant-produced mixtures, the maximum theoretical density (TMD) was considered as a first verification parameter in order to assess the consistency between the theoretical values defined during the mix design stage and the experimental values obtained from the produced specimens. This comparison is useful to evaluate whether the volumetric assumptions adopted during the design phase remain valid under plant production conditions.

Table 23 TMD comparison for plant-produced mixtures

Mix ID	Theoretical Maximum Density [Mg/m³]	Experimental Maximum Density [Mg/m³]	Experimental - theoretical difference
BI.0_2.20-0-A-1	2.590	2.5917	-0.0017
BI.0_2.46-1	2.586	2.5857	0.0003
BI.8_2.20-0-A-1	2.573	2.5958	-0.0228

The experimental TMD values of the plant-produced mixtures are generally close to the corresponding theoretical values with the exception for BI.8_2.20-0-A-1 where such difference shows an experimental value sensibly different with predicted value probably due to a different composition with respect to the declared one.

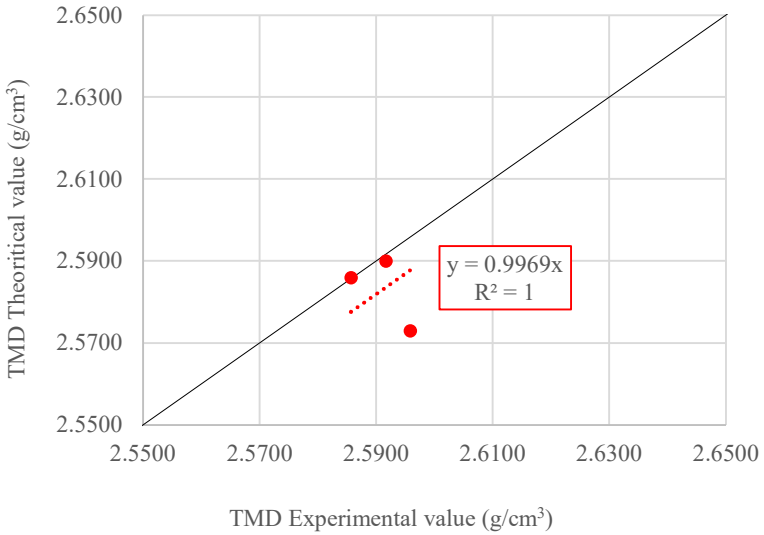

Figure 66 Experimental vs theoretical TMD comparison for plant mixtures

3.4.1.2 Gradation curves and statistical analysis

The gradation of the plant-produced mixtures was analyzed in order to verify the consistency of the aggregate skeleton with the target gradation curve adopted during the mix design phase. Since aggregate distribution strongly affects the volumetric and mechanical behavior of asphalt mixtures, this verification

is important to assess the reproducibility of the designed blends at plant scale.

Table 24 Particle size distribution of plant-produced mixtures

Sieve (mm)	BI.0_2.20-0-A-1	BI.0_2.46-1	BI.8_2.20-0-A-1
32	100.00	100.00	100.00
20	99.30	92.26	96.40
16	85.52	76.75	83.44
12.5	65.06	65.93	67.93
8	46.23	57.26	51.54
4	35.54	47.44	39.69
2	26.84	34.74	29.99
0.5	13.86	14.36	15.23
0.25	10.03	9.13	11.05
0.063	5.82	4.68	6.42

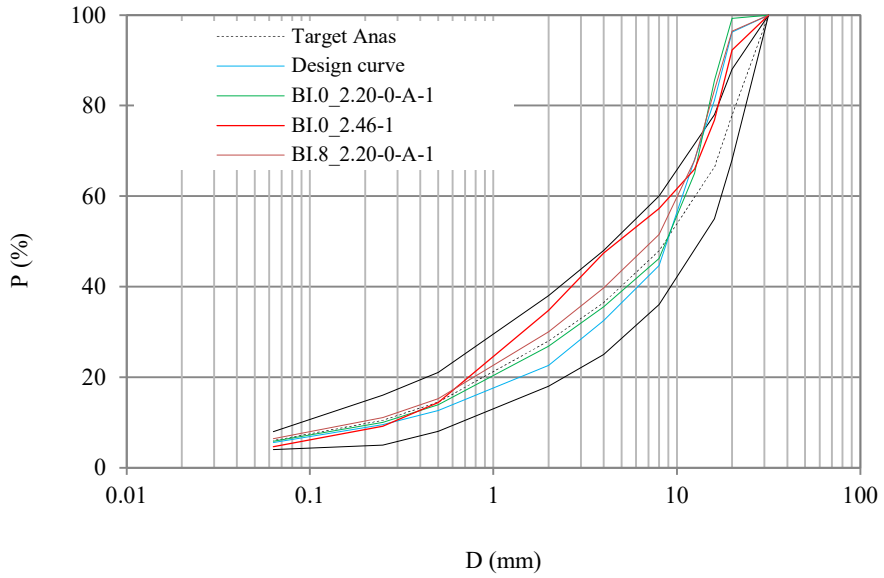

Figure 67 Gradation curves of the plant reference mixtures

As shown in Figure 67, the gradation curves of the plant-produced mixtures, obtained after ignition test, generally comply within prescribed limits [30] but did not converge neither with the target nor the laboratory design curve. It is worth noting that the red curve corresponding to mixture BI.0_2.46-1 shows a slightly different trend compared to the other mixtures. This mixture represents the earliest production, and after its production, the asphalt manufacturer modified the aggregate skeleton. This change explains the observed deviation from the other plant-produced mixtures. The BI.8_2.20-0-A-1 mixture is the most convergent to the laboratory reference curve and to the target ANAS.

Table 25 shows the differences between the ignition grading curves of the mixtures and the target ANAS. Values in black correspond to differences within the interval −5 to +5 with respect to the reference, whereas red ones identify values outside this range. The results indicate that, for most sieve sizes, the plant-produced mixtures remain within the acceptable difference range, demonstrating a satisfactory

alignment between the measured gradations and the design curve. Higher differences are observed at specific sieve sizes, mainly in the intermediate fractions, and are particularly evident for mixture BI.0_2.46-1. This behavior can be attributed to the modification of the aggregate skeleton implemented at the plant after the production of this mixture.

Table 25 Differences between measured and target gradation curves for plant-produced mixtures

Sieve (mm)	BI.0_2.20-0-A-1	BI.0_2.46-1	BI.8_2.20-0-A-1
31.5	0.0	0.0	0.0
20	3.1	-3.9	0.2
16	4.4	-4.4	2.3
8	1.6	12.6	6.9
4	3.0	14.9	7.2
2	4.2	12.1	7.4
0.5	1.2	1.7	2.6
0.25	0.5	-0.3	1.6
0.063	0.3	-0.9	0.9

3.4.1.3 Comparison between Total Binder Phase and Effective Binder Phase

For the plant-produced mixtures, the relationship between the total binder phase (TBP) defined during the mix design and the effective binder phase (EBP) measured through the ignition test was analyzed in order to verify the consistency of the binder content under industrial production conditions. This comparison is particularly relevant because plant production may affect the actual distribution of binder within the mixture due to operational variability and material handling at larger scale.

Table 26 Comparison between total binder phase (TBP) and effective binder phase (EBP) for plant-produced mixtures

Mix ID	TBP (%)	EBP (%)	Difference between TPB and EBP (%)
BI.0_2.20-0-A-1	4.01	4.030	-0.020
BI.0_2.46-1	4.14	3.970	0.170
BI.8_2.20-0-A-1	4.61	4.920	-0.310

In this study, the ignition test was used to determine the binder content of the plant-produced mixtures. The measured values represent the effective binder phase remaining after combustion, allowing a direct comparison with the design binder content.

The differences between TBP and EBP for the plant-produced mixtures remain generally limited (Table 26). All values fall within a narrow range, indicating a good agreement between the design binder content and the experimentally measured values.

These results confirm that, despite the variability associated with plant production, the binder content is reasonably well controlled and remains consistent with the mix design assumptions.

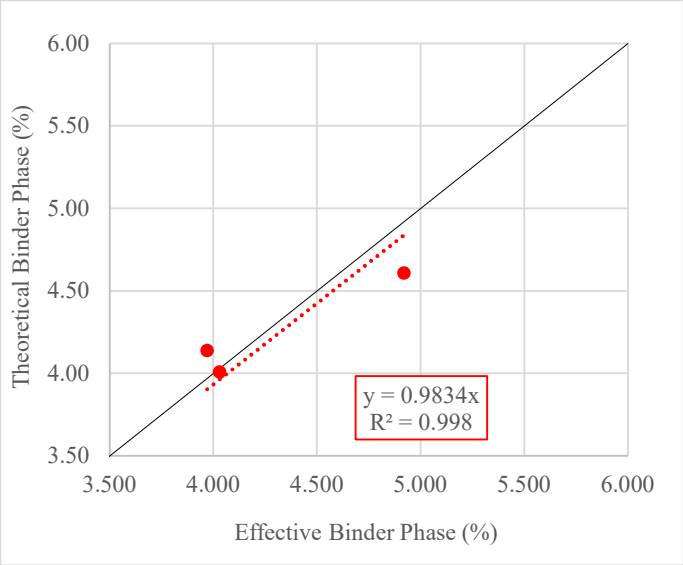

Figure 68 Control chart comparing total binder phase and effective binder phase for plant-produced mixtures

As shown in the Figure 68, the data points generally follow a linear trend close to the equality line, indicating a good agreement between TBP and EBP. The high coefficient of determination ($R^2 = 0.998$) confirms the strong correlation between the predicted and measured binder phases.

One data point shows a noticeable deviation from the general trend. This point corresponds to the mixture BI.0_2.46-1, whose different behavior is consistent with its distinct aggregate skeleton and composition, as well as the absence of a rejuvenating agent, as previously discussed.

3.4.2 Volumetric properties of plant mixtures

The volumetric properties of the plant-produced mixtures were evaluated in order to assess their consistency under industrial production conditions and to compare their behavior with that observed for laboratory mixtures, as it will be presented in 3.5.

Due to the scale of production and the inherent variability of plant processes, slight differences in volumetric properties are expected. Therefore, the analysis focuses on verifying whether the plant-produced mixtures remain within acceptable ranges and follow trends comparable to those observed in laboratory conditions.

3.4.2.1 Air void contents

For plant-produced mixtures, the air voids values were evaluated with respect to commonly adopted reference ranges [20] used to assess mixture suitability during the compaction process. In Table 27, the values falling within these ranges are in black, while those outside the acceptable limits are indicated in red, allowing a direct assessment of mixture compliance.

At 100 gyrations, only the mixtures with 2.46% neat bitumen fail to meet specifications. This is due to

a lack of convergence between the actual and target grading curve, resulting in a coarser aggregate matrix with an excessively open structure. This trend remains consistent at 180 gyrations with highest values.

Table 27 Air voids of plant-produced mixtures at different compaction levels

Specimen ID	WP.M (%)	BA.A (%)	B.M (%)	BWPR.M (%)	10 GYR (%)	100 GYR (%)	180 GYR (%)
BI.0_2.20-0-A-1-1	0.0	2.2	3.94	4.01	12.0	4.1	2.6
BI.0_2.20-0-A-1-2	0.0	2.2	3.94	4.01	12.6	4.3	2.7
BI.0_2.20-0-A-1-3	0.0	2.2	3.94	4.01	11.7	4.0	2.5
BI.0_2.46-1-1	0.0	2.46	4.14	4.14	13.5	7.1	5.8
BI.0_2.46-1-2	0.0	2.46	4.14	4.14	14.6	7.9	6.6
BI.0_2.46-1-3	0.0	2.46	4.14	4.14	13.6	7.1	5.8
BI.0_2.46-1-4	0.0	2.46	4.14	4.14	13.5	7.1	5.8
BI.0_2.46-1-5	0.0	2.46	4.14	4.14	13.9	7.4	6.1
BI.8_2.20-0-A-1-1	0.8	2.2	3.91	4.38	13.6	6.2	4.8
BI.8_2.20-0-A-1-2	0.8	2.2	3.91	4.38	12.9	5.4	4.0
BI.8_2.20-0-A-1-3	0.8	2.2	3.91	4.38	12.6	5.0	3.7
BI.8_2.20-0-A-1-4	0.8	2.2	3.91	4.38	13.2	5.5	4.0
BI.8_2.20-0-A-1-5	0.8	2.2	3.91	4.38	13.1	5.6	4.1
BI.8_2.20-0-A-1-6	0.8	2.2	3.91	4.38	13.0	5.3	3.8
BI.8_2.20-0-A-1-7	0.8	2.2	3.91	4.38	13.3	5.7	4.3
BI.8_2.20-0-A-1-8	0.8	2.2	3.91	4.38	12.2	5.0	3.7

As shown from Figure 69 to Figure 71 , the air voids diminishes with increasing compaction level, confirming the expected densification of the mixtures. Hence, for a given binder content, lower void values are observed at higher gyration levels due to improved compaction. However, in contrast with the behavior observed in laboratory, the plant-produced mixtures containing 0.8% waste plastics tend to exhibit higher air voids compared to the corresponding mixtures without plastic at the same binder content. This suggests that, under plant production conditions, the plastic behaves more like a solid inclusion within the aggregate skeleton rather than contributing to the binder phase also. The points marked with a cross (×) correspond to mixture BI.0_2.46-1 and are reported only for reference as previously explained.

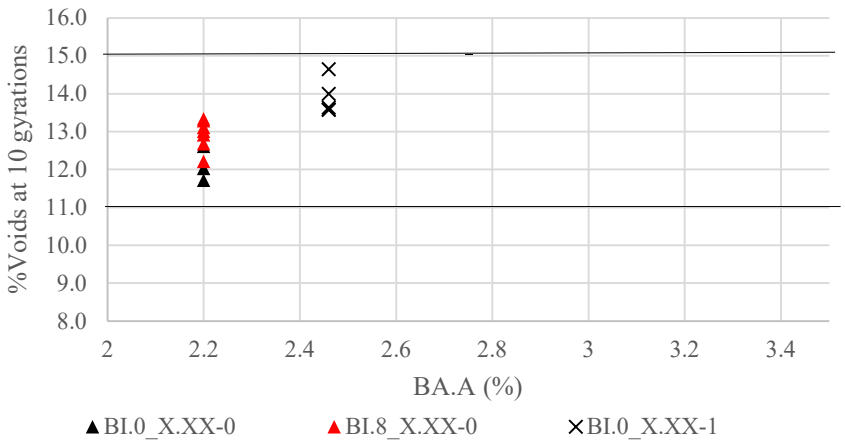

Figure 69 Air voids in BA.A domain for plant mixtures at 10 gyrations

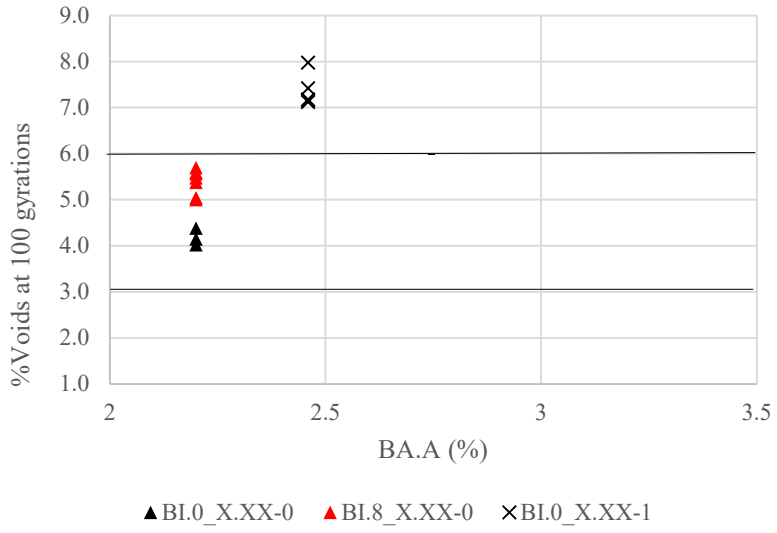

Figure 70 Air voids in BA.A domain for plant mixtures at 100 gyrations

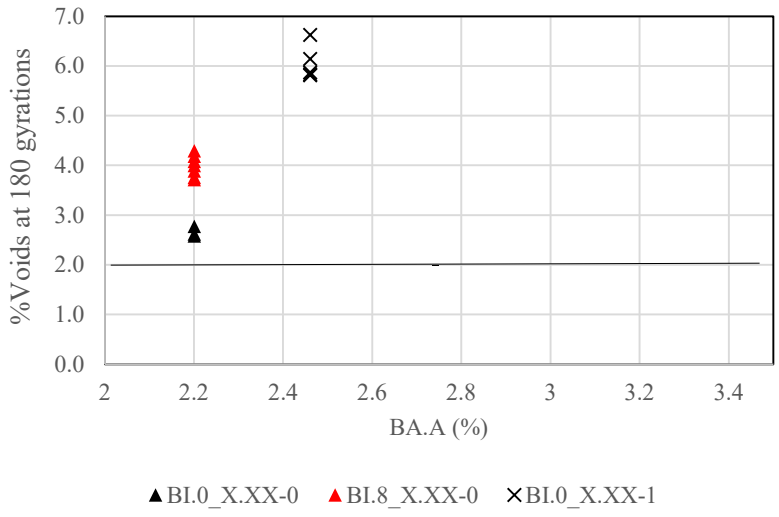

Figure 71 Air voids in BA.A domain for plant mixtures at 180 gyrations.

3.4.2.2 Voids in Mineral Aggregate (VMA)

Based on results reported in Table 28, the VMA values of the plant-produced mixtures are generally above the minimum specification limit, indicating that the aggregate skeleton provides sufficient space to accommodate the binder phase. The only exception for 2.20% neat bitumen unmodified blend.

Table 28 VMA values of the plant-produced mixtures and comparison with the specification limit

Test ID	WP.M	BA.A	B.M	BWPR.M	VMA
BI.0_2.20-0-A-1-1	0.0	2.2	3.94	4.01	12.6
BI.0_2.20-0-A-1-2	0.0	2.2	3.94	4.01	12.8
BI.0_2.20-0-A-1-3	0.0	2.2	3.94	4.01	12.6
BI.0_2.46-1-1	0.0	2.46	4.14	4.14	15.3
BI.0_2.46-1-2	0.0	2.46	4.14	4.14	16.1
BI.0_2.46-1-3	0.0	2.46	4.14	4.14	15.4
BI.0_2.46-1-4	0.0	2.46	4.14	4.14	15.3
BI.0_2.46-1-5	0.0	2.46	4.14	4.14	15.6
BI.8_2.20-0-A-1-1	0.8	2.2	3.91	4.38	17
BI.8_2.20-0-A-1-2	0.8	2.2	3.91	4.38	16.2
BI.8_2.20-0-A-1-3	0.8	2.2	3.91	4.38	15.9
BI.8_2.20-0-A-1-4	0.8	2.2	3.91	4.38	16.3
BI.8_2.20-0-A-1-5	0.8	2.2	3.91	4.38	16.4
BI.8_2.20-0-A-1-6	0.8	2.2	3.91	4.38	16.1
BI.8_2.20-0-A-1-7	0.8	2.2	3.91	4.38	16.5
BI.8_2.20-0-A-1-8	0.8	2.2	3.91	4.38	16

As it can be observed in the VMA plot as a function of the effective binder content (BWPR.M), the assumption of the binder-modifying effect of plastic is clearly reflected. In particular, the mixtures containing 0.8% waste plastic are shifted towards higher effective binder values compared to the corresponding mixtures without plastic. This rightward shift indicates that part of the plastic contributes to the binder phase, increasing the effective binder content of the mixture. However, the lack of full overlap with the reference mixtures suggests that this contribution is only partial, confirming that the plastic does not behave as a fully equivalent binder.

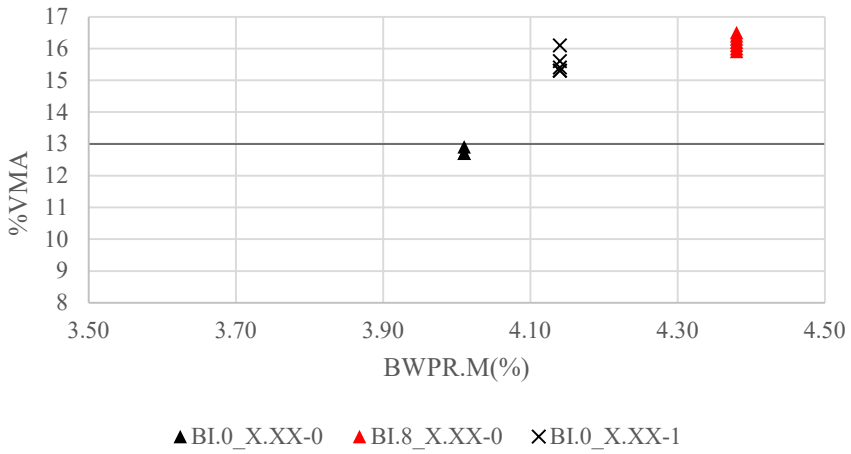

Figure 72 VMA as a function of effective binder content (BWPR.M) for plant-produced mixtures

3.4.2.3 Voids Filled with Bitumen (VFB)

Table 29 Summary of VFB values of the plant-produced mixtures

Test ID	VFB
BI.0_2.20-0-A-1-1	80.5
BI.0_2.20-0-A-1-2	79.1
BI.0_2.20-0-A-1-3	80.5
BI.0_2.46-1-1	62.1
BI.0_2.46-1-2	58.5
BI.0_2.46-1-3	61.7
BI.0_2.46-1-4	62.1
BI.0_2.46-1-5	60.7
BI.8_2.20-0-A-1-1	71.1
BI.8_2.20-0-A-1-2	75.3
BI.8_2.20-0-A-1-3	77
BI.8_2.20-0-A-1-4	74.8
BI.8_2.20-0-A-1-5	74.2
BI.8_2.20-0-A-1-6	75.9
BI.8_2.20-0-A-1-7	73.7
BI.8_2.20-0-A-1-8	76.4

As shown in Table 29, the VFB values generally fail to comply with prescriptions. For the 2.20% neat bitumen control mixtures, this non-compliance is expected: their VMA values fall below the minimum threshold, indicating that the mineral aggregate skeleton provides insufficient space to accommodate the binder. Conversely, for mixtures with 2.46%, the non – compliance stems for an excessively open structure, where the available void space is too large to bee satisfactorily saturated by the binder. The 2.20% neat bitumen modified mixtures on average meet the requirements (74.8%), demonstrating a bitumen content tailored for the adopted aggregate skeleton.

3.4.3 Mechanical properties of plant mixtures

The results reported in Table 30 are analyzed as a function of the binder-related parameters previously introduced.

Table 30 Mechanical properties of the plant-produced mixtures

Specimen ID	WP.M (%)	BA.A (%)	B.M (%)	BWPR.M (%)	STIFFNESS (MPa)	ITS (MPa)	CTI
BI.0_2.20-0-A-1-1	0.00	2.2	3.94	4.01	8956	1.867	198
BI.0_2.20-0-A-1-2	0.00	2.2	3.94	4.01	9154	1.904	224
BI.0_2.20-0-A-1-3	0.00	2.2	3.94	4.01	8263	1.951	277
BI.0_2.46-1-1	0.00	2.46	4.14	4.14	11777	1.806	374
BI.0_2.46-1-2	0.00	2.46	4.14	4.14	9514	2.095	537
BI.0_2.46-1-3	0.00	2.46	4.14	4.14	10425	2.166	386
BI.0_2.46-1-4	0.00	2.46	4.14	4.14	12053	2.011	278
BI.0_2.46-1-5	0.00	2.46	4.14	4.14	9909	2.117	413
BI.8_2.20-0-A-1-1	0.80	2.2	3.91	4.38	11413	1.827	200
BI.8_2.20-0-A-1-2	0.80	2.2	3.91	4.38	10810	1.713	105

BI.8_2.20-0-A-1-3	0.80	2.2	3.91	4.38	11214	2.043	231
BI.8_2.20-0-A-1-4	0.80	2.2	3.91	4.38	10190	1.712	142
BI.8_2.20-0-A-1-5	0.80	2.2	3.91	4.38	11349	1.952	279
BI.8_2.20-0-A-1-6	0.80	2.2	3.91	4.38	12959	2.085	326
BI.8_2.20-0-A-1-7	0.80	2.2	3.91	4.38	9652	1.941	205
BI.8_2.20-0-A-1-8	0.80	2.2	3.91	4.38	8487	1.981	190

3.4.3.1 Indirect Tensile Stiffness Modulus (ITSM)

As can be observed in Figure 73 and Figure 74, consistent with the behavior observed in the laboratory campaign, the mixtures containing 0.8% waste plastics exhibit higher stiffness values compared to the corresponding mixtures without plastic. This trend is clearly visible in all plots, indicating that the presence of plastic improves the stiffness of the mixture.

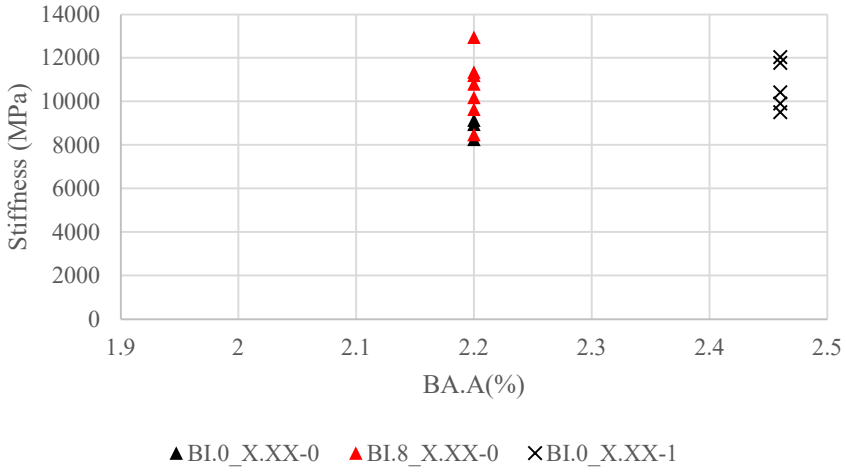

Figure 73 Stiffness modulus (ITSM) in the BA.A domain for plant-produced mixtures

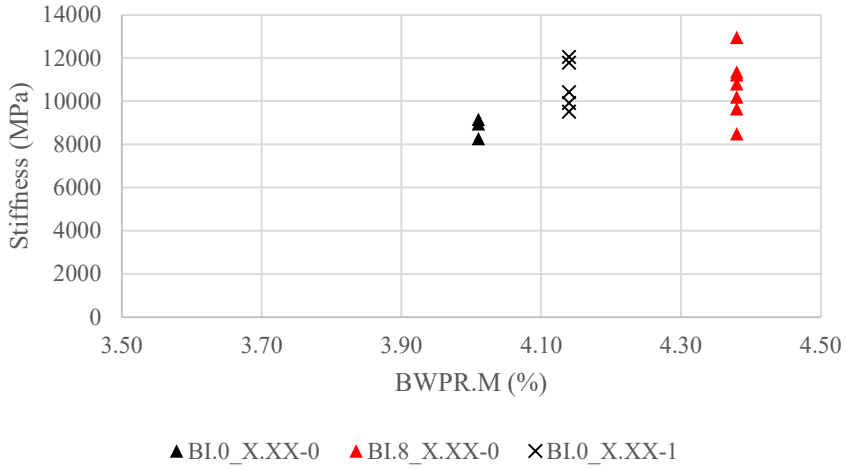

Figure 74 Stiffness modulus (ITSM) in the BWPR.M domain for plant-produced mixtures

3.4.3.2 Indirect Tensile Strength (ITS)

Consistent with the behavior theoretically expected, the modified mixtures generally show higher ITS values compared to the corresponding control mixtures. This indicates that the presence of plastic improves the internal cohesion of the mixture and enhances its resistance to tensile stresses.

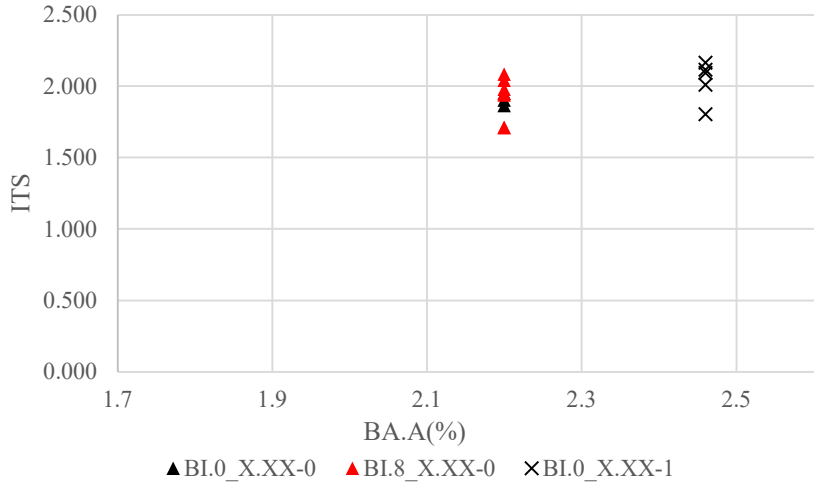

Figure 75 Indirect tensile strength (ITS) as a function of added bitumen content (B.A.A) for plant-produced mixtures

3.5 Comparison between lab and plant mixtures

Volumetrically, laboratory-prepared mixtures containing plastic exhibited lower air void contents than traditional blends. Conversely, plant-produced mixtures displayed the opposite trend reported in Figure 76, primarily due to discrepancies in their respective grading curves. In the laboratory, the design curve from optimization operations leads to an accommodation of waste plastics without volumetric expansion. In contrast, the aggregate skeleton of the plant blends aligns more strictly with target specifications, providing less internal volume to incorporate the plastic phase without increasing the overall void ratio.

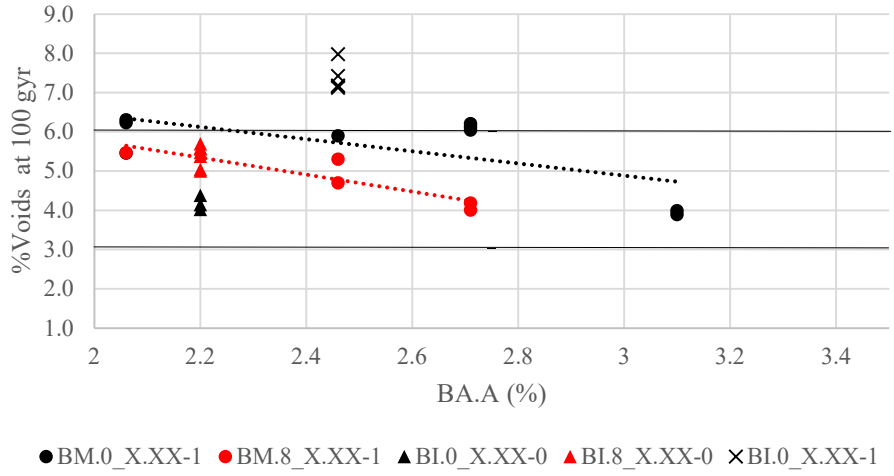

Figure 76 Air void content in BA.A domain for laboratory and plant mixtures

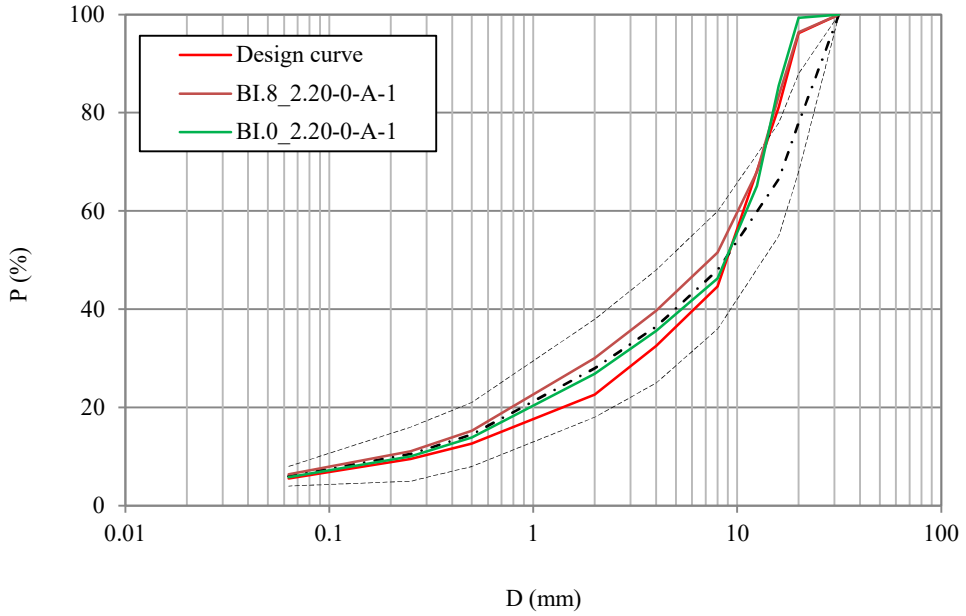

Figure 77 Summary of plant and laboratory design grading curves

Regarding VMA, mixtures with plastic consistently exhibited higher values in both laboratory and plant conditions. In contrast, VFB values were higher for laboratory mixtures containing plastic compared to those without plastic.

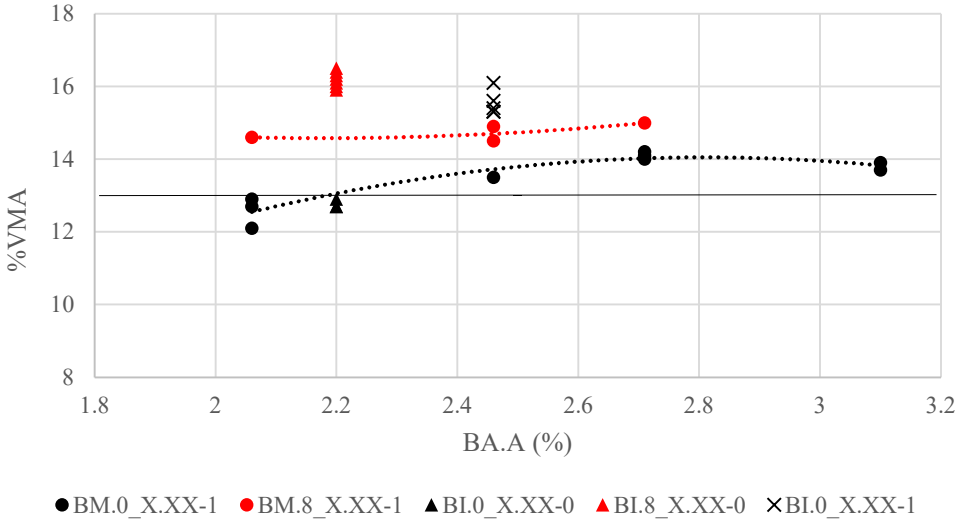

Figure 78 Variation of VMA in BA.A domain for laboratory and plant mixtures

From a mechanical point of view, the addition of plastic led to an overall improvement in performance. Both laboratory and plant mixtures with plastic showed higher stiffness modulus and ITS values compared to the reference mixtures, indicating enhanced mechanical behavior. Overall, the results indicate that mixtures containing recycled plastic can be considered suitable for application in the base layer.

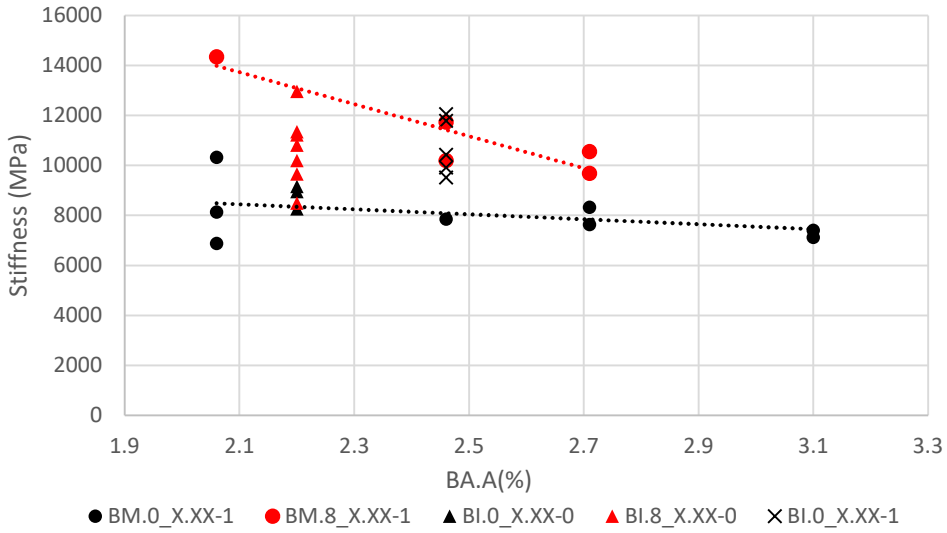

Figure 79 Stiffness modulus variation in BA.A domain for laboratory and plant-produced mixtures

However, it is recommended to further optimize these mixtures through additional plant production trials and to perform more comprehensive performance testing in the laboratory, in order to fully assess their long-term behavior.

4 Conclusions

The primarily objective of this study was to evaluate the feasibility of incorporating waste plastic into asphalt mixtures for base layer applications, specifically focusing on its impact on volumetric properties, mechanical behavior and also mix design optimization. By comparing control mixtures with 0.8% of plastic-modified blends across varying binder contents, several findings were established regarding the interaction between polymer and the mineral skeleton.

The laboratory investigation revealed a distinct difference in the volumetric response between the two mixture types, as the modified mixture achieved an optimum binder content (OBC) at 2.71% while 3.10% was found to be the most effective compromise for the control blend to maintain volumetric parameters within acceptable ranges. These OBC were further corroborated by mechanical results, where the benefits of polymer incorporation resulted both for stiffness and indirect tensile strength measurements. Such performance enhancement was further demonstrated by comparing the previous results with those of asphalt plant mixtures, where the beneficial of polymer incorporation emerged as well. The comparison of volumetric outcomes among these different production methods allowed to focus more into detail how the aggregate skeleton interacts with plastics showing the hybrid behavior of this latter.

A key finding of the research is that the addition of 0.8% waste plastic allowed for a significant reduction in neat bitumen content from 3.10% to 2.71%. This demonstrates that recycle waste plastic, beyond being a high-performing additive that enhances mechanical properties, actively supports environmental sustainability by reducing the consumption of virgin resources and repurposing waste into raw materials.

To further optimize this technology and advance this paradigm shift, future research should investigate the impact of higher mixing temperatures on the degree of plastic melting, additional long-performance test such as fatigue and rutting resistance, and full-scale pilot projects to monitor the in-situ durability of these “Green Roads”.

Bibliography

[1] Ritchie, H.; Samborska, V.; Roser, M. Plastic Pollution. OUR WORLD IN DATA,https://ourworldindata.org/plastic-pollution

[2] Lourens J. J. Meijer1, Tim van Emmerik, Ruud van der Ent, Christian Schmidt, Laurent Lebreton1. More than 1000 rivers account for 80% of global riverine plastic emissions into the ocean.

[3] Cottom et al. (2024) – with minor processing by Our World in Data

[4] Gwion B. Williams, Hairong Ma, Anna N. Khusnutdinova, Alexander F. Yakunin and Peter N. Golyshin. Harnessing extremophilic carboxylesterases for applications in polyester depolymerisation and plastic waste recycling

[5] Luzana Brasileiro, Fernando Moreno-Navarro, Raúl Tauste-Martínez, Jose Matos and Maria del Carmen Rubio-Gámez Reclaimed Polymers as Asphalt Binder Modifiers for More Sustainable Roads: A Review

[6] Isabella M. Bueno and Jamilla E. S. L. Teixeira. Waste Plastic in Asphalt Mixtures via the Dry Method: A Bibliometric Analysis

[7] Salim Barbhuiya1, Tanvir Qureshi and Bibhuti Bhusan Das. Advancing sustainable pavements: a review of low-carbon construction materials and practices

[8] Luyao Zhang, Wei Tian , Bobin Wang and Xiaomin Dai. Dynamic Life Cycle Assessment of Low-Carbon Transition in Asphalt Pavement Maintenance: A Multi-Scale Case Study Under China's Dual-Carbon Target

[9] Santagata F. et al., 2016, Road Materials and Pavement Design

[10] *Hasan & Tarefder, 2020,* A mixture design approach for mitigating cracking issue of asphalt concrete pavement

[11] Roberts, F. L., Kandhal, P. S., Brown, E. R., Lee, D. Y., & Kennedy, T. W. (1996). *Hot Mix Asphalt Materials, Mixture Design, and Construction.*

[12] Khalid A. Ghuzlan Ghazi G. Al-Khateeb† Yazeed Qasem. Rheological Properties of Polyethylene-Modified Asphalt Binder.

[13] Jitsangiam, P., Nusit, K., Teeratitayangkul, P., Ong, G. P., & Thienchai, C. (2023). Development of a modified Marshall mix design for hot-mix asphalt concrete mixed with recycled plastic based on dry mixing processes.

[14] García-Morales, M., Partal, P., Navarro, F. J., & Gallegos, C. (2006). Effect of waste polymer addition on the rheology of modified bitumen.

[15] Willis, J. R., et al. (2020)**.** *Evaluation of Waste Plastic Materials for Asphalt Binder and Mixtures.* National Cooperative Highway Research Program (NCHRP).

[16] Xu, F., Zhao, Y., & Li, K. (2020). Using waste plastics as asphalt modifier: A review.

[17] Long, G., Li, X., Yu, H., & Gong, X. (2022). Performance evaluation of asphalt mixtures incorporating waste polyethylene using the dry process.

[18] Almeida, A., Capitão, S., Bandeira, R., Fonseca, M., & Picado-Santos, L. (2020). Performance of AC mixtures containing flakes of LDPE plastic film collected from urban waste considering ageing.

[19] Kalantar, Z. N., Karim, M. R., & Mahrez, A. (2012).A review of using waste and virgin polymer in pavement.

[20] ANAS S.p.A. (2013).Capitolato Speciale d'Appalto – Norme Tecniche per la costruzione delle pavimentazioni stradali. Rome: ANAS.

[21] Ministero della Transizione Ecologica. (2022). Criteri Ambientali Minimi (CAM) per l'affidamento di servizi di progettazione e lavori per la costruzione, manutenzione e adeguamento delle infrastrutture stradali. Rome: Italian Government.

[22] European Committee for Standardization (CEN). (2012). **EN 933-1**: Tests for geometrical properties of aggregates – Part 1: Determination of particle size distribution – Sieving method. Brussels: CEN.

[23] European Committee for Standardization (CEN). (2019). **EN 12697-31**: Bituminous mixtures – Test methods – Part 31: Specimen preparation by gyratory compactor. Brussels: CEN.

[24] European Committee for Standardization (CEN). (2016). **EN 12697-35**: Bituminous mixtures – Test methods – Part 35: Laboratory mixing. Brussels: CEN.

[25] European Committee for Standardization (CEN). (2018). **EN 12697-5**: Bituminous mixtures – Test methods – Part 5: Determination of the maximum density. Brussels: CEN.

[26] European Committee for Standardization (CEN). (2020). **EN 12697-39**: Bituminous mixtures – Test methods – Part 39: Binder content by ignition method. Brussels: CEN.

[27] European Committee for Standardization (CEN). (2019). **EN 12697-31**: Bituminous mixtures – Test methods – Part 31: Specimen preparation by gyratory compactor. Brussels: CEN.

[28] European Committee for Standardization (CEN). (2020). **EN 12697-6**: Bituminous mixtures – Test methods – Part 6: Determination of bulk density of bituminous specimens. Brussels: CEN.

[29] European Committee for Standardization (CEN). (2018). **EN 12697-8**: Bituminous mixtures – Test methods – Part 8: Determination of void characteristics of bituminous specimens. Brussels: CEN.

[30] European Committee for Standardization (CEN). (2018). ***EN 12697-26****: Bituminous mixtures – Test methods – Part 26: Stiffness*. Brussels: CEN.

[31] European Committee for Standardization (CEN). (2017). **EN 12697-23**: Bituminous mixtures – Test methods – Part 23: Determination of the indirect tensile strength of bituminous specimens. Brussels: CEN.

[32] American Association of State Highway and Transportation Officials (AASHTO). (2020).*M 323: Standard specification for Superpave volumetric mix design*. Washington, DC: AASHTO.

[33] Li, N., Hao, P., Yao, Y. and Zhang, C., 2023. *The implementation of balanced mix design in asphalt materials: A review*. Construction and Building Materials, 402, p.132919.

Annexes

Nome della miscela BI.0_2.20-0-A-1
Descrizione BASE +36% GR 0/20 con rejuvenator, scheletro litico 0, compattazione 145°C stesa

Quantitativi di materiale impiegati

AGGREGATI

Frazione	%	Massa [g]	Subtotali (g)
Filler	1.5	146.7	
0/5	19	1857.8	
3/8	0	0.0	
5/15	6.5	635.6	
15/25	37	3617.8	
0/6	0	0.0	
0/20	36	3520.0	
			9777.8

BITUME DI APPORTO

		Massa [g]	
70/100	2.2	215.1	215.1

ADDITIVI

		Massa [g]	
Rejuvenator (REJ.A)	0.072	7.0	
WP (WP.M)	0	0	7.0

Massa totale della miscela [g] 10000

Massima Massa Volumica Teorica

Test ID	MMVT [Mg/m3]	MMVT medio [Mg/m3]
BI.0_2.20-0-A-1	2.597	2.592
BI.0_2.20-0-A-1	2.586	

Prova di ignizione

Mix ID	$m_{basket,prior}$ (g)	$m_{basket,prior+material}$ (g)	$m_{basket,after+material}$ (g)	B_{mix}	$B_{aggregate}$
BI.0_2.20-0-A-1	2843.8	4606.4	4535.4	4.03	4.20

Analisi granulometrica 27-01-26

Setaccio	**Passante progressivo**
[mm]	[%]
32	100.00
20	99.30
16	85.52
12.5	65.06
8	46.23
4	35.54
2	26.84
0.5	13.86
0.25	10.03
0.063	5.82
Pan	0.00

Filler perso nel lavaggio	98.5
Totale pre-lavaggio	1679.7

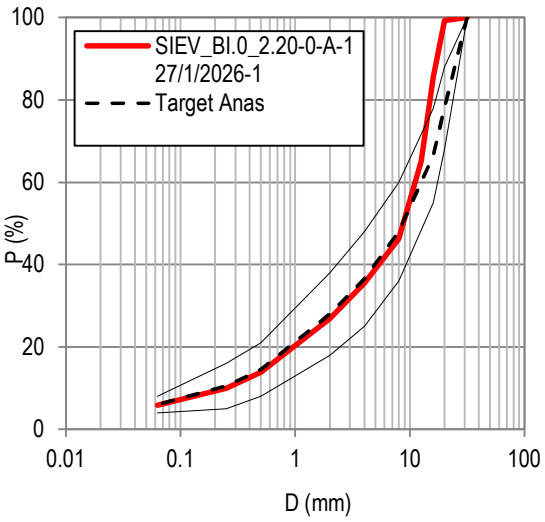

Bulk density

Test ID	M_{air} [g]	M_w [g]	M_{SSD} [g]	T [°C]	ρ_{SSD} [Mg/m^3]
BI.0_2.20-0-A-1-1	4575.5	2782.6	4592.2	20.7	2.524
BI.0_2.20-0-A-1-2	4574.5	2781.2	4593.3	20.7	2.520
BI.0_2.20-0-A-1-3	4573	2782.8	4590.7	20.8	2.525

Prova di compattazione

Test ID	v_{180}	v_{100}	v_{10}	$v_{180\ sawn}$
BI.0_2.20-0-A-1-1	2.62	4.15	12.03	1.81
BI.0_2.20-0-A-1-2	2.78	4.39	12.61	2.07
BI.0_2.20-0-A-1-3	2.59	4.03	11.71	1.37

VMA e VFB

MMVT [Mg/m^3]	2.592
B.M [%]	3.9
P_b [Mg/m^3]	1.025

Specimen ID	VMA	VFB
BI.0_2.20-0-A-1-1	12.7	79.8
BI.0_2.20-0-A-1-2	12.9	78.5
BI.0_2.20-0-A-1-3	12.7	79.8

Modulo di rigidezza a 25°C su provini tagliati

Specimen ID	E_1 (MPa)	E_2 (MPa)	Check	E_m (MPa)
BI.0_2.20-0-A-1-1 s	8848.1	9063	Passed	8956
BI.0_2.20-0-A-1-2 s	9462.5	8845.4	Passed	9154
BI.0_2.20-0-A-1-3 s	8761.8	7763.4	Passed	8263
Valore medio				8791

ITS a 25°C su provini tagliati

Specimen ID	Altezza media [mm]	Max P [kN]	Spostamento verticale [mm]	ITS [MPa]	CTI [MPa]
BI.0_2.20-0-A-1-1 s	53.7	23.623	2.221	1.867	198.11
BI.0_2.20-0-A-1-2 s	51.6	23.131	2.003	1.904	224.00
BI.0_2.20-0-A-1-3 s	50.8	23.342	1.662061	1.951	276.52

	ITS [MPa]	CTI [MPa]
Valori medi	1.907	232.9
Esito	Not Acceptable	Acceptable

Mix ID BI.8_2.20-0-A-1

Descrizione

Ricetta M73 TV36 RAP 0/25 steso il 5/12/25 in Borgaro

Aggregati

Frazione	%	Massa [g]	Subtotali (g)
Filler	1.5	145.5	
0/5	19	1842.9	
3/8	0	0.0	
5/15	6.5	630.5	
15/25	37	3588.9	
0/6	0	0.0	
0/20	36	3491.9	
			9699.7

Bitume di apporto

		Massa [g]	
70/100	2.2	213.4	213.4

Additivi

		Massa [g]	
Rejuvenator (% su mis	0.07	7.0	
WP (% su miscela)	0.80	79.9	86.9

Massa totale della miscela [g] 10000.0

Massima Massa Volumica Teorica

Test ID	MMVT [Mg/m3]	MMVT medio [Mg/m3]
BI.8_2.20-0-A-1.1	2.595	2.596
BI.8_2.20-0-A-1.2	2.597	

Prova di ignizione 30-01-25

Mix ID	$m_{basket,prior}$ (g)	$m_{basket,prior+material}$ (g)	$m_{basket,after+material}$ (g)	B_{mix}	$B_{aggregate}$
IGN_BI.8_2.20-0-A-1.1	2838.4	5376.6	5250.3	4.98	5.24
IGN_BI.8_2.20-0-A-1.2	2843.6	5420.9	5295.3	4.87	5.12

Analisi granulometrica

Setaccio	Passante progressivo
[mm]	[%]
31.5	100.00
20.0	96.40
16	83.44
12.5	67.93
8	51.54
4	39.69
2	29.99
0.5	15.23
0.25	11.05
0.063	6.42

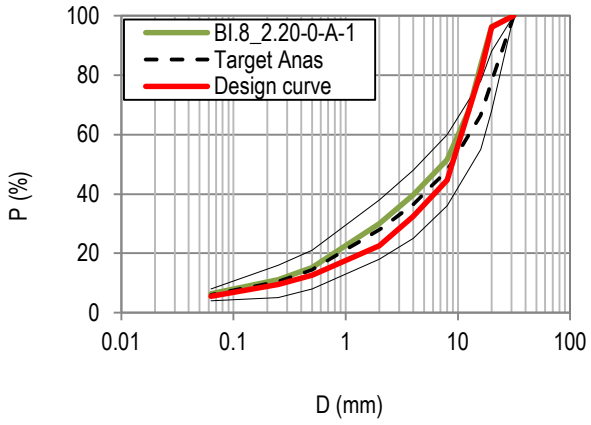

Bulk density

Test ID	M_{air} [g]	M_w [g]	M_{SSD} [g]	T [°C]	ρ_{SSD} [Mg/m^3]
BI.8_2.20-0-A-1-1	4587.8	2764.8	4619.2	18.6	2.4948
BI.8_2.20-0-A-1-2	4586.1	2770.5	4608.2	18.6	2.4920
BI.8_2.20-0-A-1-3	4585.2	2770.3	4602.3	18.6	2.4992
BI.8_2.20-0-A-1-4	4582.4	2770.4	4608.1	19.2	2.4897
BI.8_2.20-0-A-1-5	4584.5	2765.5	4605.9	19.2	2.4871
BI.8_2.20-0-A-1-6	4588.1	2774.0	4610.2	19.2	2.4948
BI.8_2.20-0-A-1-7	4585.3	2767.1	4609.4	20.8	2.4842
BI.8_2.20-0-A-1-8	4586.8	2768.8	4601.4	20.8	2.4982

Prova di compattazione

Test ID	v_{180}	v_{100}	v_{10}
BI.8_2.20-0-A-1-1	4.83	6.28	13.62
BI.8_2.20-0-A-1-2	4.00	5.48	12.91
BI.8_2.20-0-A-1-3	3.72	5.05	12.68
BI.8_2.20-0-A-1-4	4.09	5.57	13.29
BI.8_2.20-0-A-1-5	4.19	5.60	13.11
BI.8_2.20-0-A-1-6	3.89	5.38	13.01
BI.8_2.20-0-A-1-7	4.30	5.70	13.34
BI.8_2.20-0-A-1-8	3.76	5.00	12.21
Valori medi	**4.10**	**5.51**	**13.02**

VMA e VFB

Specimen ID	VMA	VFB
BI.8_2.20-0-A-1-1	17	71.1
BI.8_2.20-0-A-1-2	16.2	75.3
BI.8_2.20-0-A-1-3	15.9	77
BI.8_2.20-0-A-1-4	16.3	74.8
BI.8_2.20-0-A-1-5	16.4	74.2
BI.8_2.20-0-A-1-6	16.1	75.9
BI.8_2.20-0-A-1-7	16.5	73.7
BI.8_2.20-0-A-1-8	16	76.4

Modulo di rigidezza a 25°C

Specimen ID	E_1 (MPa)	E_2 (MPa)	Check	E_m (MPa)
BI.8_2.20-0-A-1-1	11283.1	11542.2	Passed	11412.65
BI.8_2.20-0-A-1-2	10913.5	10706	Passed	10809.75
BI.8_2.20-0-A-1-3	11358.4	11068.7	Passed	11213.55
BI.8_2.20-0-A-1-4	10145.1	10235.4	Passed	10190.25
BI.8_2.20-0-A-1-5	11549.6	11147.6	Passed	11348.6
BI.8_2.20-0-A-1-6	13100.4	12817.6	Passed	12959
BI.8_2.20-0-A-1-7	9907.4	9396.8	Passed	9652.1
BI.8_2.20-0-A-1-8	8776.4	8198.2	Passed	8487.3
Valore medio				10527

ITS a 25°C

Specimen ID	Altezza media [mm]	Max P [kN]	Spostamento verticale [mm]	ITS [MPa]	CTI [MPa]
BI.8_2.20-0-A-1-1	53.23	22.910457	2.151	1.827	200.10
BI.8_2.20-0-A-1-2	51.53	20.799303	3.836	1.713	105.23
BI.8_2.20-0-A-1-3	49.38	23.768241	2.089	2.043	230.47
BI.8_2.20-0-A-1-4	47.40	19.123	2.850	1.712	141.54
BI.8_2.20-0-A-1-5	44.70	20.555	1.647	1.952	279.17
BI.8_2.20-0-A-1-6	49.05	24.092	1.508	2.085	325.71
BI.8_2.20-0-A-1-7	49.08	22.443	2.236	1.941	204.50
BI.8_2.20-0-A-1-8	50.50	23.571	2.462	1.981	189.60

	ITS [MPa]	CTI [MPa]
Valori medi	1.907	209.5
Esito	Not Acceptable	Acceptable

Nome della miscela	BL.8_2.06-1-A-1
Descrizione	BASE +35% GR 0/20 con rejuvenator, 0.8% WP, scheletro litico 1

Quantitativi di materiale impiegati

AGGREGATI

Frazione	%	Massa [g]	Subtotali (g)
Filler	2	194.3	
0/5	14	1359.8	
3/8	0	0.0	
5/15	0	0.0	
15/25	49	4759.4	
0/6	0	0.0	
0/20	35	3399.6	
			9713.1

BITUME DI APPORTO

		Massa [g]	
70/100	2.06	200.1	200.1

ADDITIVI

		Massa [g]	
Rejuvenator (REJ.A)	0.07	6.799177527	
WP (WP.M)	0.799999883	79.99998826	86.799166

Massa totale della miscela [g] 10000

Massima Massa Volumica Teorica

Test ID	MMVT [Mg/m3]	MMVT medio [Mg/m3]
BL.8_2.06-1-A-1.3	2.584	2.579
BL.8_2.06-1-A-1.4	2.575	

Prova di ignizione 00-01-00

Mix ID	$m_{basket,prior}$ (g)	$m_{basket,prior+material}$ (g)	$m_{basket,after+material}$ (g)	B_{mix}	$B_{aggregate}$
BL.8_2.06-1-A-1	2841.1	4347	4277.1	4.64	4.87
BL.8_2.06-1-A-1	2839.6	5152.2	5051.8	4.34	4.54

Analisi granulometrica 06-11-25

Setaccio	**Passante progressivo**
[mm]	[%]
32	100.00
20	94.94
16	78.79
12.5	63.22
8	42.52
4	32.07
2	23.61
0.5	14.88
0.25	12.30
0.063	8.11
Pan	0.00

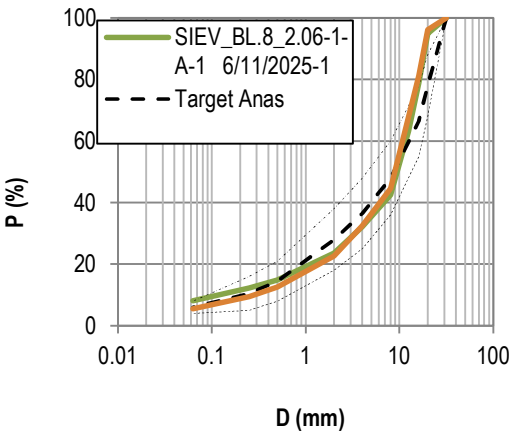

Filler perso nel lavaggio	126.5
Totale pre-lavaggio	1480.9

Bulk density

Test ID	M_{air} [g]	M_w [g]	M_{SSD} [g]	T [°C]	ρ_{SSD} [Mg/m^3]
BL.8_2.06-1-A-1-1	4525	2762.5	4531	20.5	2.554
BL.8_2.06-1-A-1-2	4525.3	2763.4	4531.5	20.5	2.555
BL.8_2.06-1-A-1-3	4525.6	2746.3	4540	21	2.518
BL.8_2.06-1-A-1-4	4524.8	2762.8	4535.7	21	2.547
0	4573	2717.7	4598.4	21.2	2.427

Prova di compattazione

Test ID	v_{180}	v_{100}	v_{10}	$v_{180\ sawn}$
BL.8_2.06-1-A-1-1	1.30	2.71	10.51	0.84
BL.8_2.06-1-A-1-2	1.27	2.60	10.52	0.50
BL.8_2.06-1-A-1-3	2.68	4.04	12.46	1.79
BL.8_2.06-1-A-1-4	1.56	2.96	11.77	0.27
Valori medi	1.70	3.08	11.31	0.00

VMA e VFB

MMVT [Mg/m^3]	2.579
B.M [%]	3.7
P_b [Mg/m^3]	1.025

Specimen ID	VMA	VFB
BL.8_2.06-1-A-1-1	12.8	89.9
BL.8_2.06-1-A-1-2	12.8	89.9
BL.8_2.06-1-A-1-3	14	81
BL.8_2.06-1-A-1-4	13.1	87.6
Valori medi	13.2	87.1

Modulo di rigidezza a 25°C su provini tagliati

Specimen ID	E_1 (MPa)	E_2 (MPa)	Check	
BL.8_2.06-1-A-1-1 s	13296.8	12723.1	Passed	E_m (MPa)
BL.8_2.06-1-A-1-2 s	10831.7	10368.3	Passed	13010
BL.8_2.06-1-A-1-3 s	12824.5	12399.9	Passed	10600
BL.8_2.06-1-A-1-4 s	11387.8	12456.6	Passed	12612
Valore medio				11922
				12036

ITS a 25°C su provini tagliati

Specimen ID	Altezza media [mm]	Max P [kN]	Spostamento verticale [mm]	ITS [MPa]	CTI [MPa]
BL.8_2.06-1-A-1-1 s	51.7	30.808	1.178	2.528	505.61
BL.8_2.06-1-A-1-2 s	51.3	33.716	1.667	2.791	394.55
BL.8_2.06-1-A-1-3 s	48.9	33.184	1.563	2.882	434.39
BL.8_2.06-1-A-1-4 s	52.5	35.039	0.553	2.833	1206.89

Valori medi	ITS [MPa]	CTI [MPa]
Esito	2.758	635.4
	Rejected	Accepted

Nome della miscela	BM.0_2.06-1-A-1
Descrizione	BASE +35% GR 0/20 con rejuvenator, miscelazione a 175°C curva ottimizzata

Quantitativi di materiale impiegati

AGGREGATI

Frazione	%	Massa [g]	Subtotali (g)
Filler	2	195.8	
0/5	14	1370.8	
3/8	0	0.0	
5/15	0	0.0	
15/25	49	4797.8	
0/6	0	0.0	
0/20	35	3427.0	
			9791.4

BITUME DI APPORTO

		Massa [g]	
70/100	2.06	201.7	201.7

ADDITIVI

		Massa [g]	
Rejuvenator (REJ.A)	0.07	6.9	
WP (WP.M)	0	0	6.9

Massa totale della miscela [g] 10000

Prova di ignizione 00-01-00

Mix ID	$m_{basket,prior}$ (g)	$m_{basket,prior+material}$ (g)	$m_{basket,after+material}$ (g)	B_{mix}	$B_{aggregate}$
BM.0_2.06-1-A-1	2839.8	5099.8	5014.4	3.78	3.93
BM.0_2.06-1-A-1	2839.7	5150.4	5058.3	3.99	4.15

Analisi granulometrica 06-11-25

Setaccio	**Passante progressivo**
[mm]	[%]
32	100.00
20	97.61
16	84.63
12.5	67.91
8	46.04
4	33.78
2	24.85
0.5	14.66
0.25	11.19
0.063	6.41
Pan	0.00

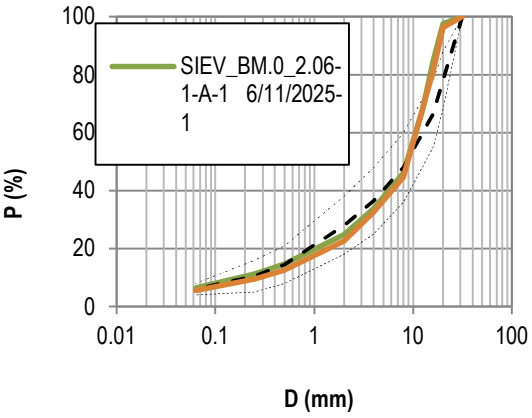

Filler perso nel lavaggio	139.3
Totale pre-lavaggio	2122.7

Bulk density

Test ID	M_{air} [g]	M_w [g]	M_{SSD} [g]	T [°C]	ρ_{SSD} [Mg/m^3]
BM.0_2.06-1-A-1-1	4609.2	2806.3	4644.1	20.1	2.504

Prova di compattazione

Test ID	v_{180}	v_{100}	v_{10}
BM.0_2.06-1-A-1-1	4.04	5.67	13.92

VMA e VFB

MMVT [Mg/m^3]	0.000
B.M [%]	5.6
P_b [Mg/m^3]	1.025

Specimen ID	VMA	VFB
BM.0_2.06-1-A-1-1	13.6	70.4
Valori medi	13.6	70.4

Nome della miscela	BM.0_2.06-1-A-2
Descrizione	BASE +35% GR 0/20 con rejuvenator, miscelazione a 165°C. Scheletro litico 1. Per

Quantitativi di materiale impiegati

AGGREGATI

Frazione	%	Massa [g]	Subtotali (g)
Filler	2	195.8	
0/5	14	1370.8	
3/8	0	0.0	
5/15	0	0.0	
15/25	49	4797.8	
0/6	0	0.0	
0/20	35	3427.0	
			9791.4

BITUME DI APPORTO

		Massa [g]	
70/100	2.06	201.7	201.7

ADDITIVI

		Massa [g]	
Rejuvenator (REJ.A)	0.07	6.9	
WP (WP.M)	0	0	6.9

Massa totale della miscela [g] 10000

Massima Massa Volumica Teorica

Test ID	MMVT [Mg/m3]	MMVT medio [Mg/m3]
BM.0_2.06-1-A-2	2.563	2.565
BM.0_2.06-1-A-2	2.566	

Prova di ignizione 00-01-00

Mix ID	$m_{basket,prior}$ (g)	$m_{basket,prior+material}$ (g)	$m_{basket,after+material}$ (g)	B_{mix}	$B_{aggregate}$
BM.0_2.06-1-A-2	2845.1	4147	4101.5	3.49	3.62

Analisi granulometrica 06-11-25

Setaccio	**Passante progressivo**
[mm]	[%]
32	100.00
20	100.00
16	83.96
12.5	61.68
8	41.84
4	29.08
2	18.73
0.5	10.51
0.25	8.34
0.063	5.43
Pan	0.00

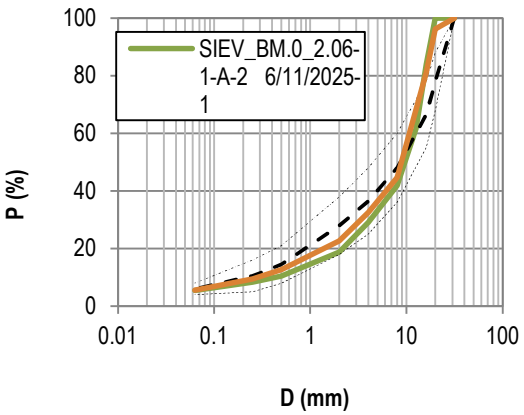

Filler perso nel lavaggio	68.2
Totale pre-lavaggio	1256.4

Bulk density

Test ID	M_{air} [g]	M_w [g]	M_{SSD} [g]	T [°C]	ρ_{SSD} [Mg/m^3]
BM.0_2.06-1-A-2-1	4610.4	2781.1	4659.7	20.9	2.449
BM.0_2.06-1-A-2-2	4610	2790.7	4665.8	20.9	2.454
BM.0_2.06-1-A-2-3	4610.7	2791.8	4652.8	20.9	2.473

Prova di compattazione

Test ID	v_{180}	v_{100}	v_{10}
BM.0_2.06-1-A-2-1	4.49	6.31	15.35
BM.0_2.06-1-A-2-2	4.32	6.24	15.32
BM.0_2.06-1-A-2-3	3.58	5.47	14.57
Valori medi	4.13	6.01	15.08

$v_{180\ sawn}$
4.60
4.31
3.48

VMA e VFB

MMVT [Mg/m^3]	0.000
B.M [%]	3.8
P_b [Mg/m^3]	1.025

Specimen ID	VMA	VFB
BM.0_2.06-1-A-2-1	12.9	65.1
BM.0_2.06-1-A-2-2	12.7	66.3
BM.0_2.06-1-A-2-3	12.1	70.1
Valori medi	12.6	67.2

Modulo di rigidezza a 25°C su provini tagliati

Specimen ID	E_1 (MPa)	E_2 (MPa)	Check	E_m (MPa)
BM.0_2.06-1-A-2-1	7949.6	8308.8	Passed	8129.2
BM.0_2.06-1-A-2-2	6720.1	7023.2	Passed	6871.65
BM.0_2.06-1-A-2-3	10850	9798	Passed	10324
Valore medio				8442

ITS a 25°C su provini tagliati

Specimen ID	Altezza media [mm]	Max P [kN]	Spostamento verticale [mm]	ITS [MPa]	CTI [MPa]
BM.0_2.06-1-A-2-1	56.5	19.6028	2.3722	1.472	146.23
BM.0_2.06-1-A-2-2	51.3	16.1094	2.2701	1.333	138.40
BM.0_2.06-1-A-2-3	45.9	18.3401	2.6760	1.696	149.36

Valori medi	ITS [MPa]	CTI [MPa]
Esito	1.501	144.7
	Acceptable	Acceptable

Nome della miscela	BM.0_2.46-1-A-1
Descrizione	BASE + 35% GR 0/20 con rejuvenator, miscelazione a 175°C scheletro litico 1

Quantitativi di materiale impiegati

AGGREGATI

Frazione	%	Massa [g]	Subtotali (g)
Filler	2	195.1	
0/5	14	1365.5	
3/8	0	0.0	
5/15	0	0.0	
15/25	49	4779.1	
0/6	0	0.0	
0/20	35	3413.6	
			9753.2

BITUME DI APPORTO

		Massa [g]	
70/100	2.46	239.9	239.9

ADDITIVI

		Massa [g]	
Rejuvenator (REJ.A)	0.07	6.8	
WP (WP.M)	0	0	6.8

Massa totale della miscela [g] 10000

Massima Massa Volumica Teorica

Test ID	MMVT [Mg/m3]	MMVT medio [Mg/m3]
BM.0_2.46-1-A-1.1	2.607	2.607
BM.0_2.46-1-A-1.2	2.606	

Prova di ignizione 00-01-00

Mix ID	$m_{basket,prior}$ (g)	$m_{basket,prior+material}$ (g)	$m_{basket,after+material}$ (g)	B_{mix}	$B_{aggregate}$
BM.0_2.46-1-A-1	2845.5	4167.3	4121.7	3.45	3.57
BM.0_2.46-1-A-1	2846.8	4915.7	4831.2	4.08	4.26

Analisi granulometrica 16-02-25

Setaccio	**Passante progressivo**
[mm]	[%]
32	100.00
20	100.00
16	90.98
12.5	73.36
8	48.71
4	33.68
2	22.97
0.5	13.04
0.25	10.09
0.063	6.41
Pan	0.00

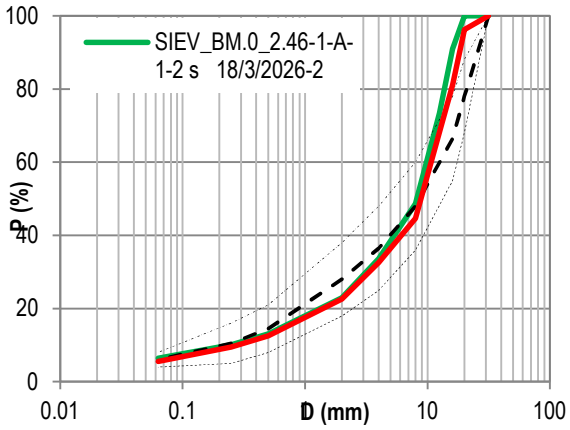

Filler perso nel lavaggio	63.7
Totale pre-lavaggio	1195.4

Bulk density

Test ID	M_{air} [g]	M_w [g]	M_{SSD} [g]	T [°C]	ρ_{SSD} [Mg/m^3]
BM.0_2.46-1-A-1-1	4578.6	2750.4	4617.3	21.6	2.447
BM.0_2.46-1-A-1-2	4578.6	2760.22	4605.4	21.6	2.476
BM.0_2.46-1-A-1-3	4580.1	2749.2	4618.9	21.6	2.445

Prova di compattazione

Test ID	v_{180}	v_{100}	v_{10}
BM.0_2.46-1-A-1-1	6.07	7.96	16.85
BM.0_2.46-1-A-1-2	4.96	5.90	15.24
BM.0_2.46-1-A-1-3	6.18	8.52	17.31
Valori medi	5.74	7.46	16.47

$v_{180\ sawn}$
4.50
3.38
4.78

VMA e VFB

MMVT [Mg/m^3]	2.607
B.M [%]	4.1
P_b [Mg/m^3]	1.025

Specimen ID	VMA	VFB
BM.0_2.46-1-A-1-1	14.5	57.9
BM.0_2.46-1-A-1-2	13.5	62.9
BM.0_2.46-1-A-1-3	14.6	57.5
Valori medi	14.2	59.4

Modulo di rigidezza a 25°C su provini tagliati

Specimen ID	E_1 (MPa)	E_2 (MPa)	Check	E_m (MPa)
BM.0_2.46-1-A-1-1	7184.4	6927.7	Passed	7056.05
BM.0_2.46-1-A-1-2	8108.3	7592	Passed	7850.15
BM.0_2.46-1-A-1-3	7745.8	7609.5	Passed	7677.65
Valore medio				7528

ITS a 25°C su provini tagliati

Specimen ID	Altezza media [mm]	Max P [kN]	Spostamento verticale [mm]	ITS [MPa]	CTI [MPa]
BM.0_2.46-1-A-1-1	50.6	16.529	2.614	1.386	124.96
BM.0_2.46-1-A-1-2	52.1	20.811	3.008	1.696	132.81
BM.0_2.46-1-A-1-3	53.8	17.332	2.362	1.368	136.46

Valori medi	ITS [MPa]	CTI [MPa]
Esito	1.483	131.4
	Acceptable	Acceptable

Nome della miscela	BM.0_2.46-1-A-2
Descrizione	BASE + 35% GR 0/20 con rejuvenator, miscelazione a 175°C scheletro litico 1 (lotto

Quantitativi di materiale impiegati

AGGREGATI

Frazione	%	Massa [g]	Subtotali (g)
Filler	2	195.1	
0/5	14	1365.5	
3/8	0	0.0	
5/15	0	0.0	
15/25	49	4779.1	
0/6	0	0.0	
0/20	35	3413.6	
			9753.2

BITUME DI APPORTO

		Massa [g]	
70/100	2.46	239.9	239.9

ADDITIVI

		Massa [g]	
Rejuvenator (REJ.A)	0.07	6.8	
WP (WP.M)	0	0	6.8

Massa totale della miscela [g] 10000

Massima Massa Volumica Teorica

Test ID	MMVT [Mg/m3]	MMVT medio [Mg/m3]
BM.0_2.46-1-A-2.1	2.607	2.610
BM.0_2.46-1-A-2.2	2.612	

Prova di ignizione 00-01-00

Mix ID	$m_{basket,prior}$ (g)	$m_{basket,prior+material}$ (g)	$m_{basket,after+material}$ (g)	B_{mix}	$B_{aggregate}$
BM.0_2.46-1-A-2	2841.7	4106.6	4058.2	3.83	3.98
BM.0_2.46-1-A-2-1 s	2839.8	4830.7	4758.4	3.63	3.77

Analisi granulometrica 26-02-26

Setaccio	**Passante progressivo**
[mm]	[%]
32	100.00
20	98.88
16	78.12
12.5	59.93
8	40.53
4	27.54
2	17.89
0.5	10.26
0.25	8.08
0.063	5.07
Pan	0.00

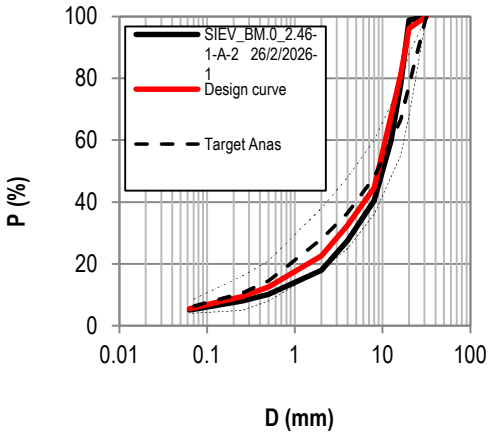

Filler perso nel lavaggio	61.7
Totale pre-lavaggio	1202.9

Bulk density

Test ID	M_{air} [g]	M_w [g]	M_{SSD} [g]	T [°C]	ρ_{SSD} [Mg/m^3]
BM.0_2.46-1-A-2-1	4578.2	2764.6	4610.7	21.4	2.475
BM.0_2.46-1-A-2-2	4577.7	2756.7	4616.6	21.4	2.456

Prova di compattazione

Test ID	v_{180}	v_{100}	v_{10}
BM.0_2.46-1-A-2-1	5.16	6.93	15.41
BM.0_2.46-1-A-2-2	5.88	7.69	16.15
Valori medi	5.52	7.31	15.78

$v_{180\ sawn}$
3.76
3.87

VMA e VFB

MMVT [Mg/m^3]	2.610
B.M [%]	4.1
P_b [Mg/m^3]	1.025

Specimen ID	VMA	VFB
BM.0_2.46-1-A-2-1	14.4	64
BM.0_2.46-1-A-2-2	15	61
Valori medi	14.7	62.5

Modulo di rigidezza a 25°C su provini tagliati

Specimen ID	E_1 (MPa)	E_2 (MPa)	Check	E_m (MPa)
BM.0_2.46-1-A-2-1	6385.5	6386.2	Passed	6385.85
BM.0_2.46-1-A-2-2	6012.9	6258.2	Passed	6135.55

ITS a 25°C su provini tagliati

Specimen ID	Altezza media [mm]	Max P [kN]	Spostamento verticale [mm]	ITS [MPa]	CTI [MPa]
BM.0_2.46-1-A-2-1	50.0	13.425736	3.077279	1.249	87.30
BM.0_2.46-1-A-2-2	49.8	15.943093	1.691	138.300	189.30

Valori medi	ITS [MPa]	CTI [MPa]
Esito	69.775	138.3
	Acceptable	Acceptable

Nome della miscela	BM.0_2.71-1-A-1
Descrizione	BASE +35% GR 0/20 con rejuvenator, miscelazione a 175°C scheletro litico 1

Quantitativi di materiale impiegati

AGGREGATI

Frazione	%	Massa [g]	Subtotali (g)
Filler	2	194.6	
0/5	14	1362.1	
3/8	0	0.0	
5/15	0	0.0	
15/25	49	4767.5	
0/6	0	0.0	
0/20	35	3405.3	
			9729.5

BITUME DI APPORTO

		Massa [g]	
70/100	2.71	263.7	263.7

ADDITIVI

		Massa [g]	
Rejuvenator (REJ.A)	0.07	6.81	
WP (WP.M)	0	0	6.8
	Massa totale della miscela [g]		10000

Massima Massa Volumica Teorica

Test ID	MMVT [Mg/m3]	MMVT medio [Mg/m3]
BM.0_2.71-1-A-1.1	2.606	2.604
BM.0_2.71-1-A-1.2	2.601	

Prova di ignizione 00-01-00

Mix ID	$m_{basket,prior}$ (g)	$m_{basket,prior+material}$ (g)	$m_{basket,after+material}$ (g)	B_{mix}	$B_{aggregate}$
BM.0_2.71-1-A-1	2839.7	4221.3	4166.9	3.94	4.10

Analisi granulometrica

Setaccio	**Passante progressivo**
[mm]	[%]
32	100.00
20	100.00
16	82.70
12.5	58.42
8	39.17
4	28.67
2	19.64
0.5	10.72
0.25	8.39
0.063	5.25
Pan	0.00

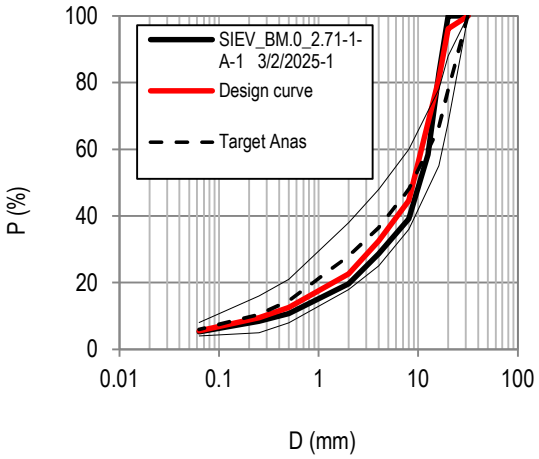

Filler perso nel lavaggio	69.7
Totale pre-lavaggio	1327.2

Bulk density

Test ID	M_{air} [g]	M_w [g]	M_{SSD} [g]	T [°C]	ρ_{SSD} [Mg/m^3]
BM.0_2.71-1-A-1-1	4568	2760	4588.2	21.4	2.494
BM.0_2.71-1-A-1-2	4569.6	2758.7	4589.1	21.4	2.491
BM.0_2.71-1-A-1-3	4566.3	2738.1	4598.8	20.7	2.449
BM.0_2.71-1-A-1-4	4568	2759.1	4589.8	20.5	2.491

Prova di compattazione

Test ID	v_{180}	v_{100}	v_{10}
BM.0_2.71-1-A-1-1	4.23	6.05	15.01
BM.0_2.71-1-A-1-2	4.31	6.21	14.76
BM.0_2.71-1-A-1-3	5.92	7.90	16.64
BM.0_2.71-1-A-1-4	4.34	6.13	14.81
Valori medi	4.70	6.57	15.30

$v_{180\ sawn}$
2.80
2.85
4.44
2.96

VMA e VFB

MMVT [Mg/m^3]	2.604
B.M [%]	4.4
P_b [Mg/m^3]	1.025

Specimen ID	VMA	VFB
BM.0_2.71-1-A-1-1	14	69.8
BM.0_2.71-1-A-1-2	14.1	69.3
BM.0_2.71-1-A-1-3	15.5	61.9
BM.0_2.71-1-A-1-4	14.2	68.7
Valori medi	14.5	67.4

Modulo di rigidezza a 25°C su provini tagliati

Specimen ID	E_1 (MPa)	E_2 (MPa)	Check	E_m (MPa)
BM.0_2.71-1-A-1-1	8359.6	8290.5	Passed	8325.05
BM.0_2.71-1-A-1-2	8418	8237.2	Passed	8327.6
BM.0_2.71-1-A-1-3	6985.7	5933.2	Passed	6459.45
BM.0_2.71-1-A-1-4	7803.2	7459.8	Passed	7631.5
Valore medio				7686

ITS a 25°C su provini tagliati

Specimen ID	Altezza media [mm]	Max P [kN]	Spostamento verticale [mm]	ITS [MPa]	CTI [MPa]
BM.0_2.71-1-A-1-1	55.7	21.879124	1.887119	1.669	208.34
BM.0_2.71-1-A-1-2	51.6	18.640896	2.119	1.535	170.67
BM.0_2.71-1-A-1-3	51.2	13.341208	3.305845	1.106	78.84
BM.0_2.71-1-A-1-4	51.4	19.370156	1.92553	1.600	195.76

Valori medi	ITS [MPa]	CTI [MPa]
Esito	1.477	163.4
	Not Acceptable	Acceptable

Nome della miscela	BM.0_3.10-1-A-1
Descrizione	BASE + 35% GR 0/20 con rejuvenator, miscelazione a 175°C scheletro litico 1. Reali

Quantitativi di materiale impiegati

AGGREGATI

Frazione	%	Massa [g]	Subtotali (g)
Filler	2	193.9	
0/5	14	1357.0	
3/8	0	0.0	
5/15	0	0.0	
15/25	49	4749.4	
0/6	0	0.0	
0/20	35	3392.5	
			9692.7

BITUME DI APPORTO

		Massa [g]	
70/100	3.1	300.5	300.5

ADDITIVI

		Massa [g]	
Rejuvenator (REJ.A)	0.07	6.8	
WP (WP.M)	0	0	6.8

Massa totale della miscela [g] 10000

Massima Massa Volumica Teorica

Test ID	MMVT [Mg/m3]	MMVT medio [Mg/m3]
BM.0_3.10-1-A-1.1	2.566	2.569
BM.0_3.10-1-A-1.2	2.573	

Prova di ignizione 00-01-00

Mix ID	$m_{basket,prior}$ (g)	$m_{basket,prior+material}$ (g)	$m_{basket,after+material}$ (g)	B_{mix}	$B_{aggregate}$
BM.0_3.10-1-A-1	2846.3	4176.4	4112.5	4.80	5.05

Analisi granulometrica

Setaccio	Passante progressivo
[mm]	[%]
32	100.00
20	100.00
16	89.24
12.5	69.03
8	49.65
4	35.71
2	22.90
0.5	12.60
0.25	9.57
0.063	5.98
Pan	0.00

Filler perso nel lavaggio	75.7
Totale pre-lavaggio	1266.2

#REF!

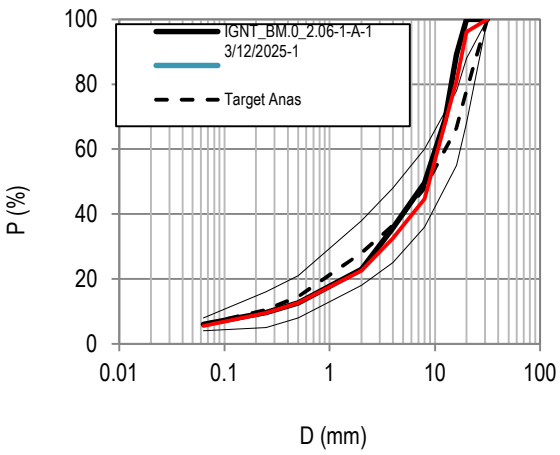

Bulk density

Test ID	M_{air} [g]	M_w [g]	M_{SSD} [g]	T [°C]	ρ_{SSD} [Mg/m^3]
BM.0_3.10-1-A-1-1	4539.5	2751.2	4549.1	20.7	2.520
BM.0_3.10-1-A-1-2	4542.8	2750.7	4553.3	20.7	2.515
BM.0_3.10-1-A-1-3	4537.4	2756.9	4543.2	20.7	2.535

Prova di compattazione

Test ID	v_{180}	v_{100}	v_{10}
BM.0_3.10-1-A-1-1	1.92	3.90	13.45
BM.0_3.10-1-A-1-2	2.10	4.00	13.21
BM.0_3.10-1-A-1-3	1.32	3.08	12.59
Valori medi	1.78	3.66	13.08

$v_{180\ sawn}$
1.24
1.44
0.58

VMA e VFB

MMVT [Mg/m^3]	2.569
B.M [%]	4.7
P_b [Mg/m^3]	1.025

Specimen ID	VMA	VFB
BM.0_3.10-1-A-1-1	13.7	86.4
BM.0_3.10-1-A-1-2	13.9	85
BM.0_3.10-1-A-1-3	13.2	90.3
Valori medi	13.6	87.2

Modulo di rigidezza a 25°C su provini tagliati

Specimen ID	E_1 (MPa)	E_2 (MPa)	Check	E_m (MPa)
BM.0_3.10-1-A-1-1 s	7521.3	7273.8	Passed	7398
BM.0_3.10-1-A-1-2 s	7105.9	7144	Passed	7125
BM.0_3.10-1-A-1-3 s	7945.3	7947.9	Passed	7947

ITS a 25°C su provini tagliati

Specimen ID	Altezza media [mm]	Max P [kN]	Spostamento verticale [mm]	ITS [MPa]	CTI [MPa]
BM.0_3.10-1-A-1-1 s	47.0	19.301	2.236	1.742	183.53
BM.0_3.10-1-A-1-2 s	47.2	14.728	3.191	1.326	97.90
BM.0_3.10-1-A-1-3 s	47.1	16.624	3.298	1.500	107.12

Valori medi	ITS [MPa]	CTI [MPa]
Esito	1.522	129.5
	Acceptable	Acceptable

Nome della miscela BM.8_2.06-1-A-1
Descrizione BASE +35% GR 0/20 con rejuvenator, scheletro litico 1

Quantitativi di materiale impiegati

AGGREGATI

Frazione	%	Massa [g]	Subtotali (g)
Filler	2	194.3	
0/5	14	1359.8	
3/8	0	0.0	
5/15	0	0.0	
15/25	49	4759.5	
0/6	0	0.0	
0/20	35	3399.6	
			9713.2

BITUME DI APPORTO

		Massa [g]	
70/100	2.06	200.1	200.1

ADDITIVI

		Massa [g]	
Rejuvenator (REJ.A)	0.07	6.8	
WP (WP.M)	0.80	79.9	86.7

Massa totale della miscela [g] 10000

Massima Massa Volumica Teorica

Test ID	MMVT [Mg/m3]	MMVT medio [Mg/m3]
BM.8_2.06-1-A-1.1	2.584	2.579
BM.8_2.06-1-A-1.2	2.575	

Prova di ignizione 00-01-00

Mix ID	$m_{basket,prior}$ (g)	$m_{basket,prior+material}$ (g)	$m_{basket,after+material}$ (g)	B_{mix}	$B_{aggregate}$
BM.8_2.06-1-A-1-2	2843.2	5045.5	4951.5	4.27	4.46
BM.8_2.06-1-A-1-2	2839.6	5173.1	5068.3	4.49	4.70

Analisi granulometrica 03-12-25

Setaccio	**Passante progressivo**
[mm]	[%]
32	100.00
20	97.57
16	82.06
12.5	61.47
8	42.08
4	30.80
2	22.26
0.5	13.05
0.25	10.02
0.063	5.90
Pan	0.00

Filler perso nel lavaggio	124.3
Totale pre-lavaggio	2057

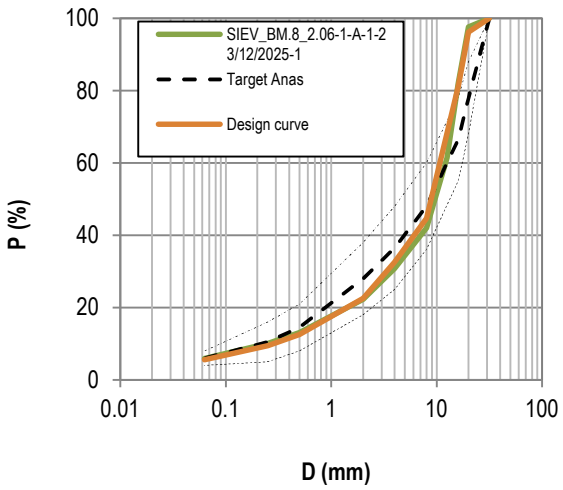

Bulk density

Test ID	M_{air} [g]	M_w [g]	M_{SSD} [g]	T [°C]	ρ_{SSD} [Mg/m^3]
BM.8_2.06-1-A-1-1	4570.1	2770.1	4604.3	20.1	2.487
BM.8_2.06-1-A-1-2	4570	2764.5	4603.9	20.5	2.480

Prova di compattazione

Test ID	v_{180}	v_{100}	v_{10}
BM.8_2.06-1-A-1-1	3.57	5.48	14.41
BM.8_2.06-1-A-1-2	3.85	5.56	14.39
Valori medi	3.71	5.52	14.40

$v_{180\ sawn}$
2.27
0.00

VMA e VFB

MMVT [Mg/m^3]	2.579
B.M [%]	3.7
P_b [Mg/m^3]	1.025

Modulo di rigidezza a 25°C su provini tagliati

Specimen ID	E_1 (MPa)	E_2 (MPa)	Check	E_m (MPa)
BM.8_2.06-1-A-1-1 s	14591.2	14107	Passed	14349

ITS a 25°C su provini tagliati

Specimen ID	Altezza media [mm]	Max P [kN]	Spostamento verticale [mm]	ITS [MPa]	CTI [MPa]
BM.8_2.06-1-A-1-1 s	51.1	24.567435	2.13415	2.040	225.28

	ITS [MPa]	CTI [MPa]
Valori medi	2.040	225.3
Esito	Rejected	Accepted

Nome della miscela	BM.8_2.46-1-A-1
Descrizione	BASE +35% GR 0/20 con rejuvenator, miscelazione a 175°C curva ottimizzata

Quantitativi di materiale impiegati

AGGREGATI

Frazione	%	Massa [g]	Subtotali (g)
Filler	2	193.5	
0/5	14	1354.5	
3/8	0	0.0	
5/15	0	0.0	
15/25	49	4740.9	
0/6	0	0.0	
0/20	35	3386.3	
			9675.3

BITUME DI APPORTO

		Massa [g]	
70/100	2.46	238.0	238.0

ADDITIVI

		Massa [g]	
Rejuvenator (REJ.A)	0.07	6.8	
WP (WP.M)	0.799439145	79.9	86.716605

Massa totale della miscela [g] 10000

Prova di ignizione 00-01-00

Mix ID	$m_{basket,prior}$ (g)	$m_{basket,prior+material}$ (g)	$m_{basket,after+material}$ (g)	B_{mix}	$B_{aggregate}$
BM.8_2.46-1-A-1-2	2839.7	5057.6	4957.4	4.52	4.73
BM.8_2.46-1-A-1-3	2839.7	5138.7	5030.5	4.71	4.94

Analisi granulometrica 04-12-25

Setaccio	**Passante progressivo**
[mm]	[%]
32	100.00
20	97.45
16	85.94
12.5	65.73
8	43.24
4	30.91
2	22.60
0.5	13.59
0.25	10.51
0.063	6.14
Pan	0.00

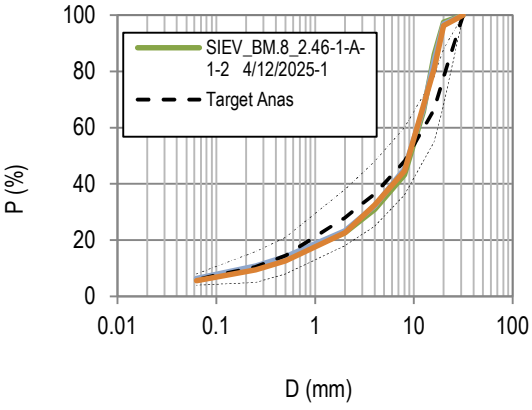

Filler perso nel lavaggio	130.1
Totale pre-lavaggio	2063.7

Bulk density

Test ID	M_{air} [g]	M_w [g]	M_{SSD} [g]	T [°C]	ρ_{SSD} [Mg/m^3]
BM.8_2.46-1-A-1-1	4549.6	2748.2	4571.6	19.4	2.491
BM.8_2.46-1-A-1-2	4540.3	2726.4	4568.4	19.4	2.461
BM.8_2.46-1-A-1-3	4539.5	2739.5	4568.1	19.4	2.479

Prova di compattazione

Test ID	v_{180}	v_{100}	v_{10}
BM.8_2.46-1-A-1-1	3.03	4.70	13.36
BM.8_2.46-1-A-1-2	4.21	6.27	15.30
BM.8_2.46-1-A-1-3	3.52	5.31	13.86
Valori medi	3.59	5.43	14.17

$v_{180\ sawn}$
1.35
-
2.11

VMA e VFB

Specimen ID	VMA	VFB
BM.8_2.46-1-A-1-1	14.5	79.1
BM.8_2.46-1-A-1-2	15.5	73.1
BM.8_2.46-1-A-1-3	14.9	76.6
Valori medi	15.0	76.3

Modulo di rigidezza a 25°C su provini tagliati

Specimen ID	E_1 (MPa)	E_2 (MPa)	Check	E_m (MPa)
BM.8_2.46-1-A-1-1 s	11625.5	11837.9	Passed	11732
BM.8_2.46-1-A-1-3 s	10341.9	10038	Passed	10190
Valore medio				10961

ITS a 25°C su provini tagliati

Specimen ID	Altezza media [mm]	Max P [kN]	Spostamento verticale [mm]	ITS [MPa]	CTI [MPa]
BM.8_2.46-1-A-1-1 s	52.7	24.2792	1.943368	1.954	236.95
BM.8_2.46-1-A-1-3 s	51.6	21.906526	2.649	1.801	160.17

Valori medi	ITS [MPa]	CTI [MPa]
Esito	1.878	198.6
	Rejected	Accepted

Nome della miscela	BM.8_2.71-1-A-1
Descrizione	BASE +35% GR 0/20 con rejuvenator, miscelazione a 175°C scheletro litico 1

Quantitativi di materiale impiegati

AGGREGATI

Frazione	%	Massa [g]	Subtotali (g)
Filler	2	193.0	
0/5	14	1351.2	
3/8	0	0.0	
5/15	0	0.0	
15/25	49	4729.3	
0/6	0	0.0	
0/20	35	3378.1	
			9651.7

BITUME DI APPORTO

		Massa [g]	
70/100	2.71	261.6	261.6

ADDITIVI

		Massa [g]	
Rejuvenator (REJ.A)	0.07	6.8	
WP (WP.M)	0.80	80.00	86.76
		Massa totale della miscela [g]	10000

Massima Massa Volumica Teorica

Test ID	MMVT [Mg/m3]	MMVT medio [Mg/m3]
BM.8_2.71-1-A-1.1	2.568	2.568
BM.8_2.71-1-A-1.2	2.567	

Prova di ignizione 18-02-26

Mix ID	$m_{basket,prior}$ (g)	$m_{basket,prior+material}$ (g)	$m_{basket,after+material}$ (g)	B_{mix}	$B_{aggregate}$
BM.8_2.71-1-A-1	2846.6	4465.7	4385.2	4.97	5.23

Analisi granulometrica

Setaccio	**Passante progressivo**
[mm]	[%]
32	100.00
20	99.02
16	91.06
12.5	71.49
8	49.94
4	36.38
2	25.28
0.5	14.61
0.25	11.19
0.063	7.00
Pan	0.00

Filler perso nel lavaggio	107.7
Totale pre-lavaggio	1523.5

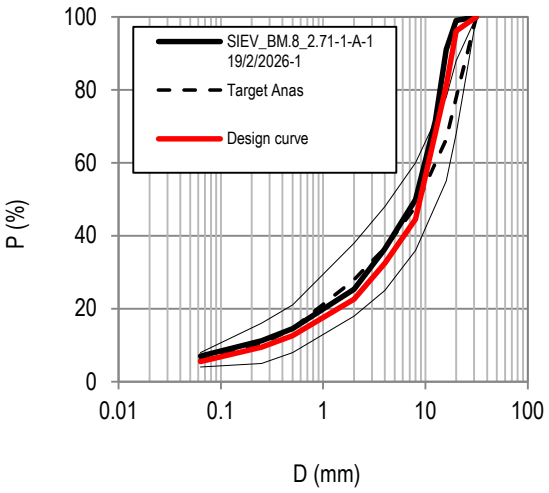

Bulk density

Test ID	M_{air} [g]	M_w [g]	M_{SSD} [g]	T [°C]	ρ_{SSD} [Mg/m^3]
BM.8_2.71-1-A-1-1	4528.5	2732.6	4537.6	20.8	2.504
BM.8_2.71-1-A-1-2	4527.3	2723.5	4541.3	20.8	2.486
BM.8_2.71-1-A-1-3	4525.9	2731.8	4535.8	20.8	2.504

Prova di compattazione

Test ID	v_{180}	v_{100}	v_{10}
BM.8_2.71-1-A-1-1	2.48	4.01	12.52
BM.8_2.71-1-A-1-2	3.19	4.79	13.74
BM.8_2.71-1-A-1-3	2.48	4.20	12.25
Valori medi	2.72	4.33	12.84

$v_{180\ sawn}$
1.61
1.72
1.56

VMA e VFB

MMVT [Mg/m^3]	2.568
B.M [%]	4.3
P_b [Mg/m^3]	1.025

Specimen ID	VMA	VFB
BM.8_2.71-1-A-1-1	15	83.4
BM.8_2.71-1-A-1-2	15.6	79.6
BM.8_2.71-1-A-1-3	15	83.4
Valori medi	15.2	82.1

Modulo di rigidezza a 25°C su provini tagliati

Specimen ID	E_1 (MPa)	E_2 (MPa)	Check	E_m (MPa)
BM.8_2.71-1-A-1-1 s	10447.9	8923.8	Passed	9686
BM.8_2.71-1-A-1-2 s	7438.4	7407.5	Passed	7423
BM.8_2.71-1-A-1-3 s	10375.2	10728.8	Passed	10552
Valore medio				9220

ITS a 25°C su provini tagliati

Specimen ID	Altezza media [mm]	Max P [kN]	Spostamento verticale [mm]	ITS [MPa]	CTI [MPa]
BM.8_2.71-1-A-1-1 s	49.8	24.289121	1.733274	2.069	281.32
BM.8_2.71-1-A-1-2 s	48.8	21.332514	2.157	1.855	202.59
BM.8_2.71-1-A-1-3 s	54.3	24.952121	2.07468	1.950	221.49

Valori medi	ITS [MPa]	CTI [MPa]
Esito	1.958	235.1
	Not Acceptable	Acceptable